Heavy Fermions: Electrons at the Edge of Magnetism

Piers Coleman
Rutgers University, Piscataway, NJ, USA

1 INTRODUCTION: 'ASYMPTOTIC FREEDOM' IN A CRYOSTAT

The term *heavy fermion* was coined by Steglich *et al*. (1976) in the late 1970s to describe the electronic excitations in a new class of intermetallic compound with an electronic density of states as much as 1000 times larger than copper. Since the original discovery of heavy-fermion behavior in $CeAl_3$ by Andres, Graebner and Ott (1975), a diversity of heavy-fermion compounds, including superconductors, antiferromagnets (AFMs), and insulators have been discovered. In the last 10 years, these materials have become the focus of intense interest with the discovery that intermetallic AFMs can be tuned through a quantum phase transition into a heavy-fermion state by pressure, magnetic fields, or chemical doping (von Löhneysen *et al*., 1994; von Löhneysen, 1996; Mathur *et al*., 1998). The 'quantum critical point' (QCP) that separates the heavy-electron ground state from the AFM represents a kind of singularity in the material phase diagram that profoundly modifies the metallic properties, giving them a a predisposition toward superconductivity and other novel states of matter.

One of the goals of modern condensed matter research is to couple magnetic and electronic properties to develop new classes of material behavior, such as high-temperature superconductivity or colossal magnetoresistance materials, spintronics, and the newly discovered multiferroic materials. Heavy-electron materials lie at the very brink of magnetic instability, in a regime where quantum fluctuations of the magnetic and electronic degrees are strongly coupled. As such, they are an important test bed for the development of our understanding about the interaction between magnetic and electronic quantum fluctuations.

Heavy-fermion materials contain rare-earth or actinide ions, forming a matrix of localized magnetic moments. The active physics of these materials results from the immersion of these magnetic moments in a quantum sea of mobile conduction electrons. In most rare-earth metals and insulators, local moments tend to order antiferromagnetically, but, in heavy-electron metals, the quantum-mechanical jiggling of the local moments induced by delocalized electrons is fierce enough to melt the magnetic order.

The mechanism by which this takes place involves a remarkable piece of quantum physics called the *Kondo effect* (Kondo, 1962, 1964; Jones, 2007). The Kondo effect describes the process by which a free magnetic ion, with a Curie magnetic susceptibility at high temperatures, becomes screened by the spins of the conduction sea, to ultimately form a spinless scatering center at low temperatures and low magnetic fields (Figure 1a). In the Kondo effect, this screening process is continuous, and takes place once the

Handbook of Magnetism and Advanced Magnetic Materials. Edited by Helmut Kronmüller and Stuart Parkin. Volume 1: *Fundamentals and Theory*. ISBN: 978-0-470-02217-7.

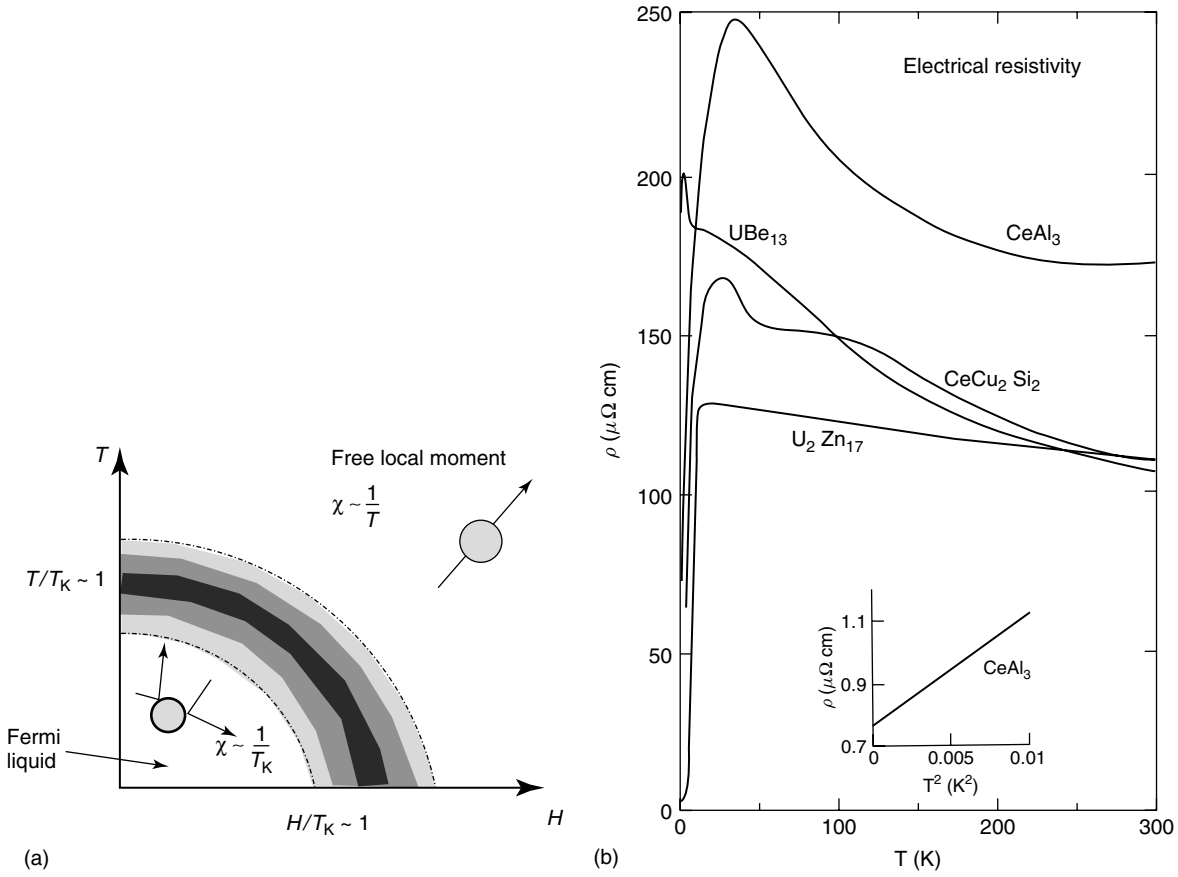

Figure 1. (a) In the Kondo effect, local moments are free at high temperatures and high fields, but become 'screened' at temperatures and magnetic fields that are small compared with the 'Kondo temperature' T_K, forming resonant scattering centers for the electron fluid. The magnetic susceptibility χ changes from a Curie-law $\chi \sim \frac{1}{T}$ at high temperature, but saturates at a constant paramagnetic value $\chi \sim \frac{1}{T_K}$ at low temperatures and fields. (b) The resistivity drops dramatically at low temperatures in heavy fermion materials, indicating the development of phase coherence between the scatering of the lattice of screened magnetic ions. (Reproduced from J.L. Smith and P.S. Riseborough, *J. Mag. Mat.* 47–48, 1985, copyright © 1985, with permission from Elsevier.)

magnetic field, or the temperature drops below a characteristic energy scale called the *Kondo temperature* T_K. Such 'quenched' magnetic moments act as strong elastic scattering potentials for electrons, which gives rise to an increase in resistivity produced by isolated magnetic ions. When the same process takes place inside a heavy-electron material, it leads to a spin quenching at every site in the lattice, but now, the strong scattering at each site develops coherence, leading to a sudden drop in the resistivity at low temperatures (Figure 1b).

Heavy-electron materials involve the dense lattice analog of the single-ion Kondo effect and are often called *Kondo lattice* compounds (Doniach, 1977). In the lattice, the Kondo effect may be alternatively visualized as the dissolution of localized and neutral magnetic f spins into the quantum conduction sea, where they become mobile excitations. Once mobile, these free spins acquire charge and form electrons with a radically enhanced effective mass (Figure 2). The net effect of this process is an increase in the volume of the electronic Fermi surface, accompanied by a profound transformation in the electronic masses and interactions.

A classic example of such behavior is provided by the intermetallic crystal $CeCu_6$. Superficially, this material is copper, alloyed with 14% Cerium. The Cerium Ce^{3+} ions in this material are Ce^{3+} ions in a $4f^1$ configuration with a localized magnetic moment with $J = 5/2$. Yet, at low temperatures, they lose their spin, behaving as if they were Ce^{4+} ions with delocalized f electrons. The heavy electrons that develop in this material are a thousand times 'heavier' than those in metallic copper, and move with a group velocity that is slower than sound. Unlike copper, which has Fermi temperature of the order 10 000 K, that of $CeCu_6$ is of the order 10 K, and above this temperature, the heavy electrons disintegrate to reveal the underlying magnetic moments of the Cerium ions, which manifest themselves as a Curie-law susceptibility $\chi \sim \frac{1}{T}$. There are many hundreds of different

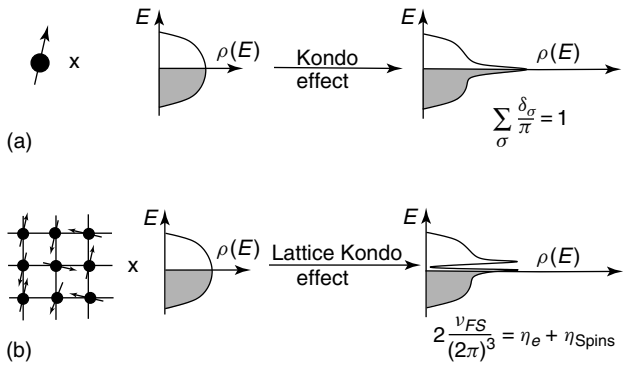

Figure 2. (a) Single-impurity Kondo effect builds a single fermionic level into the conduction sea, which gives rise to a resonance in the conduction electron density of states. (b) Lattice Kondo effect builds a fermionic resonance into the conduction sea in each unit cell. The elastic scattering of this lattice of resonances leads to the formation of a heavy-electron band, of width T_K.

varieties of heavy-electron material, many developing new and exotic phases at low temperatures.

This chapter is intended as a perspective on the the current theoretical and experimental understanding of heavy-electron materials. There are important links between the material in this chapter and the proceeding chapter on the Kondo effect by Jones (2007), the chapter on quantum criticality by Sachdev (2007), and the perspective on spin fluctuation theories of high-temperature superconductivity by Norman (2007). For completeness, I have included references to an extensive list of review articles spanning 30 years of discovery, including books on the Kondo effect and heavy fermions (Hewson, 1993; Cox and Zawadowski, 1999), general reviews on heavy-fermion physics (Stewart, 1984; Lee *et al*., 1986; Ott, 1987; Fulde, Keller and Zwicknagl, 1988; Grewe and Steglich, 1991), early views of Kondo and mixed valence physics (Gruner and Zawadowski, 1974; Varma, 1976), the solution of the Kondo impurity model by renormalization group and the strong coupling expansion (Wilson, 1976; Nozières and Blandin, 1980), the Bethe Ansatz method (Andrei, Furuya and Lowenstein, 1983; Tsvelik and Wiegman, 1983), heavy-fermion superconductivity (Sigrist and Ueda, 1991a; Cox and Maple, 1995), Kondo insulators (Aeppli and Fisk, 1992; Tsunetsugu, Sigrist and Ueda, 1997; Riseborough, 2000), X-ray spectroscopy (Allen *et al*., 1986), optical response in heavy fermions (Degiorgi, 1999), and the latest reviews on non-Fermi liquid behavior and quantum criticality (Stewart, 2001; Coleman, Pépin, Si and Ramazashvili, 2001; Varma, Nussinov and van Saarlos, 2002; von Löhneysen, Rosch, Vojta and Wolfe, 2007; Miranda and Dobrosavljevic, 2005; Flouquet, 2005). There are inevitable apologies, for this chapter is highly selective and, partly owing to lack of space, it neither covers dynamical mean-field theory (DMFT) approaches to heavy-fermion physics (Georges, Kotliar, Krauth and Rozenberg, 1996; Cox and Grewe, 1988; Jarrell, 1995; Vidhyadhiraja, Smith, Logan and Krishnamurthy, 2003) nor the extensive literature on the order-parameter phenomenology of heavy-fermion superconductors (HFSCs) reviewed in Sigrist and Ueda (1991a).

1.1 Brief history

Heavy-electron materials represent a frontier in a journey of discovery in electronic and magnetic materials that spans more than 70 years. During this time, the concepts and understanding have undergone frequent and often dramatic revision.

In the early 1930s, de Haas, de Boer and van der Berg (1933) in Leiden, discovered a 'resistance minimum' that develops in the resistivity of copper, gold, silver, and many other metals at low temperatures (Figure 3). It took a further 30 years before the purity of metals and alloys improved to a point where the resistance minimum could be linked to the presence of magnetic impurities (Clogston *et al*., 1962; Sarachik, Corenzwit and Longinotti, 1964). Clogston, Mathias, and collaborators at Bell Labs (Clogston *et al*., 1962) found they could tune the conditions under which iron impurities in Niobium were magnetic, by alloying with molybdenum. Beyond a certain concentration of molybdenum, the iron impurities become magnetic and a resistance minimum was observed to develop.

In 1961, Anderson formulated the first microscopic model for the formation of magnetic moments in metals. Earlier work by Blandin and Friedel (1958) had observed that localized d states form resonances in the electron sea. Anderson extended this idea and added a new ingredient: the Coulomb interaction between the d-electrons, which he modeled by term

$$H_I = U n_\uparrow n_\downarrow \tag{1}$$

Anderson showed that local moments formed once the Coulomb interaction U became large. One of the unexpected consequences of this theory is that local moments develop an antiferromagnetic coupling with the spin density of the surrounding electron fluid, described by the interaction (Anderson, 1961; Kondo, 1962, 1964; Schrieffer and Wolff, 1966; Coqblin and Schrieffer, 1969)

$$H_I = J\vec{\sigma}(0)\cdot\vec{S} \tag{2}$$

where $\vec{S}$ is the spin of the local moment and $\vec{\sigma}(0)$ is the spin density of the electron fluid. In Japan, Kondo (1962) set out to examine the consequences of this result. He found that when he calculated the scattering rate $\frac{1}{\tau}$ of

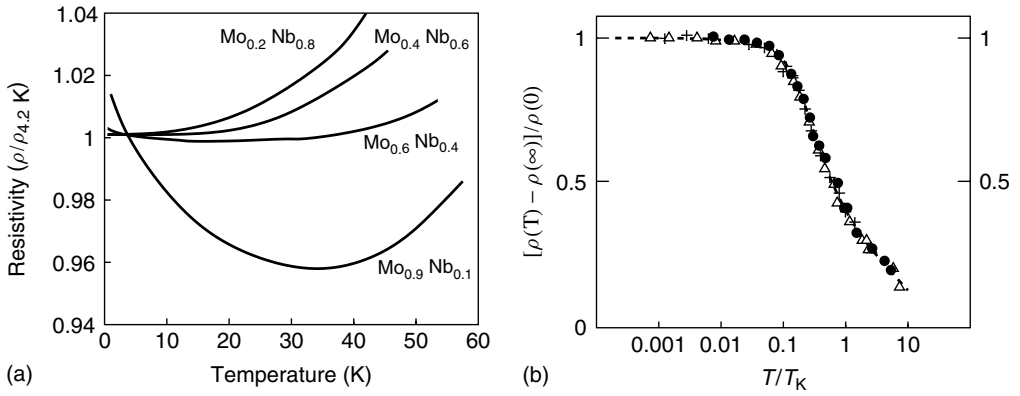

Figure 3. (a) Resistance minimum in Mo_xNb_{1-x}. (Reproduced from M. Sarachik, E. Corenzwit, and L.D. Longinotti, *Phys. Rev.* **135**, 1964, A1041, copyright © by the American Physical Society, with permission of the APS.) (b) Temperature dependence of excess resistivity produced by scattering off a magnetic ion, showing, universal dependence on a single scale, the Kondo temperature. Original data from White and Geballe (1979).

electrons of a magnetic moment to one order higher than Born approximation,

$$\frac{1}{\tau} \propto \left[J\rho + 2(J\rho)^2 \ln \frac{D}{T} \right]^2 \tag{3}$$

where ρ is the density of state of electrons in the conduction sea and D is the width of the electron band. As the temperature is lowered, the logarithmic term grows, and the scattering rate and resistivity ultimately rises, connecting the resistance minimum with the antiferromagnetic interaction between spins and their surroundings.

A deeper understanding of the logarithmic term in this scattering rate required the renormalization group concept (Anderson and Yuval, 1969, 1970, 1971; Fowler and Zawadowskii, 1971; Wilson, 1976; Nozières, 1976; Nozières and Blandin, 1980). The key idea here is that the physics of a spin inside a metal depends on the energy scale at which it is probed. The 'Kondo' effect is a manifestation of the phenomenon of 'asymptotic freedom' that also governs quark physics. Like the quark, at high energies, the local moments inside metals are asymptotically free, but at temperatures and energies below a characteristic scale the Kondo temperature,

$$T_K \sim D e^{-1/(2J\rho)} \tag{4}$$

where ρ is the density of electronic states; they interact so strongly with the surrounding electrons that they become screened into a singlet state, or 'confined' at low energies, ultimately forming a Landau–Fermi liquid (Nozières, 1976; Nozières and Blandin, 1980).

Throughout the 1960s and 1970s, conventional wisdom had it that magnetism and superconductivity are mutually exclusive. Tiny concentrations of magnetic impurities produce a lethal suppression of superconductivity in conventional metals. Early work on the interplay of the Kondo effect and superconductivity by Maple *et al*. (1972) did suggest that the Kondo screening suppresses the pair-breaking effects of magnetic moments, but the implication of these results was only slowly digested. Unfortunately, the belief in the mutual exclusion of local moments and superconductivity was so deeply ingrained that the first observation of superconductivity in the 'local moment' metal UBe_{13} (Bucher *et al*., 1975) was dismissed by its discoverers as an artifact produced by stray filaments of uranium. Heavy-electron metals were discovered by Andres, Graebner and Ott (1975), who observed that the intermetallic $CeAl_3$ forms a metal in which the Pauli susceptibility and linear specific heat capacity are about 1000 times larger than in conventional metals. Few believed their speculation that this might be a lattice version of the Kondo effect, giving rise to a narrow band of 'heavy' f electrons in the lattice. The discovery of superconductivity in $CeCu_2Si_2$ in a similar f-electron fluid, a year later by Steglich *et al*. (1976), was met with widespread disbelief. All the measurements of the crystal structure of this material pointed to the fact that the Ce ions were in a Ce^{3+} or $4f^1$ configuration. Yet, this meant one local moment per unit cell – which required an explanation of how these local moments do not destroy superconductivity, but, rather, are part of its formation.

Doniach (1977), made the visionary proposal that a heavy-electron metal is a dense Kondo lattice (Kasuya, 1956), in which every single local moment in the lattice undergoes the Kondo effect (Figure 2). In this theory, each spin is magnetically screened by the conduction sea. One of the great concerns of the time, raised by Nozières (1985), was whether there could ever be sufficient conduction electrons in a dense Kondo lattice to screen each local moment.

Theoretical work on this problem was initially stalled for want of any controlled way to compute properties of the Kondo lattice. In the early 1980s, Anderson (1981) proposed a way out of this log-jam. Taking a cue from the success of the $1/S$ expansion in spin-wave theory, and the $1/N$ expansion in statistical mechanics and particle physics, he noted that the large magnetic spin degeneracy $N = 2j + 1$ of f moments could be used to generate an expansion in the small parameter $1/N$ about the limit where $N \to \infty$. Anderson's idea prompted a renaissance of theoretical development (Ramakrishnan, 1981; Gunnarsson and Schönhammer, 1983; Read and Newns, 1983a,b; Coleman, 1983, 1987a; Auerbach and Levin, 1986), making it possible to compute the X-ray absorption spectra of these materials and, for the first time, examine how heavy f bands form within the Kondo lattice. By the mid-1980s, the first de Haas van Alphen experiments (Reinders *et al*., 1986; Taillefer and Lonzarich, 1988) had detected cyclotron orbits of heavy electrons in $CeCu_6$ and UPt_3. With these developments, the heavy-fermion concept was cemented.

On a separate experimental front, in Ott, Rudigier, Fisk and Smith (1983), and Ott *et al*. (1984) returned to the material UBe_{13}, and, by measuring a large discontinuity in the bulk specific heat at the resistive superconducting transition, confirmed it as a bulk heavy-electron superconductor. This provided a vital independent confirmation of Steglich's discovery of heavy electron superconductivity, assuaging the old doubts and igniting a huge new interest in heavy-electron physics. The number of heavy-electron metals and superconductors grew rapidly in the mid-1980s (Sigrist and Ueda, 1991b). It became clear from specific heat, NMR, and ultrasound experiments on HFSCs that the gap is anisotropic, with lines of nodes strongly suggesting an electronic, rather than a phonon mechanism of pairing. These discoveries prompted theorists to return to earlier spin-fluctuation-mediated models of anisotropic pairing. In the early summer of 1986, three new theoretical papers were received by *Physical Review*, the first by Monod, Bourbonnais and Emery (1986) working in Orsay, France, followed closely (6 weeks later) by papers from Scalapino, Loh and Hirsch (1986) at UC Santa Barbara, California, and Miyake, Rink and Varma (1986) at Bell Labs, New Jersey. These papers contrasted heavy-electron superconductivity with superfluid He-3. Whereas He-3 is dominated by ferromagnetic interactions, which generate triplet pairing, these works showed that, in heavy-electron systems, soft antiferromagnetic spin fluctuations resulting from the vicinity to an antiferromagnetic instability would drive anisotropic d-wave pairing (Figure 4). The almost coincident discovery of high-temperature superconductivity the very same year, 1986, meant that these early works on heavy-electron superconductivity were destined to exert huge influence on the evolution of ideas about high-temperature

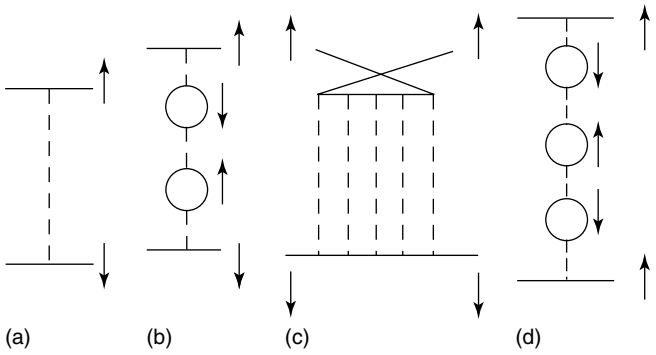

Figure 4. Figure from Monod, Bourbonnais and Emery (1986), one of three path-breaking papers in 1986 to link d-wave pairing to antiferromagnetism. (a) The bare interaction, (b), (c), and (d), the paramagnon-mediated interaction between antiparallel or parallel spins. (Reproduced from M.T.B. Monod, C. Bourbonnais, and V. Emery, *Phys. Rev. B.* **34**, 1986, 7716, copyright © 1986 by the American Physical Society, with permission of the APS.)

superconductivity. Both the resonating valence bond (RVB) and the spin-fluctuation theory of d-wave pairing in the cuprates are, in my opinion, close cousins, if not direct descendents of these early 1986 papers on heavy-electron superconductivity.

After a brief hiatus, interest in heavy-electron physics reignited in the mid-1990s with the discovery of QCPs in these materials. High-temperature superconductivity introduced many important new ideas into our conception of electron fluids, including

- Non-Fermi liquid behavior: the emergence of metallic states that cannot be described as fluids of renormalized quasiparticles.
- Quantum phase transitions and the notion that zero temperature QCPs might profoundly modify finite temperature properties of metal.

Both of these effects are seen in a wide variety of heavy-electron materials, providing an vital alternative venue for research on these still unsolved aspects of interlinked, magnetic, and electronic behavior.

In 1994 Hilbert von Löhneysen and collaborators discovered that by alloying small amounts of gold into $CeCu_6$, one can tune $CeCu_{6-x}Au_x$ through an antiferromagnetic QCP, and then reverse the process by the application of pressure (von Löhneysen, 1996; von Löhneysen *et al*., 1994). These experiments showed that a heavy-electron metal develops 'non-Fermi liquid' properties at a QCP, including a linear temperature dependence of the resistivity and a logarithmic dependence of the specific heat coefficient on temperature. Shortly thereafter, Mathur *et al*. (1998), at Cambridge showed that when pressure is used to drive the AFM $CeIn_3$

through a quantum phase transition, heavy-electron superconductivity develops in the vicinity of the quantum phase transition. Many new examples of heavy-electron system have come to light in the last few years which follow the same pattern. In one fascinating development, (Monthoux and Lonzarich, 1999) suggested that if quasi-two-dimensional versions of the existing materials could be developed, then the superconducting pairing would be less frustrated, leading to a higher transition temperature. This led experimental groups to explore the effect of introducing layers into the material $CeIn_3$, leading to the discovery of the so-called $1-1-5$ compounds, in which an XIn_2 layer has been introduced into the original cubic compound. (Petrovic *et al*., 2001; Sidorov *et al*., 2002). Two notable members of this group are $CeCoIn_5$ and, most recently, $PuCoGa_5$ (Sarrao *et al*., 2002). The transition temperature rose from 0.5 to 2.5 K in moving from $CeIn_3$ to $CeCoIn_5$. Most remarkably, the transition temperature rises to above 18 K in the $PuCoGa_5$ material. This amazing rise in T_c, and its close connection with quantum criticality, are very active areas of research, and may hold important clues (Curro *et al*., 2005) to the ongoing quest to discover room-temperature superconductivity.

1.2 Key elements of heavy-fermion metals

Before examining the theory of heavy-electron materials, we make a brief tour of their key properties. Table 1 shows a selective list of heavy fermion compounds

1.2.1 Spin entropy: a driving force for new physics

The properties of heavy-fermion compounds derive from the partially filled f orbitals of rare-earth or actinide ions (Stewart, 1984; Lee *et al*., 1986; Ott, 1987; Fulde, Keller and Zwicknagl, 1988; Grewe and Steglich, 1991). The large nuclear charge in these ions causes their f orbitals to collapse inside the inert gas core of the ion, turning them into localized magnetic moments.

Moreover, the large spin-orbit coupling in f orbitals combines the spin and angular momentum of the f states into a

Table 1. Selected heavy-fermion compounds.

Type	Material	T^* (K)	$T_c,\ x_c,\ B_c$	Properties	ρ	m J mol^{-1}K^{-2} γ_n	References
Metal	$CeCu_6$	10	–	Simple HF metal	T^2	1600	Stewart, Fisk and Wire (1984a) and Onuki and Komatsubara (1987)
Superconductors	$CeCu_2Si_2$	20	$T_c = 0.17$ K	First HFSC	T^2	800–1250	Steglich *et al*. (1976) and Geibel *et al*. (1991a,b)
	UBe_{13}	2.5	$T_c = 0.86$ K	Incoherent metal→HFSC	$\rho_c \sim 150\,\mu\Omega$ cm	800	Ott, Rudigier, Fisk and Smith (1983, 1984)
	$CeCoIn_5$	38	$T_c = 2.3$	Quasi 2D HFSC	T	750	Petrovic *et al*. (2001) and Sidorov *et al*. (2002)
Kondo insulators	$Ce_3Pt_4Bi_3$	$T_\chi \sim 80$	–	Fully gapped KI	$\sim e^{\Delta/T}$	–	Hundley *et al*. (1990) and Bucher, Schlessinger, Canfield and Fisk (1994)
	CeNiSn	$T_\chi \sim 20$	–	Nodal KI	Poor metal	–	Takabatake *et al*. (1990, 1992) and Izawa *et al*. (1999)
Quantum critical	$CeCu_{6-x}Au_x$	$T_0 \sim 10$	$x_c = 0.1$	Chemically tuned QCP	T	$\sim\frac{1}{T_0}\ln\left(\frac{T_0}{T}\right)$	von Löhneysen *et al*. (1994) and von Löhneysen (1996)
	$YbRh_2Si_2$	$T_0 \sim 24$	$B_\perp = 0.06$ T $B_\parallel = 0.66$ T	Field-tuned QCP	T	$\sim\frac{1}{T_0}\ln\left(\frac{T_0}{T}\right)$	Trovarelli *et al*. (2000), Paschen *et al*. (2004), Custers *et al*. (2003) and Gegenwart *et al*. (2005)
SC + other order	UPd_2Al_3	110	$T_{AF} = 14$ K, $T_{sc} = 2$ K	AFM + HFSC	T^2	210	Geibel *et al*. (1991a), Sato *et al*. (2001) and Tou *et al*. (1995)
	URu_2Si_2	75	$T_1 = 17.5$ K, $T_{sc} = 1.3$ K	Hidden order and HFSC	T^2	120/65	Palstra *et al*. (1985) and Kim *et al*. (2003)

Unless otherwise stated, T^* denotes the temperature of the maximum in resistivity. T_c, x_c, and B_c denote critical temperature, doping, and field. ρ denotes the temperature dependence in the normal state. $\gamma_n = C_V/T$ is the specific heat coefficient in the normal state.

state of definite J, and it is these large quantum spin degrees of freedom that lie at the heart of heavy-fermion physics.

Heavy-fermion materials display properties which change qualitatively, depending on the temperature, so much so, that the room-temperature and low-temperature behavior almost resembles two different materials. At room temperature, high magnetic fields, and high frequencies, they behave as local moment systems, with a Curie-law susceptibility

$$\chi = \frac{M^2}{3T} \qquad M^2 = (g_J \mu_B)^2 J(J+1) \tag{5}$$

where M is the magnetic moment of an f state with total angular momentum J and the gyromagnetic ratio g_J. However, at temperatures beneath a characteristic scale, we call T^* (to distinguish it from the single-ion Kondo temperature T_K), the localized spin degrees of freedom melt into the conduction sea, releasing their spins as mobile, conducting f electrons.

A Curie susceptibility is the hallmark of the decoupled, rotational dynamics of the f moments, associated with an unquenched entropy of $\mathcal{S} = k_B \ln N$ per spin, where $N = 2J + 1$ is the spin degeneracy of an isolated magnetic moment of angular momentum J. For example, in a Cerium-heavy electron material, the $4f^1$ ($L = 3$) configuration of the Ce^{3+} ion is spin-orbit coupled into a state of definite $J = L - S = 5/2$ with $N = 6$. Inside the crystal, the full rotational symmetry of each magnetic f ion is often reduced by crystal fields to a quartet ($N = 4$) or a Kramer's doublet $N = 2$. At the characteristic temperature T^*, as the Kondo effect develops, the spin entropy is rapidly lost from the material, and large quantities of heat are lost from the material. Since the area under the specific heat curve determines the entropy,

$$S(T) = \int_0^T \frac{C_V}{T'} \mathrm{d}T' \tag{6}$$

a rapid loss of spin entropy at low temperatures forces a sudden rise in the specific heat capacity. Figure 5 illustrates this phenomenon with the specific heat capacity of UBe_{13}. Notice how the specific heat coefficient C_V/T rises to a value of order 1 J mol^{-1}K^2, and starts to saturate at about 1 K, indicating the formation of a Fermi liquid with a linear specific heat coefficient. Remarkably, just as the linear specific heat starts to develop, UBe_{13} becomes superconducting, as indicated by the large specific heat anomaly.

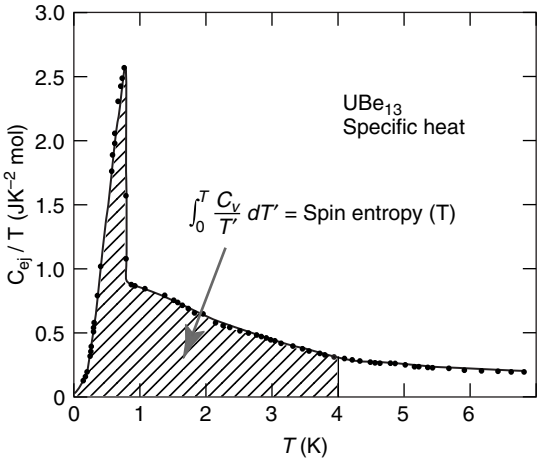

Figure 5. Showing the specific heat coefficient of UBe_{13} after (Ott, Rudigier, Fisk and Smith, 1985). The area under the C_V/T curve up to a temperature T provides a measure of the amount of unquenched spin entropy at that temperature. The condensation entropy of HFSCs is derived from the spin-rotational degrees of freedom of the local moments, and the large scale of the condensation entropy indicates that spins partake in the formation of the order parameter. (Reproduced from H.R. Ott, H. Rudigier, Z. Fisk, and J.L. Smith, in W.J.L. Buyers (ed.): *Proceedings of the NATO Advanced Study Institute on Moment Formation in Solids, Vancouver Island*, August 1983, Valence Fluctuations in Solids (Plenum, 1985), p. 309. with permission of Springer Science and Business Media.)

1.2.2 'Local' Fermi liquids with a single scale

The standard theoretical framework for describing metals is Landau–Fermi liquid theory (Landau, 1957), according to which the excitation spectrum of a metal can be adiabatically connected to those of a noninteracting electron fluid. Heavy-fermion metals are extreme examples of Landau–Fermi liquids which push the idea of adiabaticity into an regime where the bare electron interactions, on the scale of electron volts, are hundreds, even thousands of times larger than the millivolt Fermi energy scale of the heavy-electron quasiparticles. The Landau–Fermi liquid that develops in these materials shares much in common with the Fermi liquid that develops around an isolated magnetic impurity (Nozières, 1976; Nozières and Blandin, 1980), once it is quenched by the conduction sea as part of the Kondo effect. There are three key features of this Fermi liquid:

- *Single scale:* T^* The quasiparticle density of states $\rho^* \sim 1/T^*$ and scattering amplitudes $A_{\mathbf{k}\sigma,\mathbf{k}'\sigma'} \sim T^*$ scale approximately with a single scale T^*.
- *Almost incompressible:* Heavy-electron fluids are 'almost incompressible', in the sense that the charge susceptibility $\chi_c = \mathrm{d}N_e/\mathrm{d}\mu \ll \rho^*$ is unrenormalized and typically more than an order of magnitude smaller than the quasiparticle density of states ρ^*. This is because the lattice of spins severely modifies the quasiparticle density of states, but leaves the charge density of the fluid $n_e(\mu)$, and its dependence on the chemical potential μ unchanged.

- *Local:* Quasiparticles scatter when in the vicinity of a local moment, giving rise to a small momentum dependence to the Landau scattering amplitudes (Yamada, 1975; Yoshida and Yamada, 1975; Engelbrecht and Bedell, 1995).

Landau–Fermi liquid theory relates the properties of a Fermi liquid to the density of states of the quasiparticles and a small number of interaction parameters (Baym and Pethick, 1992). If $E_{\mathbf{k}\sigma}$ is the energy of an isolated quasiparticle, then the quasiparticle density of states $\rho^* = \sum_{\mathbf{k}\sigma} \delta(E_{\mathbf{k}\sigma} - \mu)$ determines the linear specific heat coefficient

$$\gamma = \mathrm{Lim}_{T\to 0}\left(\frac{C_V}{T}\right) = \frac{\pi^2 k_\mathrm{B}^2}{3}\rho^* \tag{7}$$

In conventional metals, the linear specific heat coefficient is of the order 1–10 mJ mol^{-1} K^{-2}. In a system with quadratic dispersion, $E_\mathbf{k} = \frac{\hbar^2 k^2}{2m^*}$, the quasiparticle density of states and effective mass m^* are directly proportional

$$\rho^* = \left(\frac{k_F}{\pi^2\hbar^2}\right) m^* \tag{8}$$

where k_F is the Fermi momentum. In heavy-fermion compounds, the scale of ρ^* varies widely, and specific heat coefficients in the range 100–1600 mJ mol^{-1} K^{-2} have been observed. From this simplified perspective, the quasiparticle effective masses in heavy-electron materials are two or three orders of magnitude 'heavier' than in conventional metals.

In Landau–Fermi liquid theory, a change $\delta n_{\mathbf{k}'\sigma'}$ in the quasiparticle occupancies causes a shift in the quasiparticle energies given by

$$\delta E_{\mathbf{k}\sigma} = \sum_{\mathbf{k}'\sigma'} \mathrm{f}_{\mathbf{k}\sigma,\mathbf{k}\sigma'}\delta n_{\mathbf{k}'\sigma'} \tag{9}$$

In a simplified model with a spherical Fermi surface, the Landau interaction parameters only depend on the relative angle $\theta_{\mathbf{k},\mathbf{k}'}$ between the quasiparticle momenta, and are expanded in terms of Legendre Polynomials as

$$\mathrm{f}_{\mathbf{k}\sigma,\mathbf{k}\sigma'} = \frac{1}{\rho^*}\sum_l (2l+1)P_l(\theta_{\mathbf{k},\mathbf{k}'})[F_l^s + \sigma\sigma' F_l^a] \tag{10}$$

The dimensionless 'Landau parameters' $F_l^{s,a}$ parameterize the detailed quasiparticle interactions. The s-wave ($l = 0$) Landau parameters that determine the magnetic and charge susceptibility of a Landau–Fermi liquid are given by Landau (1957), and Baym and Pethick (1992)

$$\chi_s = \mu_\mathrm{B}^2 \frac{\rho^*}{1+F_0^a} = \mu_\mathrm{B}^2\rho^*\left[1 - A_0^a\right]$$

$$\chi_c = \mathrm{e}^2\frac{\rho^*}{1+F_0^s} = \mathrm{e}^2\rho^*\left[1 - A_0^s\right] \tag{11}$$

where the quantities

$$A_0^{s,a} = \frac{F_0^{s,a}}{1+F_0^{s,a}} \tag{12}$$

are the s-wave Landau scattering amplitudes in the charge (s) and spin (a) channels, respectively (Baym and Pethick, 1992).

The assumption of local scattering and incompressibility in heavy electron fluids simplifies the situation, for, in this case, only the $l = 0$ components of the interaction remain and the quasiparticle scattering amplitudes become

$$A_{\mathbf{k}\sigma,\mathbf{k}'\sigma'} = \frac{1}{\rho^*}\left(A_0^s + \sigma\sigma' A_0^a\right) \tag{13}$$

Moreover, in local scattering, the Pauli principle dictates that quasiparticles scattering at the same point can only scatter when in opposite spin states, so that

$$A_{\uparrow\uparrow}^{(0)} = A_0^s + A_0^a = 0 \tag{14}$$

and hence $A_0^s = -A_0^a$. The additional assumption of incompressibility forces $\chi_c/(e^2\rho^*) \ll 1$, so that now $A_0^s = -A_0^a \approx 1$ and all that remains is a single parameter ρ^*.

This line of reasoning, first developed for the single impurity Kondo model by Nozières and Blandin (1980) and, Nozières (1976) and later extended to a bulk Fermi liquid by Engelbrecht and Bedell (1995), enables us to understand two important scaling trends amongst heavy-electron systems. The first consequence, deduced from equation (11), is that the dimensionless Sommerfeld ratio, or 'Wilson ratio' $W = \left(\frac{\pi^2 k_\mathrm{B}^2}{\mu_\mathrm{B}^2}\right)\frac{\chi_s}{\gamma} \approx 2$. Wilson (1976) found that this ratio is almost exactly equal to 2 in the numerical renormalization group treatment of the impurity Kondo model. The connection between this ratio and the local Fermi liquid theory was first identified by Nozières (1976), and Nozières and Blandin (1980). In real heavy-electron systems, the effect of spin-orbit coupling slightly modifies the precise numerical form for this ratio, nevertheless, the observation that $W \sim 1$ over a wide range of materials in which the density of states vary by more than a factor of 100 is an indication of the incompressible and local character of heavy Fermi liquids (Figure 6).

A second consequence of locality appears in the transport properties. In a Landau–Fermi liquid, inelastic electron–electron scattering produces a quadratic temperature dependence in the resistivity

$$\rho(T) = \rho_0 + AT^2 \tag{15}$$

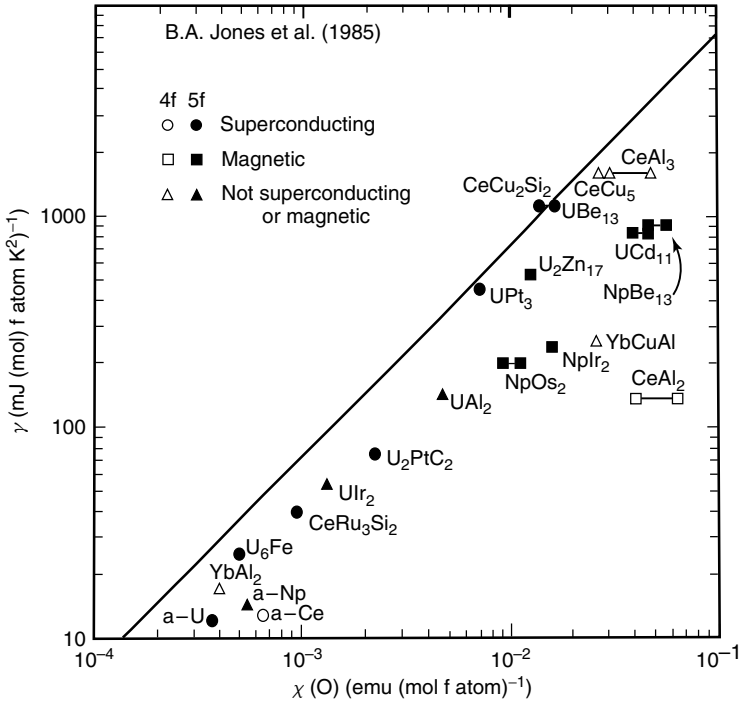

Figure 6. Plot of linear specific heat coefficient versus Pauli susceptibility to show approximate constancy of the Wilson ratio. (Reproduced from P.A. Lee, T.M. Rice, J.W. Serene, L.J. Sham, and J.W. Wilkins, *Comments Condens. Matt. Phys.* 9212, (1986) 99, with permission from Taylaor & Francis Ltd, www.informaworld.com.)

In conventional metals, resistivity is dominated by electron–phonon scattering, and the 'A' coefficient is generally too small for the electron–electron contribution to the resistivity to be observed. In strongly interacting metals, the A coefficient becomes large, and, in a beautiful piece of phenomenology, Kadowaki and Woods (1986), observed that the ratio of A to the square of the specific heat coefficient γ^2

$$\alpha_{\rm KW} = \frac{A}{\gamma^2} \approx (1 \times 10^{-5})\mu\Omega{\rm cm(mol\ K^2 mJ^{-1})} \qquad (16)$$

is approximately constant, over a range of A spanning four orders of magnitude. This can also be simply understood from the local Fermi-liquid theory, where the local scattering amplitudes give rise to an electron mean-free path given by

$$\frac{1}{k_{\rm F} l^*} \sim {\rm constant} + \frac{T^2}{(T^*)^2} \qquad (17)$$

The 'A' coefficient in the electron resistivity that results from the second term satisfies $A \propto \frac{1}{(T^*)^2} \propto \tilde{\gamma}^2$. A more detailed calculation is able to account for the magnitude of the Kadowaki–Woods constant, and its weak residual dependence on the spin degeneracy $N = 2J + 1$ of the magnetic ions (see Figure 7).

The approximate validity of the scaling relations

$$\frac{\chi}{\gamma} \approx {\rm cons}, \qquad \frac{A}{\gamma^2} \approx {\rm cons} \qquad (18)$$

for a wide range of heavy-electron compounds constitutes excellent support for the Fermi-liquid picture of heavy electrons.

A classic signature of heavy-fermion behavior is the dramatic change in transport properties that accompanies the development of a coherent heavy-fermion band structure (Figure 6). At high temperatures, heavy-fermion compounds exhibit a large saturated resistivity, induced by incoherent spin-flip scattering of the conduction electrons of the local f moments. This scattering *grows* as the temperature is lowered, but, at the same time, it becomes increasingly elastic at low temperatures. This leads to the development of phase coherence. the f-electron spins. In the case of heavy-fermion metals, the development of coherence is marked by a rapid reduction in the resistivity, but in a remarkable class of heavy fermion or 'Kondo insulators', the development of coherence leads to a filled band with a tiny insulating gap of the order $T_{\rm K}$. In this case, coherence is marked by a sudden exponential rise in the resistivity and Hall constant.

The classic example of coherence is provided by metallic $CeCu_6$, which develops 'coherence' and a maximum in

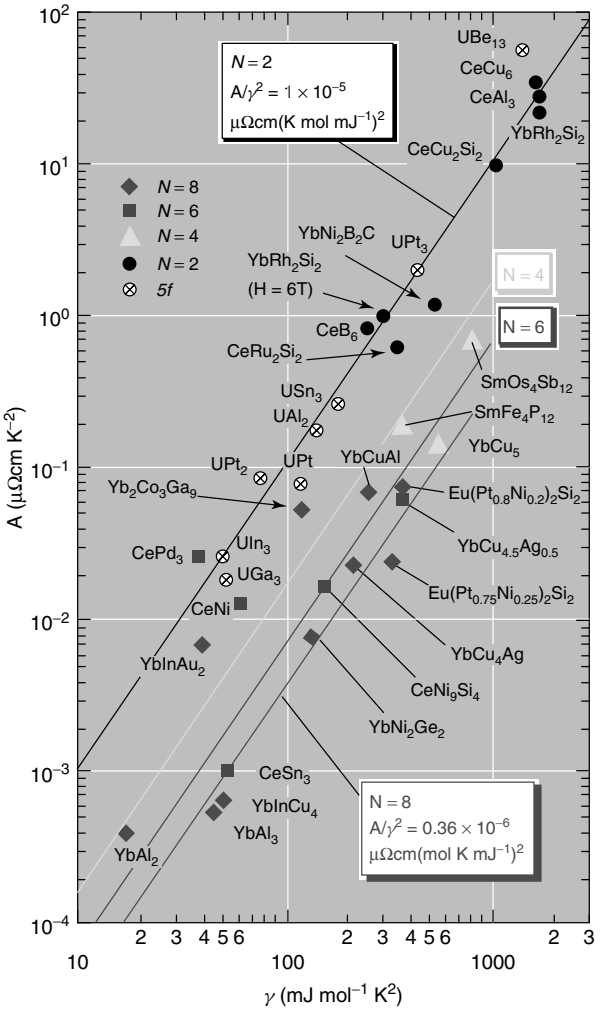

Figure 7. Approximate constancy of the Kadowaki–Woods ratio, for a wide range of heavy electrons. (After Tsujji, Kontani and Yoshimora, 2005.) When spin-orbit effects are taken into account, the Kadowaki–Woods ratio depends on the effective degeneracy $N = 2J + 1$ of the magnetic ion, which when taken into account leads to a far more precise collapse of the data onto a single curve. (Reproduced from H. Tsujji, H. Kontani, and K. Yoshimora, *Phys. Rev. Lett* 94, 2005, copyright © 2005 by the American Physical Sdociety, with permisison of the APS.057201.)

its resistivity around $T = 10\,\mathrm{K}$. Coherent heavy-electron propagation is readily destroyed by substitutional impurities. In $CeCu_6$, Ce^{3+} ions can be continuously substituted with nonmagnetic La^{3+} ions, producing a continuous crossover from coherent Kondo lattice to single impurity behavior (Figure 8).

One of the important principles of the Landau–Fermi liquid is the Fermi surface counting rule, or Luttinger's theorem (Luttinger, 1960). In noninteracting electron band theory, the volume of the Fermi surface counts the number of conduction electrons. For interacting systems, this rule survives (Martin, 1982; Oshikawa, 2000), with the unexpected corollary that

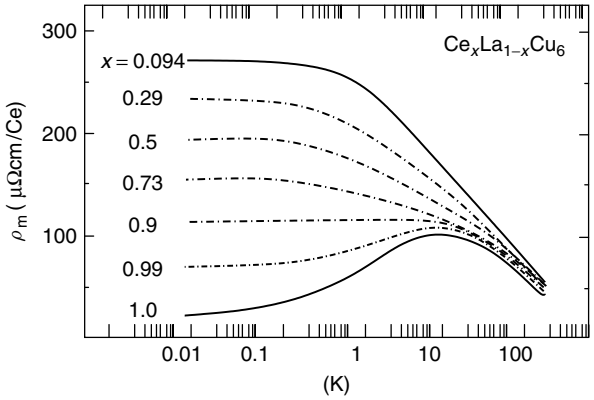

Figure 8. Development of coherence in $Ce_{1-x}La_xCu_6$. (Reproduced from Y. Onuki and T. Komatsubara, *J. Mag. Mat.* 63–64, 1987, 281, copyright © 1987, with permission of Elsevier.)

the spins of the screened local moments are also included in the sum

$$\frac{2V_{\mathrm{FS}}}{(2\pi)^3} = [n_e + n_{\mathrm{spins}}] \tag{19}$$

Remarkably, even though f electrons are localized as magnetic moments at high temperatures, in the heavy Fermi liquid, they contribute to the Fermi surface volume.

The most direct evidence for the large heavy f-Fermi surfaces derives from de Haas van Alphen and Shubnikov de Haas experiments that measure the oscillatory diamagnetism or and resistivity produced by coherent quasiparticle orbits (Figure 9). These experiments provide a direct measure of the heavy-electron mass, the Fermi surface geometry, and volume. Since the pioneering measurements on $CeCu_6$ and UPt_3 by Reinders and Springford, Taillefer, and Lonzarich in the mid-1980s (Reinders *et al*., 1986; Taillefer and Lonzarich, 1988; Taillefer *et al*., 1987), an extensive number of such measurements have been carried out (Onuki and Komatsubara, 1987; Julian, Teunissen and Wiegers, 1992; Kimura *et al*., 1998; McCollam *et al*., 2005). Two key features are observed:

- A Fermi surface volume which counts the f electrons as itinerant quasiparticles.
- Effective masses often in excess of 100 free electron masses. Higher mass quasiparticle orbits, though inferred from thermodynamics, cannot be observed with current measurement techniques.
- Often, but not always, the Fermi surface geometry is in accord with band theory, despite the huge renormalizations of the electron mass.

Additional confirmation of the itinerant nature of the f quasiparticles comes from the observation of a Drude peak in

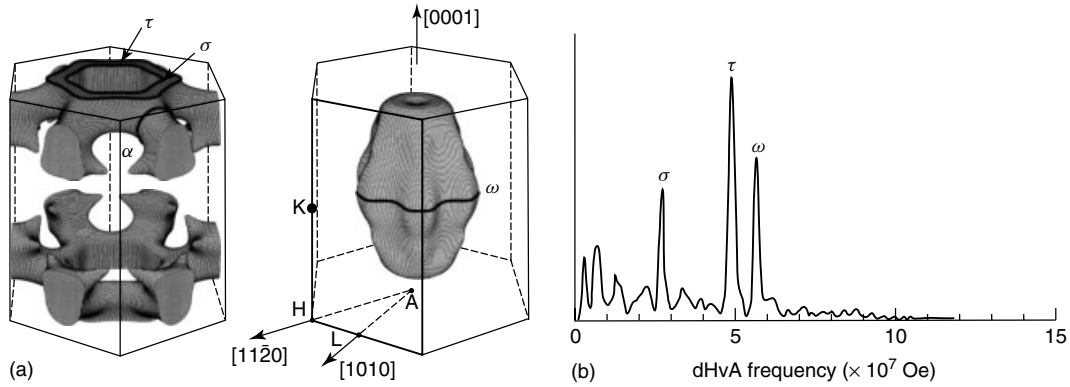

Figure 9. (a) Fermi surface of UPt_3 calculated from band theory assuming itinerant 5f electrons (Oguchi and Freeman, 1985; Wang *et al*., 1987; Norman, Oguchi and Freeman, 1988), showing three orbits (σ, ω and τ) that are identified by dHvA measurements. (After Kimura *et al*., 1998.) (b) Fourier transform of dHvA oscillations identifying σ, ω, and τ orbits shown in (a). (Kimura *et al*., 1998.)

the optical conductivity. At low temperatures, in the coherent regime, an extremely narrow Drude peak can be observed in the optical conductivity of heavy-fermion metals. The weight under the Drude peak is a measure of the plasma frequency: the diamagnetic response of the heavy-fermion metal. This is found to be extremely small, depressed by the large mass enhancement of the quasiparticles (Millis and Lee, 1987a; Degiorgi, 1999).

$$\int_{|\omega| \leq T_K} \frac{d\omega}{\pi} \sigma_{qp}(\omega) = \frac{ne^2}{m^*} \tag{20}$$

Both the optical and dHvA experiments indicate that the presence of f spins depresses both the spin and diamagnetic response of the electron gas down to low temperatures.

2 LOCAL MOMENTS AND THE KONDO LATTICE

2.1 Local moment formation

2.1.1 The Anderson model

We begin with a discussion of how magnetic moments form at high temperatures, and how they are screened again at low temperatures to form a Fermi liquid. The basic model for local moment formation is the Anderson model (Anderson, 1961)

$$H = \overbrace{\sum_{k,\sigma} \epsilon_k n_{k\sigma} + \sum_{k,\sigma} V(k)\left[c^\dagger_{k\sigma} f_\sigma + f^\dagger_\sigma c_{k\sigma}\right]}^{H_{\text{resonance}}} + \underbrace{E_f n_f + U n_{f\uparrow} n_{f\downarrow}}_{H_{\text{atomic}}} \tag{21}$$

where H_{atomic} describes the atomic limit of an isolated magnetic ion and $H_{\text{resonance}}$ describes the hybridization of the localized f electrons in the ion with the Bloch waves of the conduction sea. For pedagogical reasons, our discussion initially focuses on the case where the f state is a Kramer's doublet.

There are two key elements to the Anderson model:

- *Atomic limit:* The atomic physics of an isolated ion with a single f state, described by the model

$$H_{\text{atomic}} = E_f n_f + U n_{f\uparrow} n_{f\downarrow} \tag{22}$$

Here E_f is the energy of the f state and U is the Coulomb energy associated with two electrons in the same orbital. The atomic physics contains the basic mechanism for local moment formation, valid for f electrons, but also seen in a variety of other contexts, such as transition-metal atoms and quantum dots.
The four quantum states of the atomic model are

$$\left.\begin{array}{ll} |f^2\rangle & E(f^2) = 2E_f + U \\ |f^0\rangle & E(f^0) = 0 \end{array}\right\}\text{nonmagnetic}$$
$$|f^1\uparrow\rangle\ |f^1\downarrow\rangle\ \ E(f^1) = E_f \qquad \text{magnetic} \tag{23}$$

In a magnetic ground state, the cost of inducing a 'valence fluctuation' by removing or adding an electron to the f^1 state is positive, that is,

$$\text{removing:} \quad E(f^0) - E(f^1) = -E_f > 0 \Rightarrow \frac{U}{2} > E_f + \frac{U}{2} \tag{24}$$

$$\text{adding:} \quad E(f^2) - E(f^1) = E_f + U > 0 \Rightarrow E_f + \frac{U}{2} > -\frac{U}{2} \tag{25}$$

or (Figure 10).

$$\frac{U}{2} > E_f + \frac{U}{2} > -\frac{U}{2} \tag{26}$$

Under these conditions, a local moment is well defined, provided the temperature is lower than the valence fluctuation scale $T_{\rm VF} = \max(E_{\rm f} + U, -E_{\rm f})$. At lower temperatures, the atom behaves exclusively as a quantum top.

- *Virtual bound-state formation.* When the magnetic ion is immersed in a sea of electrons, the f electrons within the core of the atom hybridize with the Bloch states of surrounding electron sea (Blandin and Friedel, 1958) to form a resonance described by

$$H_{\rm resonance} = \sum_{k,\sigma} \epsilon_k n_{k\sigma} + \sum_{k,\sigma} \left[V(\mathbf{k}) c^\dagger_{k\sigma} f_\sigma + V(\mathbf{k})^* f^\dagger_\sigma c_{k\sigma} \right] \tag{27}$$

where the hybridization matrix element $V(\mathbf{k}) = \langle \mathbf{k} | V_{\rm atomic} | f \rangle$ is the overlap of the atomic potential between a localized f state and a Bloch wave. In the absence of any interactions, the hybridization broadens the localized f state, producing a resonance of width

$$\Delta = \pi \sum_{\mathbf{k}} |V(\mathbf{k})|^2 \delta(\epsilon_{\mathbf{k}} - \mu) = \pi V^2 \rho \tag{28}$$

where V^2 is the average of the hybridization around the Fermi surface.

There are two complementary ways to approach the physics of the Anderson model:

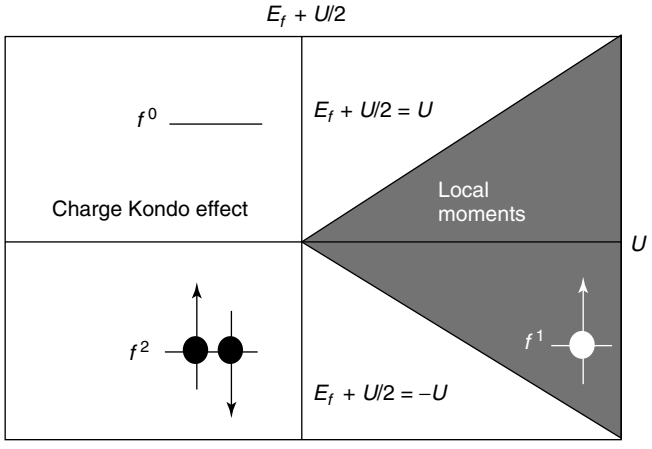

Figure 10. Phase diagram for Anderson impurity model in the atomic limit.

- The 'atomic picture', which starts with the interacting, but isolated atom ($V(k) = 0$), and considers the effect of immersing it in an electron sea by slowly dialing up the hybridization.
- The 'adiabatic picture', which starts with the noninteracting resonant ground state ($U = 0$), and then considers the effect of dialing up the interaction term U.

These approaches paint a contrasting and, at first sight, contradictory picture of a local moment in a Fermi sea. From the adiabatic perspective, the ground state is always a Fermi liquid (see 1.2.2), but from atomic perspective, provided the hybridization is smaller than U, one expects a local magnetic moment, whose low-lying degrees of freedom are purely rotational. How do we resolve this paradox?

Anderson's original work provided a mean-field treatment of the interaction. He found that at interactions larger than $U_c \sim \pi\Delta$ local moments develop with a finite magnetization $M = \langle n_\uparrow \rangle - \langle n_\downarrow \rangle$. The mean-field theory provides an approximate guide to the conditions required for moment formation, but it does not account for the restoration of the singlet symmetry of the ground state at low temperatures. The resolution of the adiabatic and the atomic picture derives from quantum spin fluctuations, which cause the local moment to 'tunnel' on a slow timescale τ_{sf} between the two degenerate 'up' and 'down' configurations.

$$e^-_\downarrow + f^1_\uparrow \rightleftharpoons e^-_\uparrow + f^1_\downarrow \tag{29}$$

These fluctuations are the origin of the Kondo effect. From the energy uncertainty principle, below a temperature $T_{\rm K}$, at which the thermal excitation energy $k_{\rm B}T$ is of the order of the characteristic tunneling rate $\frac{\hbar}{\tau_{sf}}$, a paramagnetic state with a Fermi-liquid resonance forms. The characteristic width of the resonance is then determined by the Kondo energy $k_{\rm B}T_{\rm K} \sim \frac{\hbar}{\tau_{sf}}$. The existence of this resonance was first deduced by Abrikosov (1965), and Suhl (1965), but it is more frequently called the *Kondo resonance*. From perturbative renormalization group reasoning (Haldane, 1978) and the Bethe Ansatz solution of the Anderson model (Wiegmann, 1980; Okiji and Kawakami, 1983), we know that, for large $U \gg \Delta$, the Kondo scale depends exponentially on U. In the symmetric Anderson model, where $E_f = -U/2$,

$$T_K = \sqrt{\frac{2U\Delta}{\pi^2}} \exp\left(-\frac{\pi U}{8\Delta}\right) \tag{30}$$

The temperature $T_{\rm K}$ marks the crossover from a a high-temperature Curie-law $\chi \sim \frac{1}{T}$ susceptibility to a low-temperature paramagnetic susceptibility $\chi \sim 1/T_{\rm K}$.

2.1.2 Adiabaticity and the Kondo resonance

A central quantity in the physics of f-electron systems is the f-spectral function,

$$A_f(\omega) = \frac{1}{\pi}\mathrm{Im}G_f(\omega - i\delta) \tag{31}$$

where $G_f(\omega) = -i\int_{-\infty}^{\infty} \mathrm{d}t\,\langle \mathrm{T} f_\sigma(t) f_\sigma^\dagger(0)\rangle \mathrm{e}^{i\omega t}$ is the Fourier transform of the time-ordered f-Green's function. When an f electron is added, or removed from the f state, the final state has a distribution of energies described by the f-spectral function. From a spectral decomposition of the f-Green's function, the positive energy part of the f-spectral function determines the energy distribution for electron addition, while the negative energy part measures the energy distribution of electron removal:

$$A_f(\omega) = \begin{cases} \overbrace{\sum_\lambda \left|\langle\lambda|f_\sigma^\dagger|\phi_0\rangle\right|^2 \delta(\omega - [E_\lambda - E_0])}^{\text{Energy distribution of state formed by adding one f electron}}, & (\omega > 0) \\ \underbrace{\sum_\lambda \left|\langle\lambda|f_\sigma|\phi_0\rangle\right|^2 \delta(\omega - [E_0 - E_\lambda])}_{\text{Energy distribution of state formed by removing an f electron}}, & (\omega < 0) \end{cases} \tag{32}$$

where E_0 is the energy of the ground state, and E_λ is the energy of an excited state λ, formed by adding or removing an f electron. For negative energies, this spectrum can be measured by measuring the energy distribution of photoelectrons produced by X-ray photoemission, while for positive energies, the spectral function can be measured from inverse X-ray photoemission (Allen *et al.*, 1986; Allen, Oh, Maple and Torikachvili, 1983). The weight beneath the Fermi energy peak determines the f charge of the ion

$$\langle n_f\rangle = 2\int_{-\infty}^{0} \mathrm{d}\omega A_f(\omega) \tag{33}$$

In a magnetic ion, such as a Cerium atom in a $4f^1$ state, this quantity is just a little below unity.

Figure 11 illustrates the effect of the interaction on the f-spectral function. In the noninteracting limit ($U = 0$), the f-spectral function is a Lorentzian of width Δ. If we turn on the interaction U, being careful to shifting the f-level position beneath the Fermi energy to maintain a constant occupancy, the resonance splits into three peaks, two at energies $\omega = E_f$ and $\omega = E_f + U$ corresponding to the energies for a valence fluctuation, plus an additional central 'Kondo resonance' associated with the spin fluctuations of the local moment.

At first sight, once the interaction is much larger than the hybridization width Δ, one might expect there to be no spectral weight left at low energies. But this violates the idea of adiabaticity. In fact, there are always certain adiabatic

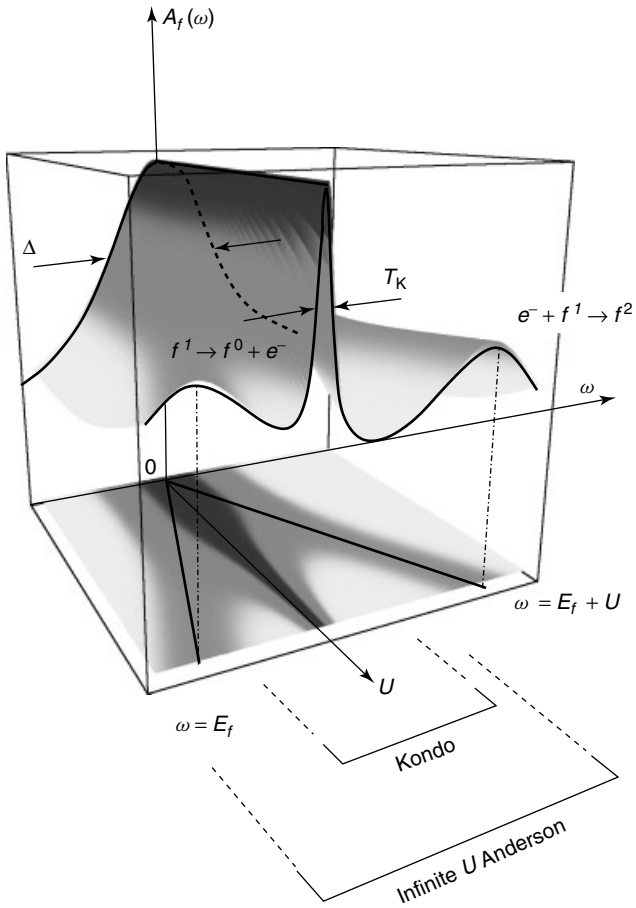

Figure 11. Schematic illustration of the evaluation of the f-spectral function $A_f(\omega)$ as interaction strength U is turned on continuously, maintaining a constant f occupancy by shifting the bare f-level position beneath the Fermi energy. The lower part of diagram is the density plot of f-spectral function, showing how the noninteracting resonance at $U = 0$ splits into an upper and lower atomic peak at $\omega = E_f$ and $\omega = E_f + U$.

invariants that do not change, despite the interaction. One such quantity is the phase shift δ_f associated with the scattering of conduction electrons of the ion; another is the height of the f-spectral function at zero energy, and it turns out that these two quantities are related. A rigorous result owing to (Langreth, 1966) tells us that the spectral function at $\omega = 0$ is directly determined by the f-phase shift, so that its noninteracting value

$$A_f(\omega = 0) = \frac{\sin^2\delta_f}{\pi\Delta} \tag{34}$$

is preserved by adiabaticity. Langreth's result can be heuristically derived by noting that δ_f is the phase of the f-Green's function at the Fermi energy, so that $G_f(0 - i\epsilon)^{-1} = |G_f^{-1}(0)|e^{-i\delta_f}$. Now, in a Fermi liquid, the scattering at the Fermi energy is purely elastic, and this implies

that $ImG_f^{-1}(0 - i\epsilon) = \Delta$, the bare hybridization width. From this, it follows that $ImG_f^{-1}(0) = |G_f^{-1}(0)| \sin\delta_f = \Delta$, so that $G_f(0) = e^{i\delta_f}/(\Delta \sin\delta_f)$, and the preceding result follows.

The phase shift δ_f is set via the Friedel sum rule, according to which the sum of the up-and-down scattering phase shifts, gives the total number of f-bound electrons, or

$$\sum_\sigma \frac{\delta_{f\sigma}}{\pi} = 2\frac{\delta_f}{\pi} = n_f \tag{35}$$

for a twofold degenerate f state. At large distances, the wave function of scattered electrons $\psi_f(r) \sim \sin(k_F r + \delta_f)/r$ is 'shifted inwards' by a distance $\delta_l/k_F = (\lambda_F/2) \times (\delta_l/\pi)$. This sum rule is sometimes called a *node counting* rule because, if you think about a large sphere enclosing the impurity, then each time the phase shift passes through π, a node crosses the spherical boundary and one more electron per channel is bound beneath the Fermi sea. Friedel's sum rule holds for interacting electrons, provided the ground state is adiabatically accessible from the noninteracting system (Langer and Ambegaokar, 1961; Langreth, 1966). Since $n_f = 1$ in an f^1 state, the Friedel sum rule tells us that the phase shift is $\pi/2$ for a twofold degenerate f state. In other words, adiabaticity tell us that the electron is *resonantly scattered* by the quenched local moment.

Photoemission studies do reveal the three-peaked structure characteristic of the Anderson model in many Ce systems, such as $CeIr_2$ and $CeRu_2$ (Allen, Oh, Maple and Torikachvili, 1983) (see Figure 12). Materials in which the Kondo resonance is wide enough to be resolved are more 'mixed valent' materials in which the f valence departs significantly from unity. Three-peaked structures have also been observed in certain U 5f materials such as UPt_3 and UAl_2 (Allen *et al*., 1985) materials, but it has not yet been resolved in UBe_{13}. A three-peaked structure has recently been observed in 4f Yb materials, such as $YbPd_3$, where the $4f^{13}$ configuration contains a single f hole, so that the positions of the three peaks are reversed relative to Ce (Liu *et al*., 1992).

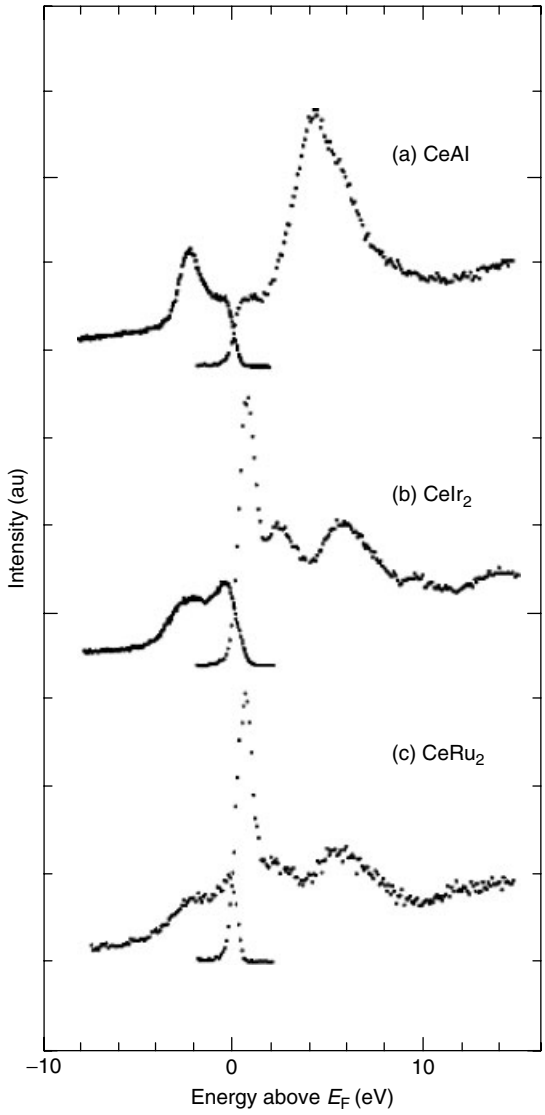

Figure 12. Showing spectral functions for three different Cerium f-electron materials, measured using X-ray photoemission (below the Fermi energy) and inverse X-ray photoemission (above the Fermi energy). CeAl is an AFM and does not display a Kondo resonance. (Reproduced from J.W. Allen, S.J. Oh, M.B. Maple and M.S. Torikachvili: *Phys. Rev.* **28**, 1983, 5347, copyright © 1983 by the American Physical Society, with permission of the APS.)

2.2 Hierarchies of energy scales

2.2.1 Renormalization concept

To understand how a Fermi liquid emerges when a local moment is immersed in a quantum sea of electrons, theorists had to connect physics on several widely spaced energy scales. Photoemission shows that the characteristic energy to produce a valence fluctuation is of the order of volts, or tens of thousands of Kelvin, yet the characteristic physics we are interested in occurs at scales hundreds or thousands of times smaller. How can we distill the essential effects of the atomic physics at electron volt scales on the low-energy physics at millivolt scales?

The essential tool for this task is the 'renormalization group' (Anderson and Yuval, 1969, 1970, 1971; Anderson, 1970, 1973; Wilson, 1976; Nozières and Blandin, 1980; Nozières, 1976), based on the idea that the physics at low-energy scales only depends on a small subset of 'relevant' variables from the original microscopic Hamiltonian. The extraction of these relevant variables is accomplished by

'renormalizing' the Hamiltonian by systematically eliminating the high-energy virtual excitations and adjusting the low-energy Hamiltonian to take care of the interactions that these virtual excitations induce in the low energy Hilbert space. This leads to a family of Hamiltonian's $H(\Lambda)$, each with a different high-energy cutoff Λ, which share the same low-energy physics.

The systematic passage from a Hamiltonian $H(\Lambda)$ to a renormalized Hamiltonian $H(\Lambda')$ with a smaller cutoff $\Lambda' = \Lambda/b$ is accomplished by dividing the eigenstates of H into a a low-energy subspace {L} and a high-energy subspace {H}, with energies $|\epsilon| < \Lambda' = \Lambda/b$ and a $|\epsilon| \in [\Lambda', \Lambda]$ respectively. The Hamiltonian is then broken up into terms that are block-diagonal in these subspaces,

$$H = \left[\begin{array}{c|c} H_{\rm L} & V^\dagger \\ \hline V & H_{\rm H} \end{array}\right] \tag{36}$$

where V and $V^\dagger$ provide the matrix elements between {L} and {H}. The effects of the V are then taken into account by carrying out a unitary (canonical) transformation that block-diagonalizes the Hamiltonian,

$$H(\Lambda) \to UH(\Lambda)U^\dagger = \left[\begin{array}{c|c} \tilde{H}_{\rm L} & 0 \\ \hline 0 & \tilde{H}_{\rm H} \end{array}\right] \tag{37}$$

The renormalized Hamiltonian is then given by $H(\Lambda') = \tilde{H}_{\rm L} = H_{\rm L} + \delta H$. The flow of key parameters in the Hamiltonian resulting from this process is called a *renormalization group flow*.

At certain important crossover energy scales, large tracts of the Hilbert space associated with the Hamiltonian are projected out by the renormalization process, and the character of the Hamiltonian changes qualitatively. In the Anderson model, there are three such important energy scales, (Figure 13)

- $\Lambda_I = E_f + U$, where valence fluctuations $e^- + f^1 \rightleftharpoons f^2$ into the doubly occupied f^2 state are eliminated. For $\Lambda \ll \Lambda_I$, the physics is described by the infinite U Anderson model

$$H = \sum_{k,\sigma} \epsilon_k n_{k\sigma} + \sum_{k,\sigma} V(k)\left[c^\dagger_{k\sigma} X_{0\sigma} + X_{\sigma 0} c_{k\sigma}\right] + E_f \sum_\sigma X_{\sigma\sigma}, \tag{38}$$

  where $X_{\sigma\sigma} = |f^1:\sigma\rangle\langle f^1:\sigma|$, $X_{0\sigma} = |f^0\rangle\langle f^1\sigma|$ and $X_{\sigma 0} = |f^1:\sigma\rangle\langle f^0|$ are 'Hubbard operators' that connect the states in the projected Hilbert space with no double occupancy.
- $\Lambda_{II} \sim |E_f| = -E_f$, where valence fluctuations into the empty state $f^1 \rightleftharpoons f^0 + e^-$ are eliminated to form a local moment. Physics below this scale is described by the Kondo model.
- $\Lambda = T_{\rm K}$, the Kondo temperature below which the local moment is screened to form a resonantly scattering local Fermi liquid.

In the symmetric Anderson model, $\Lambda_I = \Lambda_{II}$, and the transition to local moment behavior occurs in a one-step crossover process.

2.2.2 *Schrieffer–Wolff transformation*

The unitary or canonical transformation that eliminates the charge fluctuations at scales Λ_I and Λ_{II} was first

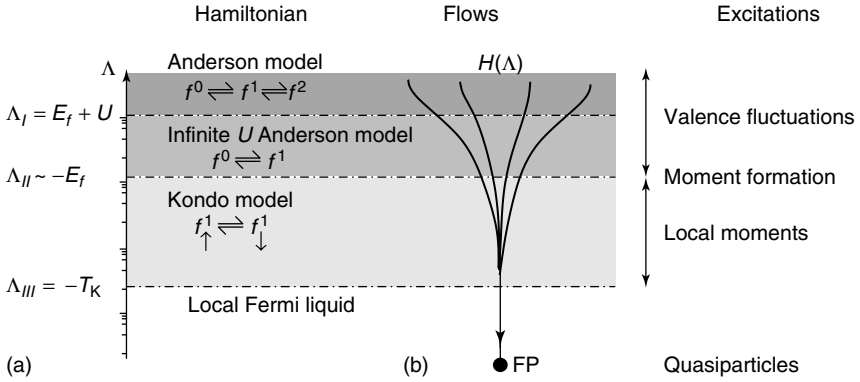

Figure 13. (a) Crossover energy scales for the Anderson model. At scales below Λ_I, valence fluctuations into the doubly occupied state are suppressed. All lower energy physics is described by the infinite U Anderson model. Below Λ_{II}, all valence fluctuations are suppressed, and the physics involves purely the spin degrees of freedom of the ion, coupled to the conduction sea via the Kondo interaction. The Kondo scale renormalizes to strong coupling below Λ_{III}, and the local moment becomes screened to form a local Fermi liquid. (b) Illustrating the idea of renormalization group flows toward a Fermi liquid fixed point.

carried out by Schrieffer and Wolff (1966), and Coqblin and Schrieffer (1969), who showed how this model gives rise to a residual antiferromagnetic interaction between the local moment and conduction electrons. The emergence of this antiferromagnetic interaction is associated with a process called *superexchange*: the virtual process in which an electron or hole briefly migrates off the ion, to be immediately replaced by another with a different spin. When these processes are removed by the canonical transformation, they induce an antiferromagnetic interaction between the local moment and the conduction electrons. This can be seen by considering the two possible spin-exchange processes

$$\begin{aligned} e^-_\uparrow + f^1_\downarrow &\leftrightarrow f^2 \leftrightarrow e^-_\downarrow + f^1_\uparrow \qquad \Delta E_I \sim U + E_f \\ h^+_\uparrow + f^1_\downarrow &\leftrightarrow f^0 \leftrightarrow h^+_\downarrow + f^1_\uparrow \qquad \Delta E_{II} \sim -E_f \end{aligned} \tag{39}$$

Both processes require that the f electron and incoming particle are in a spin-singlet. From second-order perturbation theory, the energy of the singlet is lowered by an amount $-2J$, where

$$J = V^2 \left[\frac{1}{\Delta E_1} + \frac{1}{\Delta E_2} \right] \tag{40}$$

and the factor of two derives from the two ways a singlet can emit an electron or hole into the continuum [1] and $V \sim V(k_{\rm F})$ is the hybridization matrix element near the Fermi surface. For the symmetric Anderson model, where $\Delta E_1 = \Delta E_{II} = U/2$, $J = 4V^2/U$.

If we introduce the electron spin-density operator $\vec{\sigma}(0) = \frac{1}{\mathcal{N}} \sum_{k,k'} c^\dagger_{k\alpha} \vec{\sigma}_{\alpha\beta} c_{k'\beta}$, where $\mathcal{N}$ is the number of sites in the lattice, then the effective interaction has the form

$$H_{\rm K} = -2J P_{S=0} \tag{41}$$

where $P_{S=0} = \left[\frac{1}{4} - \frac{1}{2} \vec{\sigma}(0) \cdot \vec{S}_f \right]$ is the singlet projection operator. If we drop the constant term, then the effective interaction induced by the virtual charge fluctuations must have the form

$$H_{\rm K} = J \vec{\sigma}(0) \cdot \vec{S}_f \tag{42}$$

where $\vec{S}_f$ is the spin of the localized moment. The complete 'Kondo Model', $H = H_c + H_{\rm K}$ describing the conduction electrons and their interaction with the local moment is

$$H = \sum_{\mathbf{k}\sigma} \epsilon_{\mathbf{k}} c^\dagger_{\vec{k}\sigma} c_{\vec{k}\sigma} + J \vec{\sigma}(0) \cdot \vec{S}_f \tag{43}$$

2.2.3 The Kondo effect

The antiferromagnetic sign of the superexchange interaction J in the Kondo Hamiltonian is the origin of the spin-screening physics of the Kondo effect. The bare interaction is weak, but the spin fluctuations it induces have the effect of *antiscreening* the interaction at low energies, renormalizing it to larger and larger values. To see this, we follow an Anderson's 'Poor Man's' scaling procedure (Anderson, 1973, 1970), which takes advantage of the observation that at small J the renormalization in the Hamiltonian associated with the block-diagonalization process $\delta H = \tilde{H}_{\rm L} - H_{\rm L}$ is given by second-order perturbation theory:

$$\delta H_{ab} = \langle a | \delta H | b \rangle = \frac{1}{2} \left[T_{ab}(E_a) + T_{ab}(E_b) \right] \tag{44}$$

where

$$T_{ab}(\omega) = \sum_{|\Lambda\rangle \in \{H\}} \left[\frac{V^\dagger_{a\Lambda} V_{\Lambda b}}{\omega - E_\Lambda} \right] \tag{45}$$

is the many-body 't-matrix' associated with virtual transitions into the high-energy subspace $\{H\}$. For the Kondo model,

$$V = \mathcal{P}_{\rm H} J \vec{S}(0) \cdot \vec{S}_d \mathcal{P}_{\rm L} \tag{46}$$

where $\mathcal{P}_{\rm H}$ projects the intermediate state into the high-energy subspace, while $\mathcal{P}_{\rm L}$ projects the initial state into the low-energy subspace. There are two virtual scattering processes that contribute to the antiscreening effect, involving a high-energy electron (I) or a high-energy hole (II).

Process I is denoted by the diagram

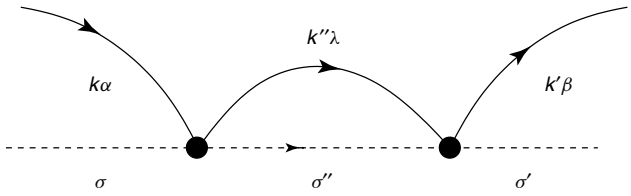

and starts in state $|b\rangle = |k\alpha, \sigma\rangle$, passes through a virtual state $|\Lambda\rangle = |c^\dagger_{k''} \alpha \sigma''\rangle$ where $\epsilon_{k''}$ lies at high energies in the range $\epsilon_{k''} \in [\Lambda/b, \Lambda]$ and ends in state $|a\rangle = |k'\beta, \sigma'\rangle$. The resulting renormalization

$$\begin{aligned} &\langle k'\beta, \sigma' | T^I(E) | k\alpha, \sigma \rangle \\ &\quad = \sum_{\epsilon_{k''} \in [\Lambda - \delta\Lambda, \Lambda]} \left[\frac{1}{E - \epsilon_{k''}} \right] J^2 \times (\sigma^a_{\beta\lambda} \sigma^b_{\lambda\alpha})(S^a_{\sigma'\sigma''} S^b_{\sigma''\sigma}) \\ &\quad \approx J^2 \rho \delta\Lambda \left[\frac{1}{E - \Lambda} \right] (\sigma^a \sigma^b)_{\beta\alpha} (S^a S^b)_{\sigma'\sigma} \end{aligned} \tag{47}$$

In *Process II*, denoted by

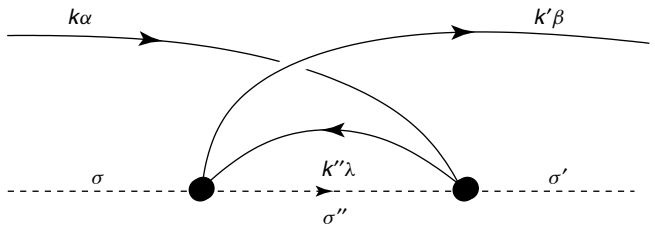

the formation of a virtual hole excitation $|\Lambda\rangle = c_{k''\lambda}|\sigma''\rangle$ introduces an electron line that crosses itself, introducing a negative sign into the scattering amplitude. The spin operators of the conduction sea and AFM reverse their relative order in process II, which introduces a relative minus sign into the T-matrix for scattering into a high-energy hole-state,

$$\begin{aligned}
&\langle k'\beta\sigma'|T^{(II)}(E)|k\alpha\sigma\rangle \\
&\quad = -\sum_{\epsilon_{k''}\in[-\Lambda,-\Lambda+\delta\Lambda]}\left[\frac{1}{E-(\epsilon_k+\epsilon_{k'}-\epsilon_{k''})}\right] \\
&\qquad \times J^2(\sigma^b\sigma^a)_{\beta\alpha}(S^aS^b)_{\sigma'\sigma} \\
&\quad = -J^2\rho\delta\Lambda\left[\frac{1}{E-\Lambda}\right](\sigma^a\sigma^b)_{\beta\alpha}(S^aS^b)_{\sigma'\sigma} \qquad (48)
\end{aligned}$$

where we have assumed that the energies ϵ_k and $\epsilon_{k'}$ are negligible compared with Λ.

Adding equations (47 and 48) gives

$$\begin{aligned}
\delta H^{int}_{k'\beta\sigma';k\alpha\sigma} &= \hat{T}^I + T^{II} = -\frac{J^2\rho\delta\Lambda}{\Lambda}[\sigma^a,\sigma^b]_{\beta\alpha}S^aS^b \\
&= 2\frac{J^2\rho\delta\Lambda}{\Lambda}\vec{\sigma}_{\beta\alpha}\cdot\vec{S}_{\sigma'\sigma} \qquad (49)
\end{aligned}$$

so the high-energy virtual spin fluctuations enhance or 'antiscreen' the Kondo coupling constant

$$J(\Lambda') = J(\Lambda) + 2J^2\rho\frac{\delta\Lambda}{\Lambda} \qquad (50)$$

If we introduce the coupling constant $g = \rho J$, recognizing that $d\ln\Lambda = -\frac{\delta\Lambda}{\Lambda}$, we see that it satisfies

$$\frac{\partial g}{\partial\ln\Lambda} = \beta(g) = -2g^2 + O(g^3) \qquad (51)$$

This is an example of a **negative** β function: a signature of an interaction that grows with the renormalization process. At high energies, the weakly coupled local moment is said to be **asymptotically free**. The solution to the scaling equation is

$$g(\Lambda') = \frac{g_o}{1-2g_o\ln(\Lambda/\Lambda')} \qquad (52)$$

and if we introduce the 'Kondo temperature'

$$T_K = D\exp\left[-\frac{1}{2g_o}\right] \qquad (53)$$

we see that this can be written

$$2g(\Lambda') = \frac{1}{\ln(\Lambda/T_K)} \qquad (54)$$

so that once $\Lambda' \sim T_K$, the coupling constant becomes of the order one – at lower energies, one reaches 'strong coupling' where the Kondo coupling can no longer be treated as a weak perturbation. One of the fascinating things about this flow to strong coupling is that, in the limit $T_K \ll D$, all explicit dependence on the bandwidth D disappears and the Kondo temperature T_K is the only intrinsic energy scale in the physics. Any physical quantity must depend in a universal way on ratios of energy to T_K, thus the universal part of the free energy must have the form

$$F(T) = T_K\Phi\frac{T}{T_K} \qquad (55)$$

where $\Phi(x)$ is universal. We can also understand the resistance created by spin-flip scattering of a magnetic impurity in the same way. The resistivity is given by $\rho_i = \frac{ne^2}{m}\tau(T,H)$, where the scattering rate must also have a scaling form

$$\tau(T,H) = \frac{n_i}{\rho}\Phi_2\left(\frac{T}{T_K},\frac{H}{T_K}\right) \qquad (56)$$

where ρ is the density of states (per spin) of electrons and n_i is the concentration of magnetic impurities and the function $\Phi_2(t,h)$ is universal. To leading order in the Born approximation, the scattering rate is given by $\tau = 2\pi\rho J^2S(S+1) = \frac{2\pi S(S+1)}{\rho}(g_0)^2$ where $g_0 = g(\Lambda_0)$ is the bare coupling at the energy scale that moments form. We can obtain the behavior at a finite temperature by replacing $g_0 \to g(\Lambda = 2\pi T)$, where upon

$$\tau(T) = \frac{2\pi S(S+1)}{\rho}\frac{1}{4\ln^2(2\pi T/T_K)} \qquad (57)$$

gives the leading high-temperature growth of the resistance associated with the Kondo effect.

The kind of perturbative analysis we have gone through here takes us down to the Kondo temperature. The physics at lower energies corresponds to the strong coupling limit of the Kondo model. Qualitatively, once $J\rho \gg 1$, the local moment is bound into a spin-singlet with a conduction electron. The number of bound electrons is $n_f = 1$, so that by the Friedel sum rule (equation (35)) in a paramagnet the phase shift $\delta_\uparrow = \delta_\downarrow = \pi/2$, the unitary limit of scattering. For more

details about the local Fermi liquid that forms, we refer the reader to the accompanying chapter on the Kondo effect by Jones (2007).

2.2.4 *Doniach's Kondo lattice concept*

The discovery of heavy-electron metals prompted Doniach (1977) to make the radical proposal that heavy-electron materials derive from a dense lattice version of the Kondo effect, described by the **Kondo Lattice model** (Kasuya, 1956)

$$H = \sum_{\mathbf{k}\sigma} \epsilon_{\mathbf{k}} c^{\dagger}_{\mathbf{k}\sigma} c_{\mathbf{k}\sigma} + J \sum_j \vec{S}_j \cdot c^{\dagger}_{\mathbf{k}\alpha} \vec{\sigma}_{\alpha\beta} c_{\mathbf{k}'\beta} \mathrm{e}^{i(\mathbf{k}'-\mathbf{k})\cdot\mathbf{R}_j} \tag{58}$$

In effect, Doniach was implicitly proposing that the key physics of heavy-electron materials resides in the interaction of neutral local moments with a charged conduction electron sea.

Most local moment systems develop an antiferromagnetic order at low temperatures. A magnetic moment at location $\mathbf{x}_0$ induces a wave of 'Friedel' oscillations in the electron spin density (Figure 14)

$$\langle \vec{\sigma}(\mathbf{x}) \rangle = -J\chi(\mathbf{x}-\mathbf{x}_0)\langle \vec{S}(\mathbf{x}_0) \rangle \tag{59}$$

where

$$\chi(\mathbf{x}) = 2\sum_{\mathbf{k},\mathbf{k}'} \left(\frac{f(\epsilon_{\mathbf{k}}) - f(\epsilon_{\mathbf{k}'})}{\epsilon_{\mathbf{k}'} - \epsilon_{\mathbf{k}}} \right) e^{i(\mathbf{k}-\mathbf{k}')\cdot\mathbf{x}} \tag{60}$$

is the nonlocal susceptibility of the metal. The sharp discontinuity in the occupancies $f(\epsilon_k)$ at the Fermi surface is responsible for Friedel oscillations in induced spin density that decay with a power law

$$\langle \vec{\sigma}(r) \rangle \sim -J\rho \frac{\cos 2k_{\mathrm{F}} r}{|k_{\mathrm{F}} r|^3} \tag{61}$$

where ρ is the conduction electron density of states and r is the distance from the impurity. If a second local moment is introduced at location $\mathbf{x}$, it couples to this Friedel oscillation with energy $J\langle \vec{S}(\mathbf{x}) \cdot \vec{\sigma}(x) \rangle$, giving rise to the 'RKKY' (Ruderman and Kittel, 1954; Kasuya, 1956; Yosida, 1957) magnetic interaction,

$$H_{\mathrm{RKKY}} = \overbrace{-J^2\chi(\mathbf{x}-\mathbf{x}')}^{J_{\mathrm{RKKY}}(\mathbf{x}-\mathbf{x}')} \vec{S}(\mathbf{x}) \cdot \vec{S}(\mathbf{x}') \tag{62}$$

where

$$J_{\mathrm{RKKY}}(r) \sim -J^2\rho \frac{\cos 2k_{\mathrm{F}} r}{k_{\mathrm{F}} r} \tag{63}$$

In alloys containing a dilute concentration of magnetic transition-metal ions, the oscillatory RKKY interaction gives rise to a frustrated, glassy magnetic state known as a *spin glass*. In dense systems, the RKKY interaction typically gives rise to an ordered antiferromagnetic state with a Néel temperature T_{N} of the order $J^2\rho$. Heavy-electron metals narrowly escape this fate.

Doniach argued that there are two scales in the Kondo lattice, the single-ion Kondo temperature T_{K} and T_{RKKY}, given by

$$\begin{aligned} T_{\mathrm{K}} &= D\mathrm{e}^{-1/(2J\rho)} \\ T_{\mathrm{RKKY}} &= J^2\rho \end{aligned} \tag{64}$$

When $J\rho$ is small, then T_{RKKY} is the largest scale and an antiferromagnetic state is formed, but, when the $J\rho$ is large, the Kondo temperature is the largest scale so a dense Kondo lattice ground state becomes stable. In this paramagnetic state, each site resonantly scatters electrons with a phase shift $\sim\pi/2$. Bloch's theorem then insures that the resonant elastic scattering at each site acts coherently, forming a renormalized band of width $\sim T_{\mathrm{K}}$ (Figure 15).

As in the impurity model, one can identify the Kondo lattice ground state with the large U limit of the Anderson lattice model. By appealing to adiabaticity, one can then link the excitations to the small U Anderson lattice model. According to this line of argument, the quasiparticle Fermi surface volume must count the number of conduction and f electrons (Martin, 1982), even in the large U limit, where it corresponds to the number of electrons *plus* the number of spins

$$2\frac{\mathcal{V}_{\mathrm{FS}}}{(2\pi)^3} = n_e + n_{\mathrm{spins}} \tag{65}$$

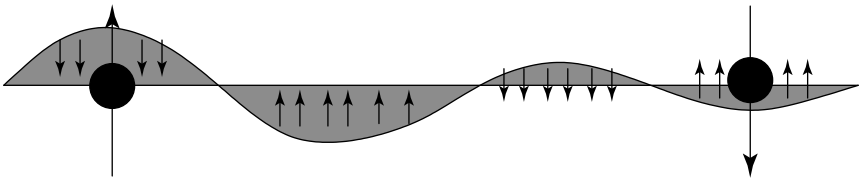

Figure 14. Spin polarization around magnetic impurity contains Friedel oscillations and induces an RKKY interaction between the spins.

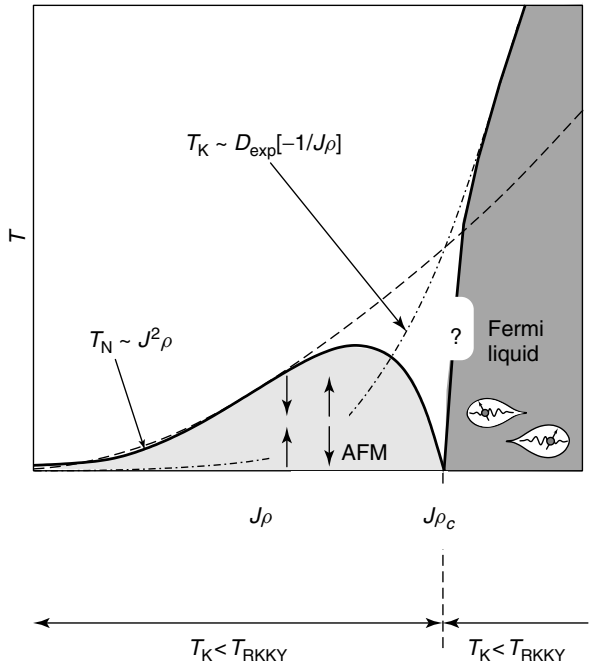

Figure 15. Doniach diagram, illustrating the antiferromagnetic regime, where $T_K < T_{RKKY}$ and the heavy-fermion regime, where $T_K > T_{RKKY}$. Experiment has told us in recent times that the transition between these two regimes is a quantum critical point. The effective Fermi temperature of the heavy Fermi liquid is indicated as a solid line. Circumstantial experimental evidence suggests that this scale drops to zero at the antiferromagnetic quantum critical point, but this is still a matter of controversy.

Using topology, and certain basic assumptions about the response of a Fermi liquid to a flux, Oshikawa (2000) was able to short circuit this tortuous path of reasoning, proving that the Luttinger relationship holds for the Kondo lattice model without reference to its finite U origins.

There are, however, aspects to the Doniach argument that leave cause for concern:

- It is purely a comparison of energy scales and does not provide a detailed mechanism connecting the heavy-fermion phase to the local moment AFM.
- Simple estimates of the value of $J\rho$ required for heavy-electron behavior give an artificially large value of the coupling constant $J\rho \sim 1$. This issue was later resolved by the observation that large spin degeneracy $2j+1$ of the spin-orbit coupled moments, which can be as large as $N = 8$ in Yb materials, enhances the rate of scaling to strong coupling, leading to a Kondo temperature (Coleman, 1983)

$$T_K = D(NJ\rho)^{\frac{1}{N}} \exp\left[-\frac{1}{NJ\rho}\right] \qquad (66)$$

Since the scaling enhancement effect stretches out across decades of energy, it is largely robust against crystal fields (Mekata *et al.*, 1986).

- Nozières' exhaustion paradox (Nozières, 1985). If one considers each local moment to be magnetically screened by a cloud of low-energy electrons within an energy T_K of the Fermi energy, one arrives at an 'exhaustion paradox'. In this interpretation, the number of electrons available to screen each local moment is of the order $T_K/D \ll 1$ per unit cell. Once the concentration of magnetic impurities exceeds $\frac{T_K}{D} \sim 0.1\%$ for ($T_K = 10\,\mathrm{K}$, $D = 10^4\,\mathrm{K}$), the supply of screening electrons would be exhausted, logically excluding any sort of dense Kondo effect. Experimentally, features of single-ion Kondo behavior persist to much higher densities. The resolution to the exhaustion paradox lies in the more modern perception that spin screening of local moments extends *up* in energy, from the Kondo scale T_K out to the bandwidth. In this respect, Kondo screening is reminiscent of Cooper pair formation, which involves electron states that extend upward from the gap energy to the Debye cutoff. From this perspective, the Kondo length scale $\xi \sim v_F/T_K$ is analogous to the coherence length of a superconductor (Burdin, Georges and Grempel, 2000), defining the length scale over which the conduction spin and local moment magnetization are coherent without setting any limit on the degree to which the correlation clouds can overlap (Figure 16).

2.3 The large N Kondo lattice

2.3.1 Gauge theories, large N, and strong correlation

The 'standard model' for metals is built upon the expansion to high orders in the strength of the interaction. This approach, pioneered by Landau, and later formulated in the language of finite temperature perturbation theory by Landau (1957), Pitaevskii (1960), Luttinger and Ward (1960), and Nozières and Luttinger (1962), provides the foundation for our understanding of metallic behavior in most conventional metals.

The development of a parallel formalism and approach for strongly correlated electron systems is still in its infancy, and there is no universally accepted approach. At the heart of the problem are the large interactions, which effectively remove large tracts of Hilbert space and impose strong constraints on the low-energy electronic dynamics. One way to describe these highly constrained Hilbert spaces is through the use of gauge theories. When written as a field theory, local constraints manifest themselves as locally conserved quantities. General principles link these conserved quantities

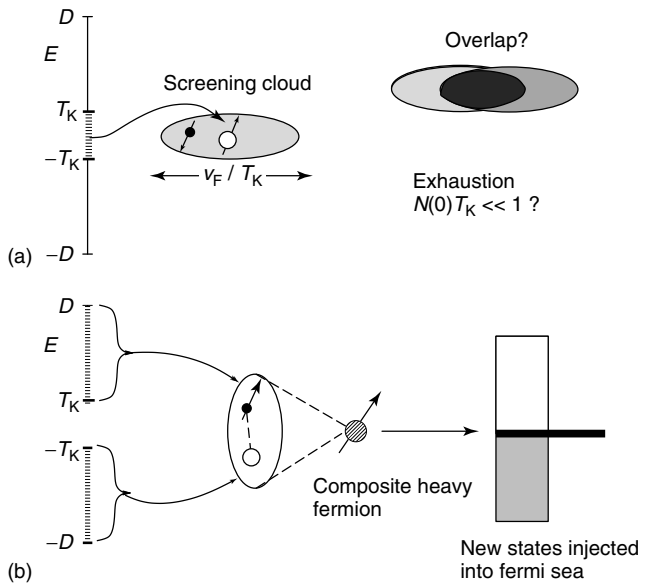

Figure 16. Contrasting (a) the 'screening cloud' picture of the Kondo effect with (b) the composite fermion picture. In (a), low-energy electrons form the Kondo singlet, leading to the exhaustion problem. In (b), the composite heavy electron is a highly localized bound-state between local moments and high-energy electrons, which injects new electronic states into the conduction sea at the chemical potential. Hybridization of these states with conduction electrons produces a singlet ground state, forming a Kondo resonance in the single impurity, and a coherent heavy electron band in the Kondo lattice.

with a set of gauge symmetries. For example, in the Kondo lattice, if a spin $S = 1/2$ operator is represented by fermions,

$$\vec{S}_j = f^\dagger_{j\alpha} \left(\frac{\vec{\sigma}}{2}\right)_{\alpha\beta} f_{j\beta} \tag{67}$$

then the representation must be supplemented by the constraint $n_f(j) = 1$ on the conserved f number at each site. This constraint means one can change the phase of each f fermion at each site arbitrarily

$$f_j \to \mathrm{e}^{i\phi_j} f_j \tag{68}$$

without changing the spin operator $\vec{S}_j$ or the Hamiltonian. This is the local gauge symmetry.

Similar issues also arise in the infinite U Anderson or Hubbard models where the 'no double occupancy' constraint can be established by using a slave boson representation (Barnes, 1976; Coleman, 1984) of Hubbard operators:

$$X_{\sigma 0}(j) = f^\dagger_{j\sigma} b_j, \qquad X_{0\sigma}(j) = b^\dagger_j f_{j\sigma} \tag{69}$$

where $f^\dagger_{j\sigma}$ creates a singly occupied f state, $f^\dagger_{j\sigma}|0\rangle \equiv |f^1, j\sigma\rangle$, while $b^\dagger$ creates an empty f^0 state, $b^\dagger_j|0\rangle = |f^0, j\rangle$. In the slave boson, the gauge charges

$$Q_j = \sum_\sigma f^\dagger_{j\sigma} f_{j\sigma} + b^\dagger_j b_j \tag{70}$$

are conserved and the physical Hilbert space corresponds to $Q_j = 1$ at each site. The gauge symmetry is now $f_{j\sigma} \to e^{i\theta_j} f_{j\sigma}$, $b_j \to e^{i\theta_j} b_j$. These two examples illustrate the link between strong correlation and gauge theories.

$$\begin{aligned} \text{Strong correlation} &\leftrightarrow \text{Constrained Hilbert space} \\ &\leftrightarrow \text{Gauge theories} \end{aligned} \tag{71}$$

A key feature of these gauge theories is the appearance of 'fractionalized fields', which carry either spin or charge, but not both. How, then, can a Landau–Fermi liquid emerge within a Gauge theory with fractional excitations?

Some have suggested that Fermi liquids cannot reconstitute themselves in such strongly constrained gauge theories. Others have advocated against gauge theories, arguing that the only reliable way forward is to return to 'real-world' models with a full fermionic Hilbert space and a finite interaction strength. A third possibility is that the gauge theory approach is valid, but that heavy quasiparticles emerge as bound-states of gauge particles. Quite independently of one's position on the importance of gauge theory approaches, the Kondo lattice poses a severe computational challenge, in no small part, because of the absence of any small parameter for resumed perturbation theory. Perturbation theory in the Kondo coupling constant J always fails below the Kondo temperature. How, then, can one develop a controlled computational tool to explore the transition from local moment magnetism to the heavy Fermi liquid?

One route forward is to seek a family of models that interpolates between the models of physical interest, and a limit where the physics can be solved exactly. One approach, as we shall discuss later, is to consider Kondo lattices in variable dimensions d, and expand in powers of $1/d$ about the limit of infinite dimensionality (Georges, Kotliar, Krauth and Rozenberg, 1996; Jarrell, 1995). In this limit, electron self-energies become momentum independent, the basis of the DMFT. Another approach, with the advantage that it can be married with gauge theory, is the use of large N expansions. The idea here is to generalize the problem to a family of models in which the f-spin degeneracy $N = 2j + 1$ is artificially driven to infinity. In this extreme limit, the key physics is captured as a mean-field theory, and finite N properties are obtained through an expansion in the small parameter $1/N$. Such large N expansions have played an important role in the context of the spherical model of statistical mechanics (Berlin and Kac, 1952) and in field theory (Witten, 1978). The next section discusses how the

gauge theory of the Kondo lattice model can be treated in a large N expansion.

2.3.2 *Mean-field theory of the Kondo lattice*

Quantum large N expansions are a kind of semiclassical limit, where $1/N \sim \hbar$ plays the role of a synthetic Planck's constant. In a Feynman path integral

$$\langle x_f(t)|x_i, 0\rangle = \int \mathcal{D}[x] \exp\left[\frac{i}{\hbar} S[x, \dot{x}]\right] \tag{72}$$

where S is the classical action and the quantum action $A = \frac{1}{\hbar}S$ is 'extensive' in the variable $\frac{1}{\hbar}$. When $\frac{1}{\hbar} \to \infty$, fluctuations around the classical trajectory vanish and the transition amplitude is entirely determined by the classical action to go from i to f. A large N expansion for the partition function Z of a quantum system involves a path integral in imaginary time over the fields ϕ

$$Z = \int \mathcal{D}[\phi] \mathrm{e}^{-NS[\phi,\dot{\phi}]} \tag{73}$$

where NS is the action (or free energy) associated with the field configuration in space and time. By comparison, we see that the large N limit of quantum systems corresponds to an alternative classical mechanics, where $1/N \sim \hbar$ emulates Planck's constant and new types of collective behavior not pertinent to strongly interacting electron systems start to appear.

Our model for a Kondo lattice of spins localized at sites j is

$$H = \sum_{\mathbf{k}\sigma} \epsilon_{\mathbf{k}} c^\dagger_{\mathbf{k}\sigma} c_{\mathbf{k}\sigma} + \sum_j H_I(j) \tag{74}$$

where

$$H_I(j) = \frac{J}{N} S_{\alpha\beta}(j) c^\dagger_{j\beta} c_{j\alpha} \tag{75}$$

is the Coqblin Schrieffer form of the Kondo interaction Hamiltonian (Coqblin and Schrieffer, 1969) between an f spin with $N = 2j + 1$ spin components and the conduction sea. The spin of the local moment at site j is represented as a bilinear of Abrikosov pseudofermions

$$S_{\alpha\beta}(j) = f^\dagger_{j\alpha} f_{j\beta} - \frac{n_f}{N}\delta_{\alpha\beta} \tag{76}$$

and

$$c^\dagger_{j\sigma} = \frac{1}{\sqrt{\mathcal{N}}} \sum_{\mathbf{k}} c^\dagger_{\mathbf{k}\sigma} \mathrm{e}^{-i\mathbf{k}\cdot\vec{R}_j} \tag{77}$$

creates an electron localized at site j, where $\mathcal{N}$ is the number of sites.

Although this is a theorists' idealization – a 'spherical cow approximation', it nevertheless captures key aspects of the physics. This model ascribes a spin degeneracy of $N = 2j + 1$ to both the f electrons *and* the conduction electrons. While this is justified for a single impurity, a more realistic lattice model requires the introduction of Clebsch–Gordon coefficients to link the spin-1/2 conduction electrons with the spin-j conduction electrons.

To obtain a mean-field theory, each term in the Hamiltonian must scale as N. Since the interaction contains two sums over the spin variables, this criterion is met by rescaling the coupling constant replacing $J \to \frac{\tilde{J}}{N}$. Another important aspect to this model is the constraint on charge fluctuations, which in the Kondo limit imposes the constraint $n_f = 1$. Such a constraint can be imposed in a path integral with a Lagrange multiplier term $\lambda(n_f - 1)$. However, with $n_f = 1$, this is not extensive in N, and cannot be treated using a mean-field value for λ. The resolution is to generalize the constraint to $n_f = Q$, where Q is an integer chosen so that as N grows, $q = Q/N$ remains fixed. Thus, for instance, if we are interested in $N = 2$, this corresponds to $q = n_f/N = \frac{1}{2}$. In the large N limit, it is then sufficient to apply the constraint on the average $\langle n_f\rangle = Q$ through a static Lagrange multiplier coupled to the difference $(n_f - Q)$.

The next step is to carry out a 'Hubbard–Stratonovich' transformation on the interaction

$$H_I(j) = -\frac{J}{N}\left(c^\dagger_{j\beta} f_{j\beta}\right)\left(f^\dagger_{j\alpha} c_{j\alpha}\right) \tag{78}$$

Here, we have absorbed the term $-\frac{J}{N} n_f c^\dagger_{j\alpha} c_{j\alpha}$ derived from the spin-diagonal part of (equation (76)) by a shift $\mu \to \mu - \frac{Jn_f}{N^2}$ in the chemical potential. This interaction has the form $-gA^\dagger A$, with $g = \frac{J}{N}$ and $A = f^\dagger_{j\alpha} c_{j\alpha}$, which we factorize using a Hubbard–Stratonovich transformation,

$$-gA^\dagger A \to A^\dagger V + \overline{V} A + \frac{\overline{V} V}{g} \tag{79}$$

so that (Lacroix and Cyrot, 1979; Read and Newns, 1983a)

$$H_I(j) \to H_I[V, j] = \overline{V}_j \left(c^\dagger_{j\sigma} f_{j\sigma}\right) + \left(f^\dagger_{j\sigma} c_{j\sigma}\right) V_j + N\frac{\overline{V}_j V_j}{J} \tag{80}$$

This is an exact transformation, provided the $V_j(\tau)$ are treated as fluctuating variables inside a path integral. The V_j can be regarded as a spinless exchange boson for the Kondo effect. In the parallel treatment of the infinite Anderson model (Coleman, 1987a), $V_j = Vb_j$ is the 'slave boson' field associated with valence fluctuations.

In diagrams:

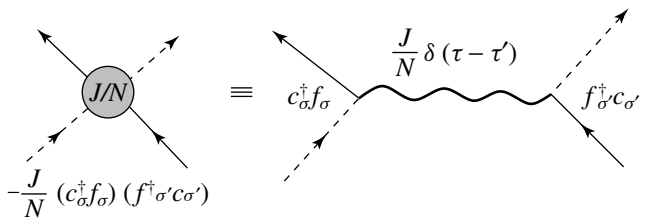

(81)

The path integral for the Kondo lattice is then

$$Z = \int \mathcal{D}[V,\lambda] \overbrace{\int \mathcal{D}[c,f] \exp\left[-\int_0^\beta \left(\sum_{k\sigma} c^\dagger_{\mathbf{k}\sigma}\partial_\tau c_{\mathbf{k}\sigma} + \sum_{j\sigma} f^\dagger_{j\sigma}\partial_\tau f_{j\sigma} + H[V,\lambda]\right)\right]}^{=\mathrm{Tr}\left[T exp\left(-\int_0^\beta H[V,\lambda]d\tau\right)\right]} \tag{82}$$

where

$$H[V,\lambda] = \sum_{\mathbf{k}\sigma} \epsilon_{\mathbf{k}} c^\dagger_{\mathbf{k}\sigma} c_{\mathbf{k}\sigma} + \sum_j \left(H_I[V_j, j] + \lambda_j[n_f(j) - Q]\right) \tag{83}$$

This is the 'Read–Newns' path integral formulation (Read and Newns, 1983a; Auerbach and Levin, 1986) of the Kondo lattice model. The path integral contains an outer integral $\int \mathcal{D}[V,\lambda]$ over the gauge fields V_j and $\lambda_j(\tau)$, and an inner integral $\int \mathcal{D}[c,f]$ over the fermion fields moving in the environment of the gauge fields. The inner path integral is equal to a trace over the time-ordered exponential of $H[V,\lambda]$.

Since the action in this path integral grows extensively with N, the large N limit is saturated by the saddle point configurations of V and λ, eliminating the the outer integral in equation (83). We seek a translationally invariant, static, saddle point, where $\lambda_j(\tau) = \lambda$ and $V_j(\tau) = V$. Since the Hamiltonian is static, the interior path integral can be written as the trace over the Hamiltonian evaluated at the saddle point,

$$Z = \mathrm{Tr} e^{-\beta H_{\mathrm{MFT}}} \qquad (N \to \infty) \tag{84}$$

where

$$H_{\mathrm{MFT}} = H[V,\lambda] = \sum_{\mathbf{k}\sigma} \epsilon_{\mathbf{k}} c^\dagger_{\mathbf{k}\sigma} c_{\mathbf{k}\sigma} + \sum_{j,\sigma}\left(\overline{V} c^\dagger_{j\sigma} f_{j\sigma} + V f^\dagger_{j\sigma} c_{j\sigma} + \lambda f^\dagger_{j\sigma} f_{j\sigma}\right) + Nn\left(\frac{\overline{V}V}{J} - \lambda_o q\right) \tag{85}$$

The saddle point is determined by the condition that the Free energy $F = -T\ln Z$ is stationary with respect to variations in V and λ. To impose this condition, we need to diagonalize H_{MFT} and compute the Free energy. First we rewrite the mean-field Hamiltonian in momentum space,

$$H_{\mathrm{MFT}} = \sum_{\mathbf{k}\sigma} \left(c^\dagger_{\mathbf{k}\sigma}, f^\dagger_{\mathbf{k}\sigma}\right) \begin{bmatrix} \epsilon_{\mathbf{k}} & \overline{V} \\ V & \lambda \end{bmatrix} \begin{pmatrix} c_{\mathbf{k}\sigma} \\ f_{\mathbf{k}\sigma} \end{pmatrix} + Nn\left(\frac{\overline{V}V}{J} - \lambda q\right) \tag{86}$$

where

$$f^\dagger_{\vec{k}\sigma} = \frac{1}{\sqrt{\mathcal{N}}} \sum_j f^\dagger_{j\sigma} e^{i\vec{k}\cdot\vec{R}_j} \tag{87}$$

is the Fourier transform of the f-electron field. This Hamiltonian can then be diagonalized in the form

$$H_{\mathrm{MFT}} = \sum_{\mathbf{k}\sigma} \left(a^\dagger_{\mathbf{k}\sigma}, b^\dagger_{\mathbf{k}\sigma}\right) \begin{bmatrix} E_{\mathbf{k}+} & 0 \\ 0 & E_{\mathbf{k}-} \end{bmatrix} \begin{pmatrix} a_{\mathbf{k}\sigma} \\ b_{\mathbf{k}\sigma} \end{pmatrix} + N\mathcal{N}_s\left(\frac{|V|^2}{J} - \lambda q\right) \tag{88}$$

where $a^\dagger_{\mathbf{k}\sigma}$ and $b^\dagger_{\mathbf{k}\sigma}$ are linear combinations of $c^\dagger_{\mathbf{k}\sigma}$ and $f^\dagger_{\vec{k}\sigma}$, which describe the quasiparticles of the theory. The momentum state eigenvalues $E = E_{\vec{k}\pm}$ are the roots of the equation

$$\mathrm{Det}\left[E\underline{1} - \begin{pmatrix} \epsilon_{\mathbf{k}} & \overline{V} \\ V & \lambda \end{pmatrix}\right] = (E-\epsilon_{\mathbf{k}})(E-\lambda) - |V|^2 = 0 \tag{89}$$

so

$$E_{\mathbf{k}\pm} = \frac{\epsilon_{\mathbf{k}} + \lambda}{2} \pm \left[\left(\frac{\epsilon_{\mathbf{k}} - \lambda}{2}\right)^2 + |V|^2\right]^{\frac{1}{2}} \tag{90}$$

are the energies of the upper and lower bands. The dispersion described by these energies is shown in Figure 17. Notice that:

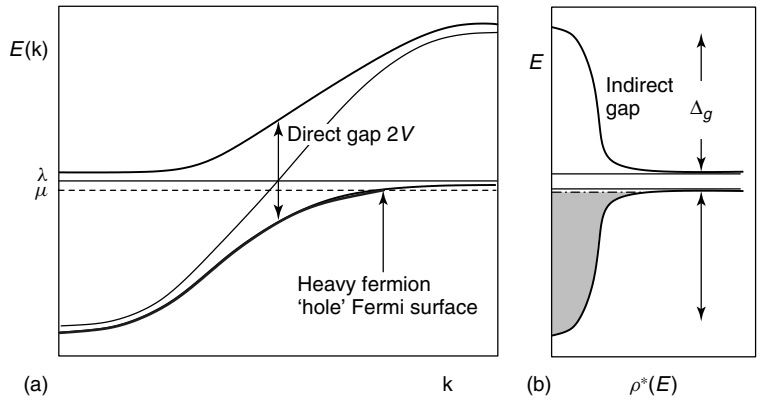

Figure 17. (a) Dispersion produced by the injection of a composite fermion into the conduction sea. (b) Renormalized density of states, showing 'hybridization gap' (Δ_g).

- hybridization between the f-electron states and the conduction electrons builds an upper and lower Fermi band, separated by an indirect 'hybridization gap' of width $\Delta_g = E_g(+) - E_g(-) \sim T_{\rm K}$, where

$$E_g(\pm) = \lambda \pm \frac{V^2}{D_\mp} \tag{91}$$

  and $\pm D_\pm$ are the top and bottom of the conduction band. The 'direct' gap between the upper and lower bands is $2|V|$.
- From (89), the relationship between the energy of the heavy electrons (E) and the energy of the conduction electrons (ϵ) is given by $\epsilon = E - |V|^2/(E-\lambda)$, so that the density of heavy-electron states $\rho^*(E) = \sum_{\mathbf{k},\pm}\delta(E - E^{(\pm)}_{\mathbf{k}})$ is related to the conduction electron density of states $\rho(\epsilon)$ by

$$\rho^*(E) = \rho\frac{{\rm d}\epsilon}{{\rm d}E} = \rho(\epsilon)\left(1 + \frac{|V|^2}{(E-\lambda)^2}\right) \sim \begin{cases} \rho\left(1+\frac{|V|^2}{(E-\lambda)^2}\right) & \text{outside hybridization gap,} \\ 0 & \text{inside hybridization gap,} \end{cases} \tag{92}$$

  so the 'hybridization gap' is flanked by two sharp peaks of approximate width $T_{\rm K}$.
- The Fermi surface volume **expands** in response to the injection of heavy electrons into the conduction sea,

$$Na^D\frac{V_{\rm FS}}{(2\pi)^3} = \left\langle \frac{1}{\mathcal{N}_s}\sum_{\mathbf{k}\sigma} n_{\mathbf{k}\sigma}\right\rangle = Q + n_c \tag{93}$$

  where a^D is the unit cell volume, $n_{\mathbf{k}\sigma} = a^\dagger_{\mathbf{k}\sigma}a_{\mathbf{k}\sigma} + b^\dagger_{\mathbf{k}\sigma}b_{\mathbf{k}\sigma}$ is the quasiparticle number operator and n_c is the number of conduction electrons per unit cell. More instructively, if $n_e = n_c/a^D$ is the electron density,

$$\overbrace{n_e}^{e^-\text{ density}} = \overbrace{N\frac{V_{\rm FS}}{(2\pi)^3}}^{\text{quasi particle density}} - \underbrace{\frac{Q}{a^D}}_{\text{positive background}} \tag{94}$$

  so the electron density n_c divides into a contribution carried by the enlarged Fermi sea, whose enlargement is compensated by the development of a positively charged background. Loosely speaking, each neutral spin in the Kondo lattice has 'ionized' to produce Q negatively charged heavy fermions, leaving behind a Kondo singlet of charge $+Qe$ (Figure 18).

To obtain V and λ, we must compute the free energy

$$\frac{F}{N} = -T\sum_{\mathbf{k},\pm}\ln\left[1 + {\rm e}^{-\beta E_{\mathbf{k}\pm}}\right] + \mathcal{N}_s\left(\frac{|V|^2}{J} - \lambda q\right) \tag{95}$$

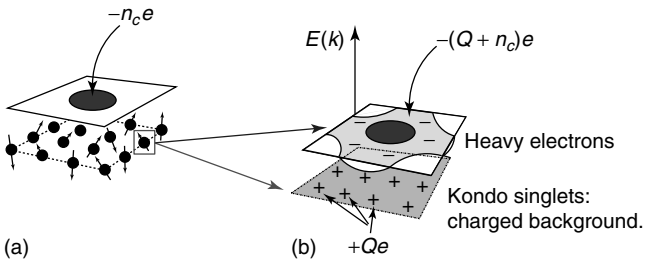

Figure 18. Schematic diagram from Coleman, Paul and Rech (2005a). (a) High-temperature state: small Fermi surface with a background of spins; (b) Low-temperature state, where large Fermi surface develops against a background of positive charge. Each spin 'ionizes' into Q heavy electrons, leaving behind a a Kondo singlet with charge $+Qe$. (Reproduced from P. Coleman, I. Paul, and J. Rech, *Phys. Rev. B* **72**, 2005, 094430, copyright © 2005 by the American Physical Society, with permission of the APS.)

At $T = 0$, the free energy converges the ground-state energy E_0, given by

$$\frac{E_0}{N\mathcal{N}_s} = \int_{-\infty}^{0} \rho^*(E)E + \left(\frac{|V|^2}{J} - \lambda q\right) \tag{96}$$

Using equation (92), the total energy is

$$\begin{aligned}\frac{E_o}{N\mathcal{N}_s} &= \int_{-D}^{0} \mathrm{d}\epsilon \rho E \mathrm{d}E + \int_{-D}^{0} \mathrm{d}E \rho |V|^2 \frac{E}{(E-\lambda)^2} \\ &\quad + \left(\frac{|V|^2}{J} - \lambda q\right) \\ &= \overbrace{-\frac{D^2\rho}{2}}^{E_c/(N\mathcal{N}_s)} + \overbrace{\frac{\Delta}{\pi}\ln\left(\frac{\lambda e}{T_{\mathrm{K}}}\right) - \lambda q}^{E_{\mathrm{K}}/(N\mathcal{N}_s)}\end{aligned} \tag{97}$$

where we have assumed that the upper band is empty and the lower band is partially filled. $T_{\mathrm{K}} = De^{-\frac{1}{J\rho}}$ as before. The first term in (97) is the conduction electron contribution to the energy E_c/Nn_s, while the second term is the lattice 'Kondo' energy $E_{\mathrm{K}}/N_{\mathcal{N}_s}$. If now we impose the constraint $\frac{\partial E_o}{\partial \lambda} = \langle n_f \rangle - Q = 0$ then $\lambda = \frac{\Delta}{\pi q}$ so that the ground-state energy can be written

$$\frac{E_{\mathrm{K}}}{N\mathcal{N}_s} = \frac{\Delta}{\pi}\ln\left(\frac{\Delta e}{\pi q T_{\mathrm{K}}}\right) \tag{98}$$

This energy functional has a 'Mexican Hat' form, with a minimum at

$$\Delta = \frac{\pi q}{e^2} T_{\mathrm{K}} \tag{99}$$

confirming that $\Delta \sim T_{\mathrm{K}}$. If we now return to the quasiparticle density of states ρ^*, we find it has the value

$$\rho^*(0) = \rho + \frac{q}{T_{\mathrm{K}}} \tag{100}$$

at the Fermi energy so the mass enhancement of the heavy electrons is then

$$\frac{m^*}{m} = 1 + \frac{q}{\rho T_{\mathrm{K}}} \sim \frac{qD}{T_{\mathrm{K}}} \tag{101}$$

2.3.3 The charge of the f electron

How does the f electron acquire its charge? We have emphasized from the beginning that the charge degrees of freedom of the original f electrons are irrelevant, indeed, absent from the physics of the Kondo lattice. So how are charged f electrons constructed out of the states of the Kondo lattice, and how do they end up coupling to the electromagnetic field?

The large N theory provides an intriguing answer. The passage from the original Hamiltonian equation (75) to the mean-field Hamiltonian equation (85) is equivalent to the substitution

$$\frac{J}{N} S_{\alpha\beta}(j) c^\dagger_{j\beta} c_{j\alpha} \longrightarrow \overline{V} f^\dagger_{j\alpha} c_{j\alpha} + V c^\dagger_{j\alpha} \mathrm{f}_{j\alpha} \tag{102}$$

In other words, the composite combination of spin and conduction electron are contracted into a single Fermi field

$$\frac{J}{N} \overbrace{S_{\alpha\beta}(j) c_{j\beta}}^{\dagger} = \left(\frac{J}{N} f^\dagger_{j\alpha} \overbrace{f_{j\beta} c_{j\beta}}^{\dagger}\right) \to V f^\dagger_{j\alpha} \tag{103}$$

The amplitude $V = \frac{J}{N} \overbrace{f_{j\beta} c_{j\beta}}^{\dagger} = -\frac{J}{N}\langle c^\dagger_{j\beta} f_{j\beta}\rangle$ involves electron states that extend over decades of energy out to the band edges. In this way, the f electron emerges as a composite bound-state of a spin and an electron. More precisely, in the long-time correlation functions,

$$\begin{aligned}&\langle \left[S_{\gamma\alpha}(i) c_{i\gamma}\right](t) \ \ \left[S_{\alpha\beta}(j) c^\dagger_{j\beta}\right](t')\rangle \\ &\xrightarrow{|t-t'| \gg \hbar/T_K} \frac{N|V^2|}{J^2} \langle f_{i\alpha}(t) f^\dagger_{j\alpha}(t')\rangle\end{aligned} \tag{104}$$

Such 'clustering' of composite operators into a single entity is well-known statistical mechanics as part of the operator product expansion (Cardy, 1996). In many-body physics, we are used to the clustering of fermions pairs into a composite boson, as in the BCS model of superconductivity, $-g\overbrace{\psi_\uparrow(x)\psi_\downarrow(x')} \to \Delta(x - x')$. The unfamiliar aspect of the Kondo effect is the appearance of a composite fermion.

The formation of these composite objects profoundly modifies the conductivity and plasma oscillations of the electron fluid. The Read–Newns path integral has two $U(1)$ gauge invariances – an external electromagnetic gauge invariance associated with the conservation of charge and an internal gauge invariance associated with the local constraints. The f electron couples to the internal gauge fields rather than the external electromagnetic fields, so why is it charged?

The answer lies in the broken symmetry associated with the development of the amplitude V. The phase of V transforms under both internal and external gauge groups. When V develops an amplitude, its phase does not actually order, but it does develop a stiffness which is sufficient to lock the internal and external gauge fields together so that, at low frequencies, they become synonymous. Written in a schematic long-wavelength form, the gauge-sensitive part of

the Kondo lattice Lagrangian is

$$\mathcal{L} = \sum_{\sigma} \int \mathrm{d}^D x \Big[c^{\dagger}_{\sigma}(x)(-i\partial_t + e\Phi(x) + \epsilon_{\mathbf{p}-e\vec{A}})c_{\sigma}(x) + f^{\dagger}_{\sigma}(x)(-i\partial_t + \lambda(x))f_{\sigma}(x) + \Big(\overline{V}(x)c^{\dagger}_{\sigma}(x)f_{\sigma}(x) + \text{ H.c}\Big)\Big] \tag{105}$$

where $\mathbf{p} = -i\vec{\nabla}$. Suppose $V(x) = |V(x)|e^{i\phi(x)}$. There are two independent gauge transformations that increase the phase ϕ of the hybridization. In the external, electromagnetic gauge transformation, the change in phase is absorbed onto the conduction electron and electromagnetic field, so if $V \to Ve^{i\alpha}$,

$$\begin{aligned} &\phi \to \phi + \alpha, \qquad c(x) \to c(x)e^{-i\alpha(x)}, \\ &e\Phi(x) \to e\Phi(x) + \dot{\alpha}(x), \quad e\vec{A} \to e\vec{A} - \vec{\nabla}\alpha(x) \end{aligned} \tag{106}$$

where $(\Phi, \vec{A})$ denotes the electromagnetic scalar and vector potential at site j and $\dot{\alpha} = \partial_t \alpha \equiv -i\partial_\tau \alpha$ denotes the derivative with respect to real time t. By contrast, in the internal gauge transformation, the phase change of V is absorbed onto the f fermion and the internal gauge field (Read and Newns, 1983a), so if $V \to Ve^{i\beta}$,

$$\begin{aligned} &\phi \to \phi + \beta, \qquad f(x) \to f(x)e^{i\beta(x)}, \\ &\lambda(x) \to \lambda(x) - \dot{\beta}(x) \end{aligned} \tag{107}$$

If we expand the mean-field free energy to quadratic order in small, slowly varying changes in $\lambda(x)$, then the change in the action is given by

$$\delta S = -\frac{\chi_Q}{2} \int \mathrm{d}^D x \mathrm{d}\tau \delta\lambda(x)^2 \tag{108}$$

where $\chi_Q = -\delta^2 F/\delta\lambda^2$ is the f-electron susceptibility evaluated in the mean-field theory. However, $\delta\lambda(x)$ is not gauge invariant, so there must be additional terms. To guarantee gauge invariance under both the internal and external transformation, we must replace $\delta\lambda$ by the covariant combination $\delta\lambda + \dot{\phi} - e\Phi$. The first two terms are required for invariance under the internal gauge group, while the last two terms are required for gauge invariance under the external gauge group. The expansion of the action to quadratic order in the gauge fields must therefore have the form

$$S \sim -\frac{\chi_Q}{2} \int \mathrm{d}\tau \sum_j (\dot{\phi} + \delta\lambda(x) - e\Phi(x))^2 \tag{109}$$

so the phase ϕ acquires a rigidity in time that generates a 'mass' or energy cost associated with *difference* of the external and internal potentials. The minimum energy static configuration is when

$$\delta\lambda(\mathbf{x}) + \dot{\phi}(\mathbf{x}) = e\Phi(\mathbf{x}) \tag{110}$$

so when the external potential changes slowly, the internal potential tracks it. It is this effect that keeps the Kondo resonance pinned at the Fermi surface. We can always choose the gauge where the phase velocity $\dot{\phi}$ is absorbed into the local gauge field λ. Recent work by Coleman, Marston and Schofield (2005b) has extended this kind of reasoning to the case where RKKY couplings generate a dispersion $j_{\mathbf{p}-\mathcal{A}}$ for the spinons, where $\mathcal{A}$ is an internal vector potential, which suppresses currents of the gauge charge n_f. In this case, the long-wavelength action has the form

$$S = \frac{1}{2} \int \mathrm{d}^3 x \mathrm{d}\tau \Big[\rho_s \left(e\vec{A} + \vec{\nabla}\phi - \vec{\mathcal{A}}\right)^2 - \chi_Q (e\Phi - \dot{\phi} - \delta\lambda)^2 \Big] \tag{111}$$

In this general form, heavy-electron physics can be seen to involve a kind of 'Meissner effect' that excludes the difference field $e\vec{A} - \vec{\mathcal{A}}$ from within the metal, locking the internal field to the external electromagnetic field, so that the f electrons, which couple to it, now become charged (Figure 19).

2.3.4 *Optical conductivity of the heavy-electron fluid*

One of the interesting consequences of the heavy-electron charge is a complete renormalization of the electronic plasma frequency (Millis, Lavagna and Lee, 1987b). The electronic

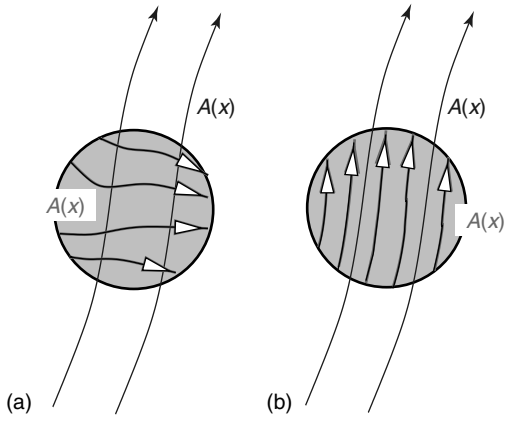

Figure 19. (a) Spin liquid, or local moment phase, internal field $\mathcal{A}$ decoupled from electromagnetic field. (b) Heavy-electron phase, internal gauge field 'locked' together with electromagnetic field. Heavy electrons are now charged and difference field $[e\vec{A}(x) - \mathcal{A}(x)]$ is excluded from the material.

plasma frequency is related via a f-sum rule to the integrated optical conductivity

$$\int_0^\infty \frac{\mathrm{d}\omega}{\pi}\sigma(\omega) = f_1 = \frac{\pi}{2}\left(\frac{n_c e^2}{m}\right) \tag{112}$$

where n_e is the density of electrons [2]. In the absence of local moments, this is the total spectral weight inside the Drude peak of the optical conductivity.

When the heavy-electron fluid forms, we need to consider the plasma oscillations of the enlarged Fermi surface. If the original conduction sea was less than half filled, then the renormalized heavy-electron band is more than half filled, forming a partially filled hole band. The density of electrons in a filled band is N/a^D, so the effective density of hole carriers is then

$$n_{\mathrm{HF}} = (N - Q - \mathcal{N}_c)/a^D = (N - Q)/a^D - n_c \tag{113}$$

The mass of the excitations is also renormalized, $m \to m^*$. The two effects produce a low-frequency 'quasiparticle' Drude peak in the conductivity, with a small total weight

$$\int_0^{\sim V} \mathrm{d}\omega\sigma(\omega) = f_2 = \frac{\pi}{2}\frac{n_{\mathrm{HF}}e^2}{m^*} \sim f_1 \times \frac{m}{m^*}\left(\frac{n_{\mathrm{HF}}}{n_c}\right) \ll f_1 \tag{114}$$

Optical conductivity probes the plasma excitations of the electron fluid at low momenta. The direct gap between the upper and lower bands of the Kondo lattice are separated by a direct hybridization gap of the order $2V \sim \sqrt{DT_{\mathrm{K}}}$. This scale is substantially larger than the Kondo temperature, and it defines the separation between the thin Drude peak of the heavy electrons and the high-frequency contribution from the conduction sea.

In other words, the total spectral weight is divided up into a small 'heavy fermion' Drude peak, of total weight f_2, where

$$\sigma(\omega) = \frac{n_{\mathrm{HF}}e^2}{m^*}\frac{1}{(\tau^*)^{-1} - i\omega} \tag{115}$$

separated off by an energy of the order $V \sim \sqrt{T_{\mathrm{K}}D}$ from an 'interband' component associated with excitations between the lower and upper Kondo bands (Millis and Lee, 1987a; Degiorgi, Anders, Gruner and Society, 2001). This second term carries the bulk $\sim f_1$ of the spectral weight (Figure 20).

Simple calculations, based on the Kubo formula, confirm this basic expectation, (Millis and Lee, 1987a; Degiorgi, Anders, Gruner and Society, 2001) showing that the relationship between the original relaxation rate of the conduction sea and the heavy-electron relaxation rate τ^* is

$$(\tau^*)^{-1} = \frac{m}{m^*}(\tau)^{-1} \tag{116}$$

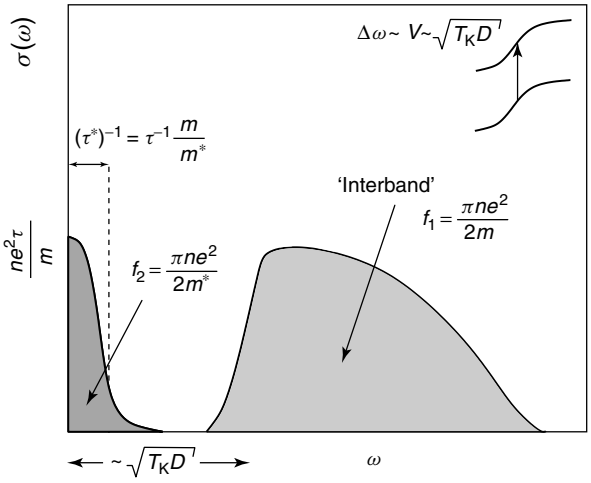

Figure 20. Separation of the optical sum rule in a heavy-fermion system into a high-energy 'interband' component of weight $f_2 \sim ne^2/m$ and a low-energy Drude peak of weight $f_1 \sim ne^2/m^*$.

Notice that this means that the residual resistivity

$$\rho_o = \frac{m^*}{ne^2\tau^*} = \frac{m}{ne^2\tau} \tag{117}$$

is unaffected by the effects of mass renormalization. This can be understood by observing that the heavy-electron Fermi velocity is also renormalized by the effective mass, $v_{\mathrm{F}}^* = \frac{m}{m^*}$, so that the mean-free path of the heavy-electron quasiparticles is unaffected by the Kondo effect.

$$l^* = v_{\mathrm{F}}^*\tau^* = v_{\mathrm{F}}\tau \tag{118}$$

The formation of a narrow Drude peak, and the presence of a direct hybridization gap, have been seen in optical measurements on heavy-electron systems (Schlessinger, Fisk, Zhang and Maple, 1997; Beyerman, Gruner, Dlicheouch and Maple, 1988; Dordevic *et al*., 2001). One of the interesting features about the hybridization gap of size $2V$ is that the mean-field theory predicts that the ratio of the direct to the indirect hybridization gap is given by $\frac{2V}{T_{\mathrm{K}}} \sim \frac{1}{\sqrt{\rho T_{\mathrm{K}}}} \sim \sqrt{\frac{m^*}{m_e}}$, so that the effective mass of the heavy electrons should scale as square of the ratio between the hybridization gap and the characteristic scale T^* of the heavy Fermi liquid

$$\frac{m^*}{m_e} \propto \left(\frac{2V}{T_{\mathrm{K}}}\right)^2 \tag{119}$$

In practical experiments, T_{K} is replaced by the 'coherence temperature' T^*, where the resistivity reaches a maximum. This scaling law is broadly followed (see Figure 21) in measured optical data (Dordevic *et al*., 2001), and provides further confirmation of the correctness of the Kondo lattice picture.

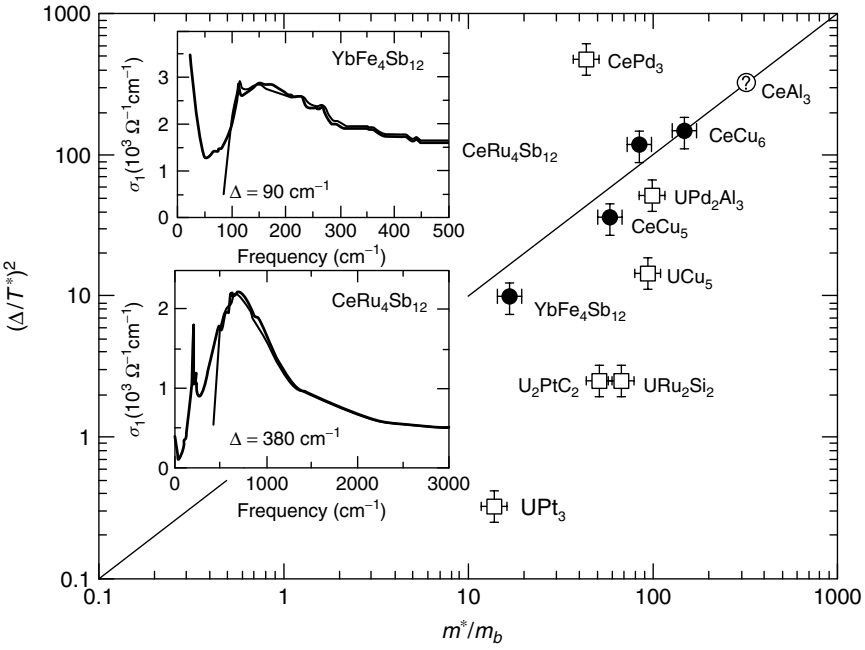

Figure 21. Scaling of the effective mass of heavy electrons with the square of the optical hybridization gap. (Reproduced from S.V. Dordevic, D.N. Basov, N.R. Dilley, E.D. Bauer, and M.B. Maple, *Phys. Rev. Lett.* **86**, 2001, 684, copyright © by the American Physical Society, with permission from the APS.)

2.4 Dynamical mean-field theory

The fermionic large N approach to the Kondo lattice provides an invaluable description of heavy-fermion physics, one that can be improved upon beyond the mean-field level. For example, the fluctuations around the mean-field theory can be used to compute the interactions, the dynamical correlation functions, and the optical conductivity (Coleman, 1987b; Millis and Lee, 1987a). However, the method does face a number of serious outstanding drawbacks:

- False phase transition: In the large N limit, the crossover between the heavy Fermi liquid and the local moment physics sharpens into a phase transition where the $1/N$ expansion becomes singular. There is no known way of eliminating this feature in the $1/N$ expansion.
- Absence of magnetism and superconductivity: The large N approach, based on the $SU(N)$ group, cannot form a two-particle singlet for $N > 2$. The $SU(N)$ group is fine for particle physics, where baryons are bound-states of N quarks, but, for condensed matter physics, we sacrifice the possibility of forming two-particle or two-spin singlets, such as Cooper pairs and spin-singlets. Antiferromagnetism and superconductivity are consequently absent from the mean-field theory.

Amongst the various alternative approaches currently under consideration, one of particular note is the DMFT. The idea of DMFT is to reduce the lattice problem to the physics of a single magnetic ion embedded within a self-consistently determined effective medium (Georges, Kotliar, Krauth and Rozenberg, 1996; Kotliar *et al*., 2006). The effective medium is determined self-consistently from the self-energies of the electrons that scatter off the single impurity. In its more advanced form, the single impurity is replaced by a cluster of magnetic ions.

Early versions of the DMFT were considered by Kuramoto and Watanabe (1987), and Cox and Grewe (1988), and others, who used diagrammatic means to extract the physics of a single impurity. The modern conceptual framework for DMFT was developed by Metzner and Vollhardt (1989), and Georges and Kotliar (1992). The basic idea behind DMFT is linked to early work of Luttinger and Ward (1960), and Kotliar *et al*. (2006), who found a way of writing the free energy as a variational functional of the full electronic Green's function

$$\mathcal{G}_{ij} = -\langle T\psi_i(\tau)\psi_j^\dagger(0)\rangle \tag{120}$$

Luttinger and Ward showed that the free energy is a variational functional of $F[\mathcal{G}]$ from which Dyson's equation relating the $\mathcal{G}$ to the bare Green's function $\mathcal{G}_0$

$$[\mathcal{G}_0^{-1} - \mathcal{G}^{-1}]_{ij} = \Sigma_{ij}[\mathcal{G}] \tag{121}$$

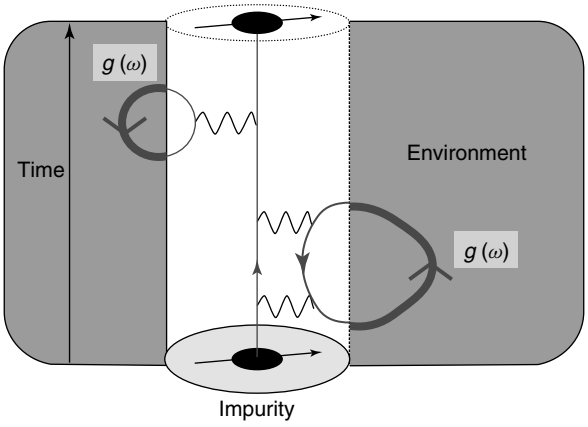

Figure 22. In the dynamical mean-field theory, the many-body physics of the lattice is approximated by a single impurity in a self-consistently determined environment. Each time the electron makes a sortie from the impurity, its propagation through the environment is described by a self-consistently determined local propagator $\mathcal{G}(\omega)$, represented by the thick gray line.

The quantity $\Sigma[\mathcal{G}]$ is a functional, a machine which takes the full propagator of the electron and outputs the self-energy of the electron. Formally, this functional is the sum of the one-particle irreducible Feynman diagrams for the self-energy: while its output depends on the input Greens function, the actual the machinery of the functional is determined solely by the interactions. The only problem is that we do not know how to calculate it.

DMFT solves this problem by approximating this functional by that of a single impurity or a cluster of magnetic impurities (Figure 22). This is an ideal approximation for a local Fermi liquid, where the physics is highly retarded in time, but local in space. The local approximation is also asymptotically exact in the limit of infinite dimensions (Metzner and Vollhardt, 1989). If one approximates the input Green function to Σ by its on-site component $\mathcal{G}_{ij} \approx \mathcal{G}\delta_{ij}$, then the functional becomes the local self-energy functional of a single magnetic impurity,

$$\Sigma_{ij}[\mathcal{G}_{ls}] \approx \Sigma_{ij}[\mathcal{G}\delta_{ls}] \equiv \Sigma_{\text{impurity}}[\mathcal{G}]\delta_{ij} \tag{122}$$

DMFT extracts the local self-energy by solving an Anderson impurity model embedded in an arbitrary electronic environment. The physics of such a model is described by a path integral with the action

$$S = -\int_0^\beta \mathrm{d}\tau \mathrm{d}\tau' f_\sigma^\dagger(\tau)\mathcal{G}_0^{-1}(\tau-\tau')f_\sigma(\tau') + U\int_0^\beta \mathrm{d}\tau n_\uparrow(\tau)n_\downarrow(\tau) \tag{123}$$

where $G_0(\tau)$ describes the bare Green's function of the f electron, hybridized with its dynamic environment. This quantity is self-consistently updated by the DMFT. There are, by now, a large number of superb numerical methods to solve an Anderson model for an arbitrary environment, including the use of exact diagonalization, diagrammatic techniques, and the use of Wilson's renormalization group (Bulla, 2006). Each of these methods is able to take an input 'environment' Green's function providing as output the impurity self-energy $\Sigma[\mathcal{G}_0] = \Sigma(i\omega_n)$.

Briefly, this is how the DMFT computational cycle works. One starts with an estimate for the environment Green's function $\mathcal{G}_0$ and uses this as input to the 'impurity solver' to compute the first estimate $\Sigma(i\omega_n)$ of the local self-energy. The interaction strength is set within the impurity solver. This local self-energy is used to compute the Green's functions of the electrons in the environment. In an Anderson lattice, the Green's function becomes

$$G(\mathbf{k},\omega) = \left[\omega - E_f - \frac{V^2}{\omega-\epsilon_{\mathbf{k}}} - \Sigma(\omega)\right]^{-1} \tag{124}$$

where V is the hybridization and $\epsilon_{\mathbf{k}}$ the dispersion of the conduction electrons. It is through this relationship that the physics of the lattice is fed into the problem. From $G(\mathbf{k},\omega)$, the local propagator is computed

$$\mathcal{G}(\omega) = \sum_{\mathbf{k}}\left[\omega - E_f - \frac{V^2}{\omega-\epsilon_{\mathbf{k}}} - \Sigma(\omega)\right]^{-1} \tag{125}$$

Finally, the new estimate for the bare environment Green's function $\mathcal{G}_0$ is then obtained by inverting the equation $\mathcal{G}^{-1} = \mathcal{G}_0^{-1} - \Sigma$, so that

$$\mathcal{G}_0(\omega) = \left[G^{-1}(\omega) + \Sigma(\omega)\right] \tag{126}$$

This quantity is then reused as the input to an 'impurity solver' to compute the next estimate of $\Sigma(\omega)$. The whole procedure is then reiterated to self-consistency. For the Anderson lattice, Cyzcholl (Schweitzer and Czycholl, 1991) has shown that remarkably good results are obtained using a perturbative expansion for Σ to the order of U^2 (Figure 23). Although this approach is not sufficient to capture the limiting Kondo behavior much, the qualitative physics of the Kondo lattice, including the development of coherence at low temperatures, is already captured by this approach. However, to go to the strongly correlated regime, where the ratio of the interaction to the impurity hybridization width $U/(\pi\Delta)$ is much larger than unity, one requires a more sophisticated solver.

There are many ongoing developments under way using this powerful new computational tool, including the incorporation of realistic descriptions of complex atoms, and the extension to 'cluster DMFT' involving clusters of magnetic moments embedded in a self-consistent environment. Let me

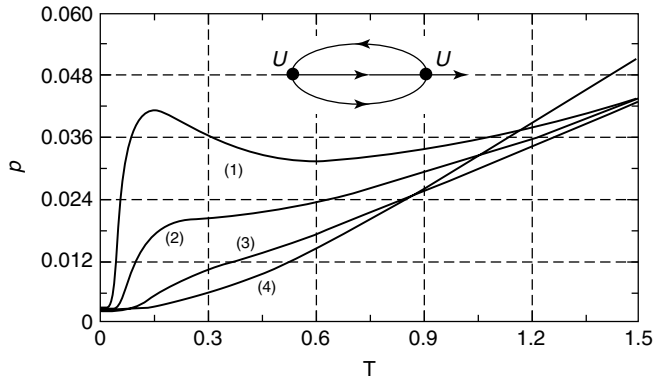

Figure 23. Resistivity for the Anderson lattice, calculated using the DMFT, computing the self-energy to order U^2. (1), (2), (3), and (4) correspond to a sequence of decreasing electron density corresponding to $n_{\mathrm{TOT}} = (0.8, 0.6, 0.4, 0.2)$ respectively. (Reproduced from H. Schweitzer and G. Czycholl, *Phys. Rev. Lett.* **67**, 1991, 3724 copyright © by the American Physical Society, with permission of the APS.)

end this brief summary with a list of a few unsolved issues with this technique

- There is, at present, no way to relate the thermodynamics of the bulk to the impurity thermodynamics.
- At present, there is no natural extension of these methods to the infinite U Anderson or Kondo models that incorporates the Green's functions of the *localized* f-electron degrees of freedom as an integral part of the DMFT.
- The method is largely a numerical black box, making it difficult to compute microscopic quantities beyond the electron-spectral functions. At the human level, it is difficult for students and researchers to separate themselves from the ardors of coding the impurity solvers, and make time to develop new conceptual and qualitative understanding of the physics.

3 KONDO INSULATORS

3.1 Renormalized silicon

The ability of a dense lattice of local moments to transform a metal into an insulator, a 'Kondo insulator' is one of the remarkable and striking consequences of the dense Kondo effect (Aeppli and Fisk, 1992; Tsunetsugu, Sigrist and Ueda, 1997; Riseborough, 2000). Kondo insulators are heavy-electron systems in which the the liberation of mobile charge through the Kondo effect gives rise to a filled heavy-electron band in which the chemical potential lies in the middle of the hybridization gap. From a quasiparticle perspective,

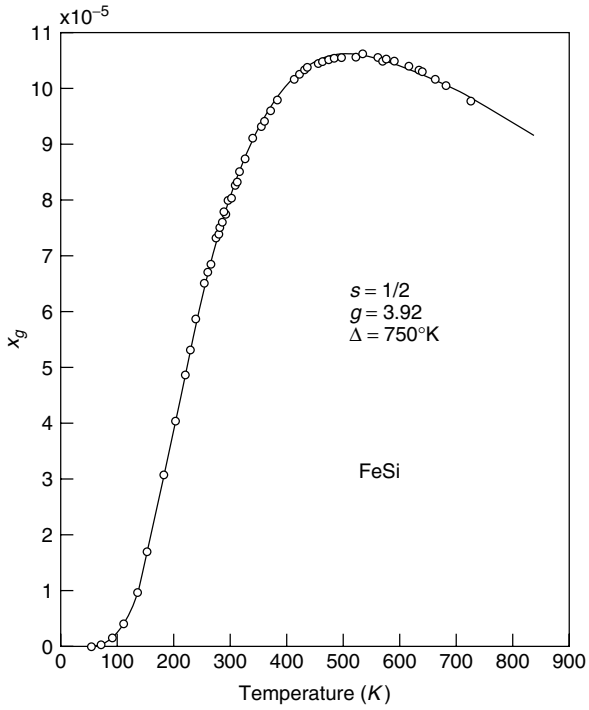

Figure 24. Schematic band picture of Kondo insulator, illustrating how a magnetic field drives a metal-insulator transition. Modified from Aeppli and Fisk (1992). (Reproduced from V. Jaccarino, G.K. Wertheim, J.H. Wernick, C.R. Walker and S. Arajs, *Phys. Rev.* **160**, 1967, 476 copyright © 1967 by the American Physical Society, with permission of the APS.)

Kondo insulators are highly renormalized 'band insulators' (Figure 24). The d-electron Kondo insulator FeSi has been referred to as *renormalized silicon*. However, like Mott–Hubbard insulators, the gap in their spectrum is driven by interaction effects, and they display optical and magnetic properties that cannot be understood with band theory.

There are about a dozen known Kondo insulators, including the rare-earth systems SmB_6 (Menth, Buehler and Geballe, 1969), YB_{12} (Iga, Kasaya and Kasuya, 1988), $CeFe_4P_{12}$ (Meisner *et al.*, 1985), $Ce_3Bi_4Pt_3$ (Hundley *et al.*, 1990), CeNiSn (Takabatake *et al.*, 1992, 1990; Izawa *et al.*, 1999) and CeRhSb (Takabatake *et al.*, 1994), and the d-electron Kondo insulator FeSi. At high temperatures, Kondo insulators are local moment metals, with classic Curie susceptibilities, but, at low temperatures, as the Kondo effect develops coherence, the conductivity and the magnetic susceptibility drop toward zero. Perfect insulating behavior is, however, rarely observed due to difficulty in eliminating impurity band formation in ultranarrow gap systems. One of the cleanest examples of Kondo-insulating behavior occurs in the d-electron system FeSi (Jaccarino *et al.*, 1967; DiTusa *et al.*, 1997). This 'flyweight' heavy-electron system provides a rather clean realization of the phenomena seen in other

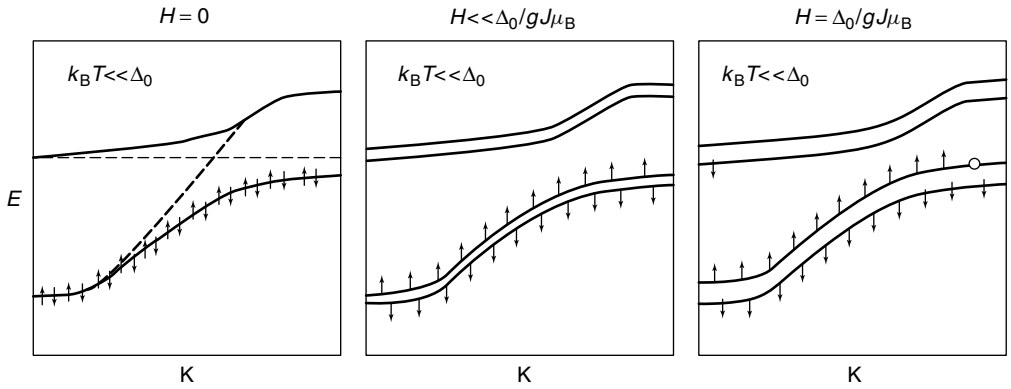

Figure 25. Temperature-dependent susceptibility in FeSi (after Jaccarino *et al*., 1967), fitted to the activated Curie form $\chi(T) = (C/T)e^{-\Delta/(k_B T)}$, with $C = (g\mu_B)^2 j(j+1)$, and $g = 3.92$, $\Delta = 750\,\mathrm{K}$. The Curie tail has been subtracted. (Reproduced from G. Aeppli and Z. Fisk, *Comm. Condens. Matter Phys.* **16** (1992) 155, with permission from Taylor & Franics Ltd, www/.nformaworld.com.)

Kondo insulators, with a spin and charge gap of about 750 K (Schlessinger, Fisk, Zhang and Maple, 1997). Unlike its rare-earth counterparts, the small spin-orbit coupling in this materials eliminates the Van Vleck contribution to the susceptibility at $T = 0$, giving rise to a susceptibility which almost completely vanishes at low temperatures (Jaccarino *et al*., 1967) (Figure 25).

Kondo insulators can be understood as 'half-filled' Kondo lattices in which each quenched moment liberates a negatively charged heavy electron, endowing each magnetic ion an extra unit of positive charge. There are three good pieces of support for this theoretical picture:

- Each Kondo insulator has its fully itinerant semiconducting analog. For example, CeNiSn is isostructural and isoelectronic with the semiconductor TiNiSi containing Ti^{4+} ions, even though the former contains Ce^{3+} ions with localized f moments. Similarly, $Ce_3Bi_4Pt_3$, with a tiny gap of the order 10 meV is isolectronic with semiconducting $Th_3Sb_4Ni_3$, with a 70 meV gap, in which the 5f-electrons of the Th^{4+} ion are entirely delocalized.
- Replacing the magnetic site with isoelectronic nonmagnetic ions is equivalent to doping, thus in $Ce_{1-x}La_xBi_4Pt_3$, each La^{3+} ion behaves as an electron donor in a lattice of effective Ce^{4+} ions. $Ce_{3-x}La_xPt_4Bi_3$ is, in fact, very similar to $CePd_3$, which contains a pseudogap in its optical conductivity, with a tiny Drude peak (Bucher *et al*., 1995).
- The magnetoresistance of Kondo insulators is large and negative, and the 'insulating gap' can be closed by the action of physically accessible fields. Thus, in $Ce_3Bi_4Pt_3$, a 30 T field is sufficient to close the indirect hybridization gap.

These equivalences support the picture of the Kondo effect liberating a composite fermion.

Figure 26(a) shows the sharp rise in the resistivity of $Ce_3Bi_4Pt_3$ as the Kondo-insulating gap forms. In Kondo insulators, the complete elimination of carriers at low temperatures is also manifested in the optical conductivity. Figure 26(b) shows the temperature dependence of the optical conductivity in $Ce_3Bi_4Pt_3$, showing the emergence of a gap in the low-frequency optical response and the loss of carriers at low energies.

The optical conductivity of the Kondo insulators is of particular interest. Like the heavy-electron metals, the development of coherence is marked by the formation of a direct hybridization gap in the optical conductivity. As this forms, a pseudogap develops in the optical conductivity. In a noninteracting band gap, the lost f-sum weight inside the pseudogap would be deposited above the gap. In heavy-fermion metals, a small fraction of this weight is deposited in the Drude peak – however, most of the weight is sent off to energies comparable with the bandwidth of the conduction band. This is one of the most direct pieces of evidence that the formation of Kondo singlets involves electron energies that spread out to the bandwidth. Another fascinating feature of the heavy-electron 'pseudogap' is that it forms at a temperature that is significantly lower than the pseudogap. This is because the pseudogap has a larger width given by the geometric mean of the coherence temperature and the bandwidth $2V \sim \sqrt{T_K D}$. The extreme upward transfer of spectral weight in Kondo insulators has not yet been duplicated in detailed theoretical models. For example, while calculations of the optical conductivity within the DMFT do show spectral weight transfer, it is not yet possible to reduce the indirect band gap to the point where it is radically smaller than the interaction scale U (Rozenberg, Kotliar and Kajueter, 1996). It may be that these discrepancies will disappear in future calculations based on the more extreme physics of the Kondo model, but these calculations have yet to be carried out.

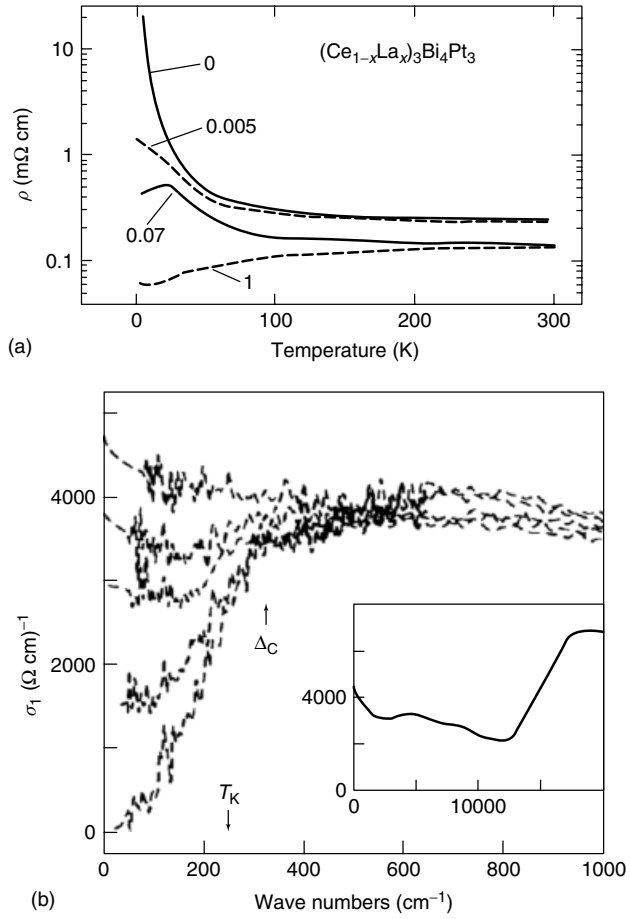

Figure 26. (a) Temperature-dependent resistivity of $Ce_3Pt_4Bi_3$ showing the sharp rise in resistivity at low temperatures. (Reproduced from M.F. Hundley, P.C. Canfield, J.D. Thompson, Z. Fisk, and J.M. Lawrence, *Phys. Rev. B.* **42**, 1990, 6842, copyright © 1990 by the American Physical Society, with permission of the APS.) Replacement of local moments with spinless *La* ions acts like a dopant. (b) Real part of optical conductivity $\sigma_1(\omega)$ for Kondo insulator $Ce_3Pt_4Bi_3$. (Reproduced from B. Bucher, Z. Schlessinger, P.C. Canfield, and Z. Fisk 03/04/2007 *Phys. Rev. Lett* **72**, 1994, 522, copyright © 1994 by the American Physical Society, with permission of the APS.) The formation of the pseudogap associated with the direct hybridization gap leads to the transfer of f-sum spectral weight to high energies of order the bandwidth. The pseudogap forms at temperatures that are much smaller than its width (see text). Insert shows $\sigma_1(\omega)$ in the optical range.

There are, however, a number of aspects of Kondo insulators that are poorly understood from the the simple hybridization picture, in particular,

- The apparent disappearance of RKKY magnetic interactions at low temperatures.
- The nodal character of the hybridization gap that develops in the narrowest gap Kondo insulators CeNiSn and CeRhSb.
- The nature of the metal-insulator transition induced by doping.

3.2 Vanishing of RKKY interactions

There are a number of experimental indications that the low-energy magnetic interactions vanish at low frequencies in a Kondo lattice. The low-temperature product of the susceptibility and temperature χT reported (Aeppli and Fisk, 1992) to scale with the inverse Hall constant $1/R_H$, representing the exponentially suppressed density of carriers, so that

$$\chi \sim \frac{1}{R_{\mathrm{H}} T} \sim \frac{\mathrm{e}^{-\Delta/T}}{T} \tag{127}$$

The important point here is that the activated part of the susceptibility has a vanishing Curie–Weiss temperature. A similar conclusion is reached from inelastic neutron scattering measurements of the magnetic susceptibility $\chi'(q,\omega) \sim$ in CeNiSn and FeSi, which appears to lose all of its momentum dependence at low temperatures and frequencies. There is, to date, no theory that can account for these vanishing interactions.

3.3 Nodal Kondo insulators

The narrowest gap Kondo insulators, CeNiSn and CeRhSb, are effectively semimetals, for although they do display tiny pseudogaps in their spin and charge spectra, the purest samples of these materials develop metallic behavior (Izawa *et al.*, 1999). What is particularly peculiar (Figure 27) about these two materials is that the NMR relaxation rate $1/(T_1)$ shows a T^3 temperature dependence from about 10 to 1 K, followed by a linear Korringa behavior at lower temperatures. The usual rule of thumb is that the NMR relaxation rate is proportional to a product of the temperature and the thermal average of the electronic density of states $N^*(\omega)$

$$\frac{1}{T_1} \sim T\overline{N(\omega)^2} \sim T[N(\omega \sim T)]^2 \tag{128}$$

where $\overline{N(\omega)^2} = \int \mathrm{d}\epsilon \left(-\frac{\partial f(\omega)}{\partial \omega}\right) N(\omega)^2$ is the thermally smeared average of the squared density of states. This suggests that the electronic density of states in these materials has a 'V' shaped form, with a finite value at $\omega = 0$. Ikeda and Miyake (1996) have proposed that the Kondo-insulating state in these materials develops in a crystal-field state with an axially symmetric hybridization vanishing along a single crystal axis. In such a picture, the finite density of states does not derive from a Fermi surface, but from the angular average of the coherence peaks in the density of states. The

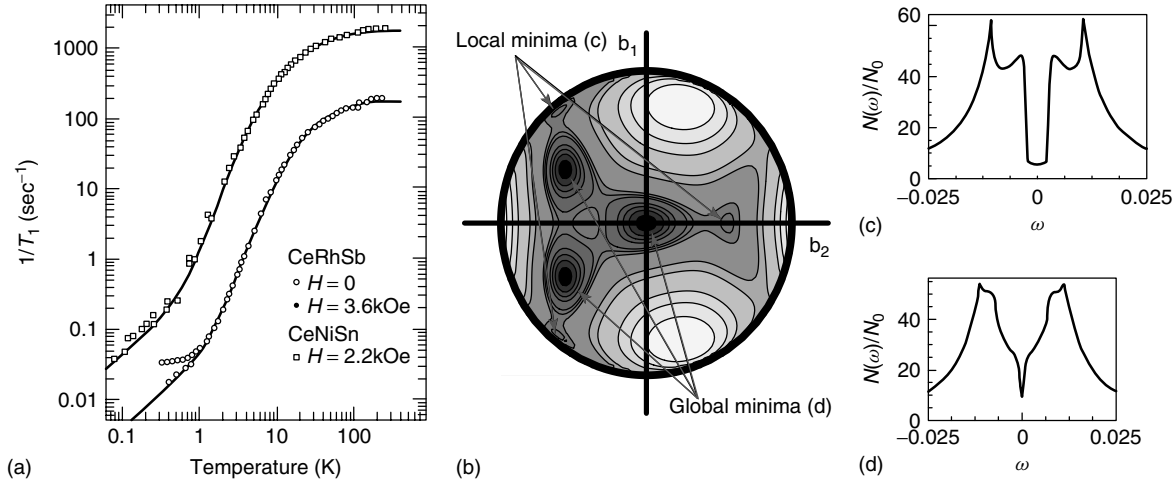

Figure 27. (a) NMR relaxation rate $1/T_1$ in CeRhSb and CeNiSn, showing a T^3 relaxation rate sandwiched between a low- and a high-temperature T-linear Korringa relaxation rate, suggesting a V-shaped density of states. (Reproduced from K. Nakamura, Y. Kitaoka, K. Asayama, T. Takabatake, H. Tanaka, and H. Fujii, *J. Phys. Soc Japan* **63**, 1994, 33, with permission of the Physical Society of Japan.) (b) Contour plot of the ground-state energy in mean-field theory for the narrow gap Kondo insulators, as a function of the two first components of the unit vector $\hat{b}$ (the third one is taken as positive). The darkest regions correspond to lowest values of the free energy. Arrows point to the three global and three local minima that correspond to nodal Kondo insulators. (Reproduced from J. Moreno and P. Coleman, *Phys. Rev. Lett.* **84**, 2000, 342, copyright © 2000 by the American Physical Society, with permission of the APS.) (c) Density of states of Ikeda and Miyake (1996) state that appears as the global minimum of the Kinetic energy. (Reproduced from H. Ikeda, and K. Miyake *J. Phys. Soc. Jpn.* **65**, 1996, 1769, with permission of the Physical Society of Japan.) (d) Density of states of the MC state (Moreno and Coleman, 2000) that appears as a local minimum of the Kinetic energy, with more pronounced 'V'-shaped density of states.

odd thing about this proposal is that CeNiSn and CeRhSb are monoclinic structures, and the low-lying Kramers doublet of the f state can be any combination of the $|\pm\frac{1}{2}\rangle$, $|\pm\frac{3}{2}\rangle$, or $|\pm\frac{5}{2}\rangle$ states:

$$|\pm = b_1|\pm 1/2\rangle + b_2|\pm 5/2\rangle + b_3|\mp 3/2\rangle \qquad (129)$$

where $\hat{b} = (b_1, b_2, b_3)$ could, in principle, point anywhere on the unit sphere, depending on details of the monoclinic crystal field. The Ikeda Miyake model corresponds to three symmetry-related points in the space of crystal-field ground states,

$$\hat{b} = \begin{cases} (\mp\frac{\sqrt{2}}{4}, -\frac{\sqrt{5}}{4}, \frac{3}{4}) \\ (0, 0, 1) \end{cases} \qquad (130)$$

where a node develops along the x, y, or z axis, respectively. But the nodal crystal-field states are isolated 'points' amidst a continuum of fully gapped crystal-field states. Equally strangely, neutron scattering results show no crystal-field satellites in the dynamical spin susceptibility of CeNiSn, suggesting that the crystal electric fields are quenched (Alekseev *et al*., 1994), and that the nodal physics is a many-body effect (Kagan, Kikoin and Prokof'ev, 1993; Moreno and Coleman, 2000). One idea is that Hund's interactions provide the driving force for this selection mechanism. Zwicknagl, Yaresko and Fulde (2002) have suggested that Hund's couplings select the orbitals in multi f electron heavy-electron metals such as UPt_3. Moreno and Coleman (2000) propose a similar idea in which virtual valence fluctuations into the f^2 state generate a many-body or a Weiss effective field that couples to the orbital degrees of freedom, producing an effective *crystal* field that adjusts itself in order to minimize the kinetic energy of the f electrons. This hypothesis is consistent with the observation that the Ikeda Miyake state corresponds to the Kondo-insulating state with the lowest kinetic energy, providing a rational for the selection of the nodal configurations. Moreno and Coleman also found another nodal state with a more marked V-shaped density of states that may fit the observed properties more precisely. This state is also a local minimum of the electron Kinetic energy. These ideas are still in their infancy, and more work needs to be done to examine the controversial idea of a Weiss crystal field, both in the insulators and in the metals.

4 HEAVY-FERMION SUPERCONDUCTIVITY

4.1 A quick tour

Since the discovery (Steglich *et al*., 1976) of superconductivity in $CeCu_2Si_2$, the list of known HFSCs has grown to

include more than a dozen (Sigrist and Ueda, 1991b) materials with a great diversity of properties (Sigrist and Ueda, 1991a; Cox and Maple, 1995). In each of these materials, the jump in the specific heat capacity at the superconducting phase transition is comparable with the normal state specific heat

$$\frac{(C_v^s - C_v^n)}{C_V} \sim 1 - 2 \tag{131}$$

and the integrated entropy beneath the C_v/T curve of the superconductor matches well with the corresponding area for the normal phase obtained when superconductivity is suppressed by disorder or fields

$$\int_0^{T_c} \mathrm{d}T \frac{(C_v^s - C_v^n)}{T} = 0 \tag{132}$$

Since the normal state entropy is derived from the f moments, it follows that these same degrees of freedom are involved in the development of the superconucting state. With the exception of a few anomalous cases, (UBe_{13}, $PuCoGa_5$, and $CeCoIn_5$), heavy-fermion superconductivity develops out of the coherent, paramagnetic heavy Fermi liquid, so heavy fermion superconductivity can be said to involve the pairing of heavy f electrons.

Independent confirmation of the 'heavy' nature of the pairing electrons comes from observed size of the London penetration depth λ_{L} and superconducting coherence length ξ in these systems, both of which reflect the enhanced effective mass. The large mass renormalization enhances the penetration depth, whilst severely contracting the coherence length, making these extreme type-II superconductors. The London penetration depth of HFSCs agree well with the value expected on the assumption that only spectral weight in the quasiparticle Drude peak condenses to form a superconductor by

$$\frac{1}{\mu_o \lambda_{\mathrm{L}}^2} = \frac{ne^2}{m^*} = \int_{\omega \in \mathrm{D.}P} \frac{\mathrm{d}\omega}{\pi} \sigma(\omega) \ll \frac{ne^2}{m} \tag{133}$$

London penetration depths in these compounds are a factor of 20–30 times *longer* (Broholm *et al*., 1990) than in superconductors, reflecting the large enhancement in effective mass. By contrast, the coherence lengths $\xi \sim v_{\mathrm{F}}/\Delta \sim hk_{\mathrm{F}}/(m^*\Delta)$ are severely contracted in a HFSC. The orbitally limited upper critical field is determined by the condition that an area ξ^2 contains a flux quantum $\xi^2 B_c \sim \frac{h}{2e}$. In UBe_{13}, a superconductor with 0.9 K transition temperature, the upper critical field is about 11 T, a value about 20 times larger than a conventional superconductor of the same transition temperature.

Table 2 shows a selected list of HFSCs. 'Canonical' HFSCs, such as $CeCu_2Si_2$ and UPt_3, develop superconductivity out of a paramagnetic Landau–Fermi liquid. 'Preordered' superconductors, such as UPt_2Al_3 (Geibel *et al*., 1991a,b), $CePt_3Si$, and URu_2Si_2, develop another kind of order before going superconducting at a lower temperature. In the case of URu_2Si_2, the nature of the upper ordering transition is still unidentified, but, in the other examples, the upper transition involves the development of antiferromagnetism. 'Quantum critical' superconductors, including $CeIn_3$ and $CeCu_2(Si_{1-x}Ge_x)_2$, develop superconductivity when pressure is tuned close to a QCP. $CeIn_3$ develops superconductivity at the pressure-tuned antiferromagnetic quantum critical point at 2.5 GPa (25 kbar). $CeCu_2$ $(Si,Ge)_2$ has two islands, one associated with antiferromagnetism at low pressure and a second at still higher pressure, thought to be associated with critical valence fluctuations (Yuan *et al*., 2006).

'Strange' superconductors, which include UBe_{13}, the 115 material $CeCoIn_5$, and $PuCoGa_5$, condense into the superconducting state out of an incoherent or strange metallic state. UBe_{13} has a resistance of the order 150 μΩcm at its transition temperature. $CeCoIn_5$ bears superficial resemblance to a high-temperature superconductor, with a linear temperature resistance in its normal state, while its cousin, $PuCoGa_5$ transitions directly from a Curie paramagnet of unquenched f spins into an anisotropically paired, singlet superconductor. These particular materials severely challenge our theoretical understanding, for the heavy-electron quasiparticles appear to form as part of the condensation process, and we are forced to address how the f-spin degrees of freedom incorporate into the superconducting parameter.

4.2 Phenomenology

The main body of theoretical work on heavy-electron systems is driven by experiment, and focuses directly on the phenomenology of the superconducting state. For these purposes, it is generally sufficient to assume a Fermi liquid of preformed mobile heavy electrons, an electronic analog of superfluid Helium-3, in which the quasiparticles interact through a phenomenological BCS model. For most purposes, the Landau–Ginzburg theory is sufficient. I regret that, in this short review, I do not have time to properly represent and discuss the great wealth of fascinating phenomenology, the wealth of multiple phases, and the detailed models that have been developed to describe them. I refer the interested reader to reviews on this subject. (Sigrist and Ueda, 1991a).

On theoretical grounds, the strong Coulomb interactions of the f electrons that lead to moment formation in heavy-fermion compounds are expected to heavily suppress the formation of conventional s-wave pairs in these systems. A large body of evidence favors the idea that the gap function and the anomalous Green function between paired heavy electrons $F_{\alpha\beta}(x) = \langle c_\alpha^\dagger(x) c_\beta^\dagger(0) \rangle$ is spatially

Table 2. Selected HFSCs.

Type	Material	T_c (K)	Knight shift (singlet)	Remarks	Gap symmetry	References
Canonical	$CeCu_2Si_2$	0.7	Singlet	First HFSC	Line nodes	Steglich *et al*. (1976)
	UPt_3	0.48	?	Double transition to T-violating state	Line and point nodes	Stewart, Fisk, Willis and Smith (1984b)
Preordered	UPd_2Al_3	2	Singlet	Néel AFM $T_N = 14\,K$	Line nodes $\Delta \sim \cos 2\chi$	Geibel *et al*. (1991a), Sato *et al*. (2001) and Tou *et al*. (1995)
	URu_2Si_2	1.3	Singlet	Hidden order at $T_0 = 17.5\,K$	Line nodes	Palstra *et al*. (1985) and Kim *et al*. (2003)
	$CePt_3Si$	0.8	Singlet and Triplet	Parity-violating crystal. $T_N = 3.7\,K$	Line nodes	Bauer *et al*. (2004)
Quantum critical	$CeIn_3$	0.2 (2.5 GPa)	Singlet	First quantum critical HFSC	Line nodes	Mathur *et al*. (1998)
	$CeCu_2\ (Si_{1-x}Ge_x)_2$	0.4 (P = 0) 0.95 (5.4 GPa)	Singlet	Two islands of SC as function of pressure	Line nodes	Yuan *et al*. (2006)
Quadrupolar	$PrOs_4Sb_{12}$	1.85	Singlet	Quadrupolar fluctuations	Point nodes	Isawa *et al*. (2003)
Strange	$CeCoIn_5$	2.3	Singlet	Quasi-2D $\rho_n \sim T$	Line nodes $d_{x^2-y^2}$	Petrovic *et al*. (2001)
	UBe_{13}	0.86	?	Incoherent metal at T_c	Line nodes	Andres, Graebner and Ott (1975)
	$PuCoGa_5$	18.5	Singlet	Direct transition Curie metal → HFSC	Line nodes	Sarrao *et al*. (2002)

anisotropic, forming either p-wave triplet or d-wave singlet pairs.

In BCS theory, the superconducting quasiparticle excitations are determined by a one-particle Hamiltonian of the form

$$H = \sum_{\mathbf{k},\sigma} \epsilon_{\mathbf{k}} f^{\dagger}_{\mathbf{k}\alpha} f_{\mathbf{k}\alpha} + \sum_{\mathbf{k}} [f^{\dagger}_{\mathbf{k}\alpha} \Delta_{\alpha\beta}(\mathbf{k}) f^{\dagger}_{-\mathbf{k}\beta} + f_{-\mathbf{k}\beta} \overline{\Delta}_{\beta\alpha}(\mathbf{k}) f_{\mathbf{k}\alpha}] \tag{134}$$

where

$$\Delta_{\alpha\beta}(\mathbf{k}) = \begin{cases} \Delta(\mathbf{k})(i\sigma_2)_{\alpha\beta} & \text{(singlet)} \\ \vec{d}(\mathbf{k}) \cdot (i\sigma_2 \vec{\sigma})_{\alpha\beta} & \text{(triplet)} \end{cases} \tag{135}$$

For singlet pairing, $\Delta(\mathbf{k})$ is an even parity function of $\mathbf{k}$, while for triplet pairing, $\vec{d}(\mathbf{k})$ is a an odd-parity function of $\mathbf{k}$ with three components.

The excitation spectrum of an anisotropically paired singlet superconductor is given by

$$E_{\mathbf{k}} = \sqrt{\epsilon^2_{\mathbf{k}} + |\Delta_{\mathbf{k}}|^2} \tag{136}$$

This expression can also be used for a triplet superconductor that does not break the time-reversal symmetry by making the replacement $|\Delta_{\mathbf{k}}|^2 \equiv \vec{d}^{\dagger}(\mathbf{k}) \cdot \vec{d}(\mathbf{k})$.

Heavy-electron superconductors are anisotropic superconductors, in which the gap function vanishes at points, or, more typically, along lines on the Fermi surface. Unlike s-wave superconductors, magnetic and nonmagnetic impurities are equally effective at pair breaking and suppressing T_c in these materials. A node in the gap is the result of sign changes in the underlying gap function. If the gap function vanishes along surfaces in momentum space, the intersection of these surfaces with the Fermi surface produces 'line nodes' of gapless quasiparticle excitations. As an example, consider UPt_3, where, according to one set of models (Blount, Varma and Aeppli, 1990; Joynt, 1988; Puttika and Joynt, 1988; Hess, Tokuyasu and Sauls, 1990; Machida and Ozaki, 1989), pairing involves a complex d-wave gap

$$\Delta_{\mathbf{k}} \propto k_z(\hat{k}_x \pm i k_y), \qquad |\Delta_{\mathbf{k}}|^2 \propto k_z^2(k_x^2 + k_y^2) \tag{137}$$

Here $\Delta_{\mathbf{k}}$ vanishes along the basal plane $k_z = 0$, producing a line of nodes around the equator of the Fermi surface, and along the z axis, producing a point node at the poles of the Fermi surface.

One of the defining properties of line nodes on the Fermi surface is a quasiparticle density of states that vanishes linearly with energy

$$N^*(E) = 2\sum_{\mathbf{k}} \delta(E - E_{\mathbf{k}}) \propto E \tag{138}$$

The quasiparticles surrounding the line node have a 'relativistic' energy spectrum. In a plane perpendicular to the node, $E_{\mathbf{k}} \sim \sqrt{(v_F k_1)^2 + (\alpha k_2)^2}$, where $\alpha = \mathrm{d}\Delta/\mathrm{d}k_2$ is the gradient of the gap function and k_1 and k_2 the momentum measured in the plane perpendicular to the line node. For a two-dimensional relativistic particle with dispersion $E = ck$, the density of states is given by $N(E) = \frac{|E|}{4\pi c^2}$. For the anisotropic case, we need to replace c by the geometric mean of v_F and α, so $c^2 \to v_F\alpha$. This result must then be doubled to take account of the spin degeneracy and averaged over each line node:

$$N(E) = 2\sum_{\text{nodes}} \int \frac{\mathrm{d}k_\parallel}{2\pi} \frac{|E|}{4\pi v_F \alpha} = |E| \times \sum_{\text{nodes}} \left(\int \frac{\mathrm{d}k_\parallel}{4\pi^2 v_F \alpha} \right) \tag{139}$$

In the presence of pair-breaking impurities and in a vortex state, the quasiparticle nodes are smeared, adding a small constant component to the density of states at low energies.

This linear density of states is manifested in a variety of power laws in the temperature dependence of experimental properties, most notably

- Quadratic temperature dependence of specific heat $C_V \propto T^2$, since the specific heat coefficient is proportional to the thermal average of the density of states

$$\frac{C_V}{T} \propto \overbrace{\overline{N(E)}}^{\propto T} \sim T \tag{140}$$

  where $\overline{N(E)}$ denotes the thermal average of $N(E)$.
- A ubiquitous T^3 temperature dependence in the nuclear magnetic relaxation (NMR) and nuclear quadrupole relaxation (NQR) rates $1/T_1$. The nuclear relaxation rate is proportional to the thermal average of the squared density of states, so, for a superconductor with line nodes,

$$\frac{1}{T_1} \propto T \overbrace{\overline{N(E)^2}}^{\propto T^2} \sim T^3 \tag{141}$$

  Figure 28 shows the T^3 NMR relaxation rate of the Aluminum nucleus in UPd_2Al_3.

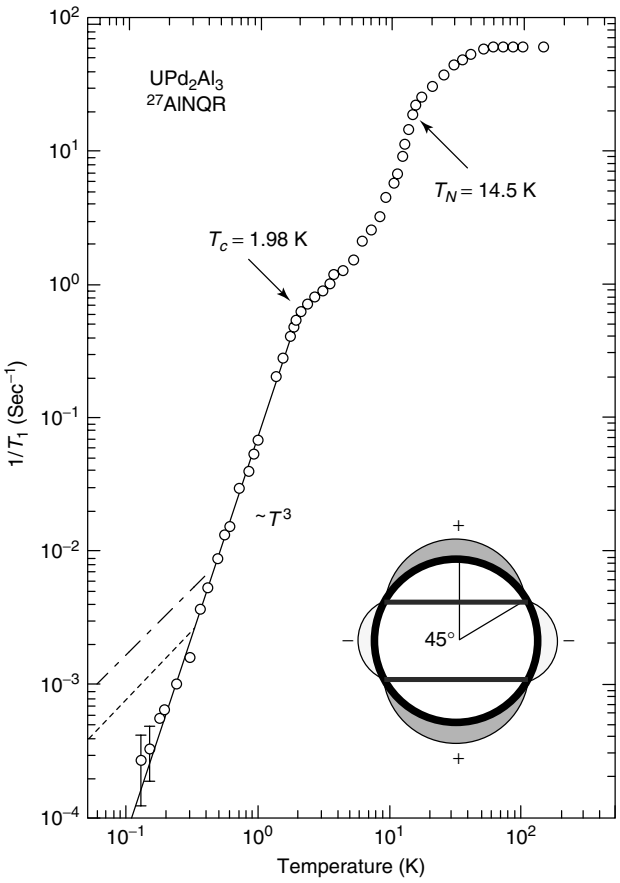

Figure 28. Temperature dependence of the ^{27}Al NQR relaxation rate $1/T_1$ for UPd_2Al_3 (after Tou *et al*., 1995) showing T^3 dependence associated with lines of nodes. Inset showing nodal structure $\Delta \propto \cos(2\theta)$ proposed from analysis of anisotropy of thermal conductivity in Won *et al*. (2004). (Reproduced from H. Tou, Y. Kitaoka, K. Asayama, C. Geibel, C. Schank, and F. Steglich, 1995, *J. Phys. Soc. Japan* **64**, 1995 725, with permission of the Physical Society of Japan.)

Although power laws can distinguish line and point nodes, they do not provide any detailed information about the triplet or singlet character of the order parameter or the location of the nodes. The observation of upper critical fields that are 'Pauli limited' (set by the spin coupling, rather than the diamagnetism), and the observation of a Knight shift in most HFSCs, indicates that they are anisotropically singlet paired. Three notable exceptions to this rule are UPt_3, UBe_{13}, and UNi_2Al_3, which do not display either a Knight shift or a Pauli-limited upper critical field, and are the best candidates for odd-parity triplet pairing. In the special case of $CePt_3Sn$, the crystal structure lacks a center of symmetry and the resulting parity violation must give a mixture of triplet and singlet pairs.

Until comparatively recently, very little was known about the positions of the line nodes in heavy-electron

superconductors. In one exception, experiments carried out almost 20 years ago on UPt_3 observed marked anisotropies in the ultrasound attenuation length and the penetration depth (Bishop *et al*., 1984; Broholm *et al*., 1990) that appear to support a line of nodes in the basal plane. The ultrasonic attenuation $\alpha_s(T)/\alpha_n$ in single crystals of UPt_3 has a T linear dependence when the polarization lies in the basal plane of the gap nodes, but a T^3 dependence when the polarization is along the c axis.

An interesting advance in the experimental analysis of nodal gap structure has recently occurred, owing to new insights into the behavior of the nodal excitation spectrum in the flux phase of HFSCs. In the 1990s, Volovik (1993) observed that the energy of heavy-electron quasiparticles in a flux lattice is 'Doppler shifted' by the superflow around the vortices, giving rise to a finite density of quasiparticle states around the gap nodes. The Doppler shift in the quasiparticle energy resulting from superflow is given by

$$E_{\mathbf{k}} \rightarrow E_{\mathbf{k}} + \vec{p} \cdot \vec{v}_s = E_{\mathbf{k}} + \vec{v}_F \cdot \frac{\hbar}{2}\vec{\nabla}\phi \tag{142}$$

where $\vec{v}_s$ is the superfluid velocity and ϕ the superfluid phase. This has the effect of shifting quasiparticle states by an energy of the order $\Delta E \sim \hbar\frac{v_F}{2R}$, where R is the average distance between vortices in the flux lattice. Writing $\pi H R^2 \sim \Phi_0$, and $\pi H_{c2}\xi^2 \sim \Phi_0$ where $\Phi_0 = \frac{h}{2e}$ is the flux quantum, H_{c2} is the upper critical field, and ξ is the coherence length, it follows that $\frac{1}{R} \sim \frac{1}{\xi}\sqrt{\frac{H}{H_{c2}}}$. Putting $\xi \sim v_F/\Delta$, where Δ is the typical size of the gap, the typical shift in the energy of nodal quasiparticles is of the order $E_H \sim \Delta\sqrt{\frac{H}{H_{c2}}}$. Now since the density of states is of the order $N(E) = \frac{|E|}{\Delta}N(0)$, where $N(0)$ is the density of states in the normal phase, it follows that the smearing of the nodal quasiparticle energies will produce a density of states of the order

$$N^*(H) \sim N(0)\sqrt{\frac{H}{H_{c2}}} \tag{143}$$

This effect, the 'Volovik effect', produces a linear component to the specific heat $C_V/T \propto \sqrt{\frac{H}{H_{c2}}}$. This enhancement of the density of states is largest when the group velocity $\vec{V}_F$ at the node is perpendicular to the applied field $\vec{H}$, and when the field is parallel to $\vec{v}_F$ at a particular node, the node is unaffected by the vortex lattice (Figure 29). This

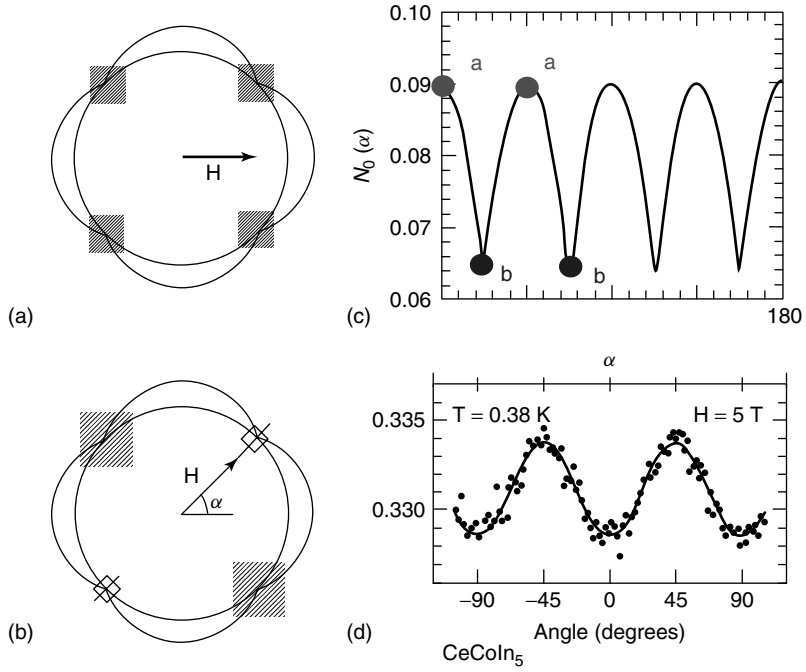

Figure 29. Schematic showing how the nodal quasiparticle density of states depends on field orientation (after Vekhter, Hirschfield, Carbotte and Nicol, 1999). (a) Four nodes are activated when the field points toward an antinode, creating a maximum in density of states. (b) Two nodes activated when the field points toward a node, creating a minimum in the density of states. (c) Theoretical dependence of density of states on angle. (After Vekhter, Hirschfield, Carbotte and Nicol, 1999.) (d) Measured angular dependence of C_v/T (after Aoki *et al*., 2004) is 45° out of phase with prediction. This discrepancy is believed to be due to vortex scattering, and is expected to vanish at lower fields. (Reproduced from I. Vekhter, P. Hirschfield, J.P. Carbotte, and E.J. Nicol, *Phys. Rev. B* **59**, 1998, R9023, copyright © 1998 by the American Physical Society, with permission of the APS.)

gives rise to an angular dependence in the specific heat coefficient and thermodynamics that can be used to measure the gap anisotropy. In practice, the situation is complicated at higher fields where the Andreev scattering of quasiparticles by vortices becomes important. The case of $CeCoIn_5$ is of particular current interest. Analyses of the field-anisotropy of the thermal conductivity in this material was interpreted early on in terms of a gap structure with $d_{x^2-y^2}$, while the anisotropy in the specific heat appears to suggest a d_{xy} symmetry. Recent theoretical work by Vorontsov and Vekhter (2006) suggests that the discrepancy between the two interpretations can be resolved by taking into account the effects of the vortex quasiparticle scattering that were ignored in the specific heat interpretation. They predict that, at lower fields, where vortex scattering effects are weaker, the sign of the anisotropic term in the specific heat reverses, accounting for the discrepancy

It is clear that, despite the teething problems in the interpretation of field-anisotropies in transport and thermodynamics, this is an important emerging tool for the analysis of gap anisotropy, and, to date, it has been used to give tentative assignments to the gap anisotropy of UPd_2Al_3, $CeCoIn_5$, and $PrOs_4Sb_{12}$.

4.3 Microscopic models

4.3.1 Antiferromagnetic fluctuations as a pairing force

The classic theoretical models for heavy-fermion superconductivity treat the heavy-electron fluids as a Fermi liquid with antiferromagnetic interactions amongst their quasiparticles (Monod, Bourbonnais and Emery, 1986; Scalapino, Loh and Hirsch, 1986; Monthoux and Lonzarich, 1999). UPt_3 provided the experimental inspiration for early theories of heavy-fermion superconductivity, for its superconducting state forms from within a well-developed Fermi liquid. Neutron scattering on this material shows signs of antiferromagnetic spin fluctuations (Aeppli *et al*., 1987), making it natural to presuppose that these might be the driving force for heavy-electron pairing.

Since the early 1970s, theoretical models had predicted that strong ferromagnetic spin fluctuations, often called *paramagnons*, could induce p-wave pairing, and this mechanism was widely held to be the driving force for pairing in superfluid He–3. An early proposal that antiferromagnetic interactions could provide the driving force for anisotropic singlet pairing was made by Hirsch (1985). Shortly thereafter, three seminal papers, by Monod, Bourbonnais and Emery (1986) (BBE), Scalapino, Loh and Hirsch (1986) (SLH) and by Miyake, Miyake, Rink and Varma (1986) (MSV), solidified this idea with a concrete demonstration that antiferromagnetic interactions drive an attractive BCS interaction in the d-wave pairing channel. It is a fascinating thought that at the same time that this set of authors was forging the foundations of our current thoughts on the link between antiferromagnetism and d-wave superconductivity, Bednorz and Mueller were in the process of discovering high-temperature superconductivity.

The BBE and SLH papers develop a paramagnon theory for d-wave pairing in a Hubbard model with a contact interaction I, having in mind a system, which in the modern context, would be said to be close to an antiferromagnetic QCP. The MSV paper starts with a model with a preexisting antiferromagnetic interaction, which, in the modern context, would be associated with the 't–J' model. It is this approach that I sketch here. The MSV model is written

$$H = \sum \epsilon_{\mathbf{k}} a^{\dagger}_{\mathbf{k}\sigma} a_{\mathbf{k}\sigma} + H_{\rm int} \tag{144}$$

where

$$H_{\rm int} = \frac{1}{2} \sum_{\mathbf{k},\mathbf{k}'} \sum_{\mathbf{q}} J(\mathbf{k}-\mathbf{k}') \vec{\sigma}_{\alpha\beta} \cdot \vec{\sigma}_{\gamma\delta} \times \left(a^{\dagger}_{\mathbf{k}+\mathbf{q}/2\alpha} a^{\dagger}_{-\mathbf{k}+\mathbf{q}/2\gamma} \right) \left(a_{-\mathbf{k}'+\mathbf{q}/2\delta} a_{\mathbf{k}'+\mathbf{q}/2\beta} \right) \tag{145}$$

describes the antiferromagnetic interactions. There are a number of interesting points to be made here:

- The authors have in mind a strong coupled model, such as the Hubbard model at large U, where the interaction cannot be simply derived from paramagnon theory. In a weak-coupled Hubbard model, a contact interaction I and bare susceptibility $\chi_0(q)$, the induced magnetic interaction can be calculated in a random phase approximation (RPA) (Miyake, Rink and Varma, 1986) as

$$J(q) = -\frac{I}{2[1 + I\chi_0(q)]} \tag{146}$$

  MSV make the point that the detailed mechanism that links the low-energy antiferromagnetic interactions to the microscopic interactions is poorly described by a weak-coupling theory, and is quite likely to involve other processes, such as the RKKY interaction, and the Kondo effect that lie outside this treatment.
- Unlike phonons, magnetic interactions in heavy-fermion systems cannot generally be regarded as retarded interactions, for they extend up to an energy scale ω_0 that is comparable with the heavy-electron bandwidth T^*. In a classic BCS treatment, the electron energy is restricted to lie within a Debye energy of the Fermi energy. But

here, $\omega_0 \sim T^*$, so all momenta are involved in magnetic interactions, and the interaction can transformed to real space as

$$H = \sum \epsilon_{\mathbf{k}} a^\dagger_{\mathbf{k}\sigma} a_{\mathbf{k}\sigma} + \frac{1}{2}\sum_{i,j} J(\mathbf{R}_i - \mathbf{R}_j)\vec{\sigma}_i \cdot \vec{\sigma}_j \quad (147)$$

where $J(\mathbf{R}) = \sum_{\mathbf{q}} e^{i\mathbf{q}\cdot\mathbf{R}} J(\mathbf{q})$ is the Fourier transform of the interaction and $\vec{\sigma}_i = a^\dagger_{i\alpha}\vec{\sigma}_{\alpha\beta}a_{i\beta}$ is the spin density at site i. Written in real space, the MSV model is seen to be an early predecessor of the t–J model used extensively in the context of high-temperature superconductivity.

To see that antiferromagnetic interactions favor d-wave pairing, one can use the 'let us decouple the interaction' in real space in terms of triplet and singlet pairs. Inserting the identity [3]

$$\vec{\sigma}_{\alpha\beta} \cdot \vec{\sigma}_{\gamma\delta} = -\frac{3}{2}(\sigma_2)_{\alpha\gamma}(\sigma_2)_{\beta\delta} + \frac{1}{2}(\vec{\sigma}\sigma_2)_{\alpha\gamma} \cdot (\sigma_2\vec{\sigma})_{\beta\delta} \quad (148)$$

into equation (147) gives

$$H_{\rm int} = -\frac{1}{4}\sum_{i,j} J_{ij}\left[3\Psi^\dagger_{ij}\Psi_{ij} - \vec{\Psi}^\dagger_{ij}\cdot\vec{\Psi}_{ij}\right] \quad (149)$$

where

$$\begin{aligned}\Psi^\dagger_{ij} &= \left(a^\dagger_{i\alpha}(-i\sigma)_{\alpha\gamma}\ a^\dagger_{j\gamma}\right)\\ \vec{\Psi}^\dagger_{ij} &= \left(a^\dagger_{i\alpha}(-i\vec{\sigma}\sigma_2)_{\alpha\gamma}\ a^\dagger_{j\gamma}\right)\end{aligned} \quad (150)$$

create singlet and triplet pairs with electrons located at sites i and j respectively. In real space, it is thus quite clear that an antiferromagnetic interaction $J_{ij} > 0$ induces attraction in the singlet channel, and repulsion in the triplet channel. Returning to momentum space, substitution of equation (148) into (145) gives

$$H_{\rm int} = -\sum_{\mathbf{k},\mathbf{k}',\mathbf{q}} J(\mathbf{k}-\mathbf{k}')\left[3\Psi^\dagger_{\mathbf{k},\ \mathbf{q}}\Psi_{\mathbf{k}',\ \mathbf{q}} - \vec{\Psi}^\dagger_{\mathbf{k},\ \mathbf{q}}\cdot\vec{\Psi}_{\mathbf{k}',\ \mathbf{q}}\right] \quad (151)$$

where $\Psi^\dagger_{\mathbf{k},\mathbf{q}} = \frac{1}{2}\left(a^\dagger_{\mathbf{k}+\mathbf{q}/2\ \alpha}(-i\sigma_2)_{\alpha\gamma}\ a^\dagger_{-\mathbf{k}-\mathbf{q}/2\ \gamma}\right)$ and $\vec{\Psi}^\dagger_{\mathbf{k},\mathbf{q}} = \frac{1}{2}\left(a^\dagger_{\mathbf{k}+\mathbf{q}/2\ \alpha}(-i\vec{\sigma}\sigma_2)_{\alpha\gamma}\ a^\dagger_{-\mathbf{k}-\mathbf{q}/2\ \gamma}\right)$ create singlet and triplet pairs at momentum $\mathbf{q}$ respectively. Pair condensation is described by the zero momentum component of this interaction, which gives

$$H_{\rm int} = \sum_{\mathbf{k},\mathbf{k}'}\left[V^{(s)}_{\mathbf{k},\mathbf{k}'}\Psi^\dagger_{\mathbf{k}}\Psi_{\mathbf{k}'} + V^{(t)}_{\mathbf{k},\mathbf{k}'}\vec{\Psi}^\dagger_{\mathbf{k}}\cdot\vec{\Psi}_{\mathbf{k}'}\right] \quad (152)$$

where $\Psi^\dagger_{\mathbf{k}} = \frac{1}{2}\left(a^\dagger_{\mathbf{k}\alpha}(-i\sigma_2)_{\alpha\beta}\ a^\dagger_{-\mathbf{k}\beta}\right)$ and $\vec{\Psi}^\dagger_{\mathbf{k},\mathbf{q}} = \frac{1}{2}\left(a^\dagger_{\mathbf{k}\alpha}(-i\vec{\sigma}\sigma_2)_{\alpha\beta}\ a^\dagger_{-\mathbf{k}\beta}\right)$ create Cooper pairs and

$$\begin{aligned}V^{(s)}_{\mathbf{k},\mathbf{k}'} &= -3[J(\mathbf{k}-\mathbf{k}') + J(\mathbf{k}+\mathbf{k}')]/2\\ V^{(t)}_{\mathbf{k},\mathbf{k}'} &= \ [J(\mathbf{k}-\mathbf{k}') - J(\mathbf{k}+\mathbf{k}')]/2\end{aligned} \quad (153)$$

are the BCS pairing potentials in the singlet and triplet channel, respectively. (Notice how the even/odd-parity symmetry of the triplet pairs pulls out the corresponding symmetrization of $J(\mathbf{k}-\mathbf{k}')$.)

For a given choice of $J(\mathbf{q})$, it now becomes possible to decouple the interaction in singlet and triplet channels. For example, on a cubic lattice of side length, if the magnetic interaction has the form

$$J(\mathbf{q}) = 2J(\cos(q_x a) + \cos(q_y a) + \cos(q_z a)) \quad (154)$$

which generates soft antiferromagnetic fluctuations at the staggered $\mathbf{Q}$ vector $\mathbf{Q} = (\pi/a, \pi/a, \pi/a)$, then the pairing interaction can be decoupled into singlet and triplet components,

$$\begin{aligned}V^s_{\mathbf{k},\mathbf{k}'} &= -\frac{3J}{2}\big[s(\mathbf{k})s(\mathbf{k}') + \mathrm{d}_{x^2-y^2}(\mathbf{k})\mathrm{d}_{x^2-y^2}(\mathbf{k}')\\ &\qquad + \mathrm{d}_{2z^2-r^2}(\mathbf{k})\mathrm{d}_{2z^2-r^2}(\mathbf{k}')\big]\\ V^t_{\mathbf{k},\mathbf{k}'} &= \frac{J}{2}\sum_{i=x,y,z} p_i(\mathbf{k})\,p_i(\mathbf{k}')\end{aligned} \quad (155)$$

where

$$\begin{aligned}s(\mathbf{k}) &= \sqrt{\tfrac{2}{3}}(\cos(k_x a)\\ &\quad + \cos(k_y a) + \cos(k_z a)) \qquad \text{(extended s-wave)}\\ \left.\begin{aligned}\mathrm{d}_{x^2-y^2}(\mathbf{k}) &= (\cos(k_x a) - \cos(k_y a)\\ \mathrm{d}_{2z^2-r^2}(\mathbf{k}) &= \tfrac{1}{\sqrt{3}}(\cos(k_x a)\\ &\quad + \cos(k_y a) - 2\cos(k_z a))\end{aligned}\right\} &\text{(d-wave)}\end{aligned} \quad (156)$$

are the gap functions for singlet pairing and

$$p_i(\mathbf{q}) = \sqrt{2}\sin(q_i a), \quad (i = x, y, z), \quad \text{(p-wave)} \quad (157)$$

describe three triplet gap functions. For $J > 0$, this particular BCS model then gives rise to extended s- and d-wave superconductivity with approximately the same transition temperatures, given by the gap equation

$$\sum_{\mathbf{k}} \tanh\left(\frac{\epsilon_{\mathbf{k}}}{2T_c}\right)\frac{1}{\epsilon_{\mathbf{k}}}\begin{Bmatrix} s(\mathbf{k})^2 \\ \mathrm{d}_{x^2-y^2}(\mathbf{k})^2 \end{Bmatrix} = \frac{2}{3J} \quad (158)$$

4.3.2 Toward a unified theory of HFSC

Although the spin-fluctuation approach described provides a good starting point for the phenomenology of heavy-fermion superconductivity (HFSC), it leaves open a wide range of questions that suggest this problem is only partially solved:

- How can we reconcile heavy-fermion superconductivity with the local moment origins of the heavy-electron quasiparticles?
- How can the incompressibility of the heavy-electron fluid be incorporated into the theory? In particular, extended s-wave solutions are expected to produce a large singlet f-pairing amplitude, giving rise to a large Coulomb energy. Interactions are expected to significantly depress, if not totally eliminate such extended s-wave solutions.
- Is there a controlled limit where a model of heavy-electron superconductivity can be solved?
- What about the 'strange' HFSCs UBe_{13}, $CeCoIn_5$, and $PuCoGa_5$, where T_c is comparable with the Kondo temperature? In this case, the superconducting order parameter must involve the f spin as a kind of 'composite' order parameter. What is the nature of this order parameter, and what physics drives T_c so high that the Fermi liquid forms at much the same time as the superconductivity develops?

One idea that may help understand the heavy-fermion pairing mechanism is Anderson's RVB theory (Anderson, 1987) of high-temperature superconductivity. Anderson proposed (Anderson, 1987; Baskaran, Zou and Anderson, 1987; Kotliar, 1988) that the parent state of the high-temperature superconductors is a two-dimensional spin liquid of RVBs between spins, which becomes superconducting upon doping with holes. In the early 1990s, Coleman and Andrei (1989) adapted this theory to a Kondo lattice. Although an RVB spin liquid is unstable with respect to the antiferromagnetic order in three dimensions, in situations close to a magnetic instability, where the energy of the antiferromagnetic state is comparable with the Kondo temperature, $E_{\rm AFM} \sim T_{\rm K}$, conduction electrons partially spin-compensate the spin liquid, stabilizing it against magnetism (Figure 30a). In the Kondo-stabilized spin liquid, the Kondo effect induces some RVBs in the f-spin liquid to escape into the conduction fluid where they pair charged electrons to form a heavy-electron superconductor.

A key observation of the RVB theory is that, when charge fluctuations are removed to form a spin fluid, there is no distinction between particle and hole (Affleck, Zou, Hsu and Anderson, 1988). The mathematical consequence of this is that the the spin-1/2 operator

$$\vec{S}_f = f^\dagger_{i\alpha}\left(\frac{\vec{\sigma}}{2}\right)_{\alpha\beta} f^\dagger_\alpha, \qquad n_f = 1 \tag{159}$$

is not only invariant under a change of phase $f_\sigma \to e^{i\phi} f_\sigma$, but it also possesses a continuous particle-hole symmetry

$$f^\dagger_\sigma \to \cos\theta\, f^\dagger_\sigma + \mathrm{sgn}\sigma \sin\theta\, f_{-\sigma} \tag{160}$$

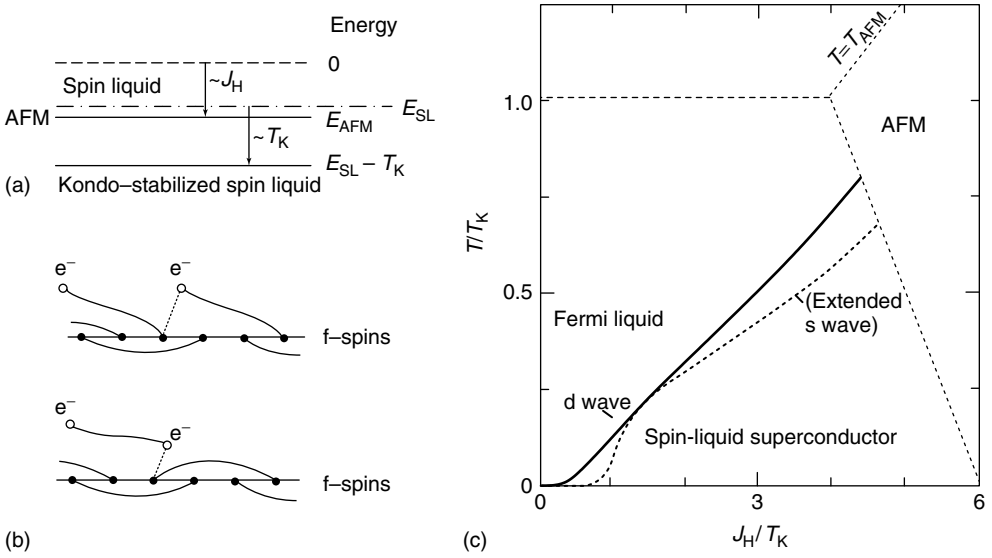

Figure 30. Kondo-stabilized spin liquid, diagram from Coleman and Andrei (1989). (a) Spin liquid stabilized by Kondo effect, (b) Kondo effect causes singlet bonds to form between spin liquid and conduction sea. Escape of these bonds into the conduction sea induces superconductivity. (c) Phase diagram computed using $SU(2)$ mean-field theory of Kondo Heisenberg model. (Reproduced from P. Coleman and N. Andrei, 1989, *J. Phys. Cond. Matt. C* **1** (1989) 4057, with permission of IOP Publishing Ltd.)

These two symmetries combine to create a *local* $SU(2)$ *gauge symmetry*. One of the implications is that the constraint $n_f = 1$ associated with the spin operator is actually part of a triplet of Gutzwiller constraints

$$f^\dagger_{i\uparrow} f_{i\uparrow} - f_{i\downarrow} f^\dagger_{i\downarrow} = 0, \quad f^\dagger_{i\uparrow} f^\dagger_{i\downarrow} = 0, \quad f_{i\downarrow} f_{i\uparrow} = 0 \tag{161}$$

If we introduce the Nambu spinors

$$\tilde{f}_i \equiv \begin{pmatrix} f_{i\uparrow} \\ f^\dagger_{i\downarrow} \end{pmatrix}, \qquad \tilde{f}^\dagger_i = (f^\dagger_{i\uparrow}, f_{i\downarrow}) \tag{162}$$

then this means that all three components of the 'isospin' of the f electrons vanish,

$$\tilde{f}^\dagger_i \vec{\tau} \tilde{f}_i = (f^\dagger_{i\uparrow}, f_{i\downarrow}) \left[\begin{pmatrix} 0 & 1 \\ 1 & 0 \end{pmatrix}, \begin{pmatrix} 0 & -i \\ i & 0 \end{pmatrix}, \begin{pmatrix} 1 & 0 \\ 0 & -1 \end{pmatrix} \right] \times \begin{pmatrix} f_{i\uparrow} \\ f^\dagger_{i\downarrow} \end{pmatrix} = 0 \tag{163}$$

where $\vec{\tau}$ is a triplet of Pauli spin operators that act on the f-Nambu spinors. In other words, in the incompressible f fluid, there can be no *s-wave* singlet pairing.

This symmetry is preserved in spin-1/2 Kondo models. When applied to the Heisenberg Kondo model

$$H = \sum_{\mathbf{k}\sigma} \epsilon_{\mathbf{k}} c^\dagger_{\mathbf{k}\sigma} c_{\mathbf{k}\sigma} + J_H \sum_{(i,j)} \mathbf{S}_i \cdot \mathbf{S}_j + J_K \sum_j c^\dagger_{j\sigma} \vec{\sigma}_{\sigma\sigma'} c_{j\sigma'} \cdot \mathbf{S}_j \tag{164}$$

where $\mathbf{S}_i = f^\dagger_{i\alpha} \left(\frac{\vec{\sigma}}{2}\right)_{\alpha\beta} f_{i\beta}$ represents an f spin at site i, it leads to an $SU(2)$ gauge theory for the Kondo lattice with Hamiltonian

$$H = \sum_{\mathbf{k}} \epsilon_{\mathbf{k}} \tilde{c}^\dagger_{\mathbf{k}} \tau_3 \tilde{c}_{\mathbf{k}} + \sum \vec{\lambda}_j \tilde{f}^\dagger_j \vec{\tau} \tilde{f}_j + \sum_{(i,j)} [\tilde{f}^\dagger_i U_{ij} \tilde{f}_j + \text{H.c}] + \frac{1}{J_\text{H}} \text{Tr}[U^\dagger_{ij} U_{ij}] + \sum_i [\tilde{f}^\dagger_i V_i \tilde{c}_i + \text{H.c}] + \frac{1}{J_\text{K}} \text{Tr}[V^\dagger_i V_i] \tag{165}$$

where λ_j is the Lagrange multiplier that imposes the Gutzwiller constraint $\vec{\tau} = 0$ at each site, $\tilde{c}_k = \begin{pmatrix} c_{k\uparrow} \\ c^\dagger_{-k\downarrow} \end{pmatrix}$ and $\tilde{c}_j = \begin{pmatrix} c_{j\uparrow} \\ c^\dagger_{j\downarrow} \end{pmatrix}$ are Nambu conduction electron spinors in the momentum and position basis, respectively, while

$$U_{ij} = \begin{pmatrix} h_{ij} & \Delta_{ij} \\ \overline{\Delta}_{ij} & -\overline{h}_{ij} \end{pmatrix} \qquad V_i = \begin{pmatrix} V_i & \overline{\alpha}_i \\ \alpha_i & -\overline{V}_i \end{pmatrix} \tag{166}$$

are matrix order parameters associated with the Heisenberg and Kondo decoupling, respectively. This model has the local gauge invariance $\tilde{f}_j \to g_j \tilde{f}_j$, $V_j \to g_j V_j$ $U_{ij} \to g_i U_{ij} g^\dagger_j$, where g_j is an $SU(2)$ matrix. In this kind of model, one can 'gauge fix' the model so that the Kondo effect occurs in the particle-hole channel ($\alpha_i = 0$). When one does so, however, the spin-liquid instability takes place preferentially in an anisotropically paired Cooper channel. Moreover, the constraint on the f electrons not only suppresses singlet s-wave pairing, it also suppresses extended s-wave pairing (Figure 30).

One of the initial difficulties with both the RVB and the Kondo-stabilized spin liquid approaches is that, in its original formulation, it could not be integrated into a large N approach. Recent work indicates that both the fermionic RVB and the Kondo-stabilized spin-liquid picture can be formulated as a controlled $SU(2)$ gauge theory by carrying out a large N expansion using the group $SP(N)$ (Read and Sachdev, 1991), originally introduced by Read and Sachdev for problems in frustrated magnetism, in place of the group $SU(N)$. The local particle-hole symmetry associated with the spin operators in $SU(2)$ is intimately related to the symplectic property of Pauli spin operators

$$\sigma_2 \vec{\sigma}^T \sigma_2 = -\vec{\sigma} \tag{167}$$

where $\vec{\sigma}^T$ is the transpose of the spin operator. This relation, which represents the sign reversal of spin operators under time-reversal, is only satisfied by a subset of the $SU(N)$ spins for $N > 2$. This subset defines the generators of the symplectic subgroup of $SU(N)$, called $SP(N)$.

Concluding this section, I want to briefly mention the challenge posed by the highest T_c superconductor, $PuCoGa_5$ (Sarrao *et al.*, 2002; Curro *et al.*, 2005). This material, discovered some 4 years ago at Los Alamos, undergoes a direct transition from a Curie paramagnet into a heavy-electron superconductor at around $T_c = 19\,\text{K}$ (Figure 31). The Curie paramagnetism is also seen in the Knight shift, which scales with the bulk susceptibility (Curro *et al.*, 2005). The remarkable feature of this material is that the specific heat anomaly has the large size ($110\,\text{mJ}\,\text{mol}^{-1}\,\text{K}^2$ (Sarrao *et al.*, 2002)) characteristic of heavy-fermion superconductivity, yet there are no signs of saturation in the susceptibility as a precursor to superconductivity, suggesting that the heavy quasiparticles do not develop from local moments until the transition. This aspect of the physics cannot be explained by the spin-fluctuation theory (Bang, Balatsky, Wastin and Thompson, 2004), and suggests that the Kondo effect takes place simultaneously with the pairing mechanism. One interesting possibility here is that the development of coherence between the Kondo effect in two different channels created by the different symmetries of the valence fluctuations into the f^6 and f^4 states might be the driver of this intriguing new superconductor (Jarrell, Pang and Cox, 1997; Coleman, Tsvelik, Andrei and Kee, 1999).

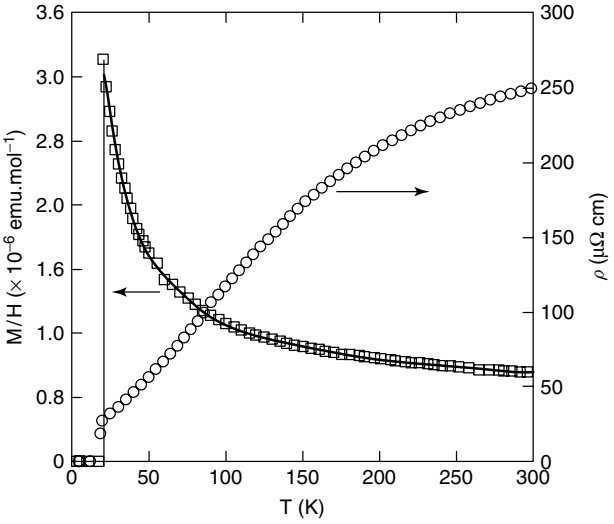

Figure 31. Temperature dependence of the magnetic susceptibility of $PuCoGa_5$. (After Sarrao *et al.*, 2002.) The susceptibility shows a direct transition from Curie–Weiss paramagnet into HFSC, without any intermediate spin quenching. (Reproduced from Sarrao, J.L., L.A. Morales, J.D. Thompson, B.L. Scott, G.R. Stewart, F. Wastlin, J. Rebizant, P. Boulet, E. Colineau, and G.H. Lander, 2002, with permission from Nature Publishing. © 2002.)

5 QUANTUM CRITICALITY

5.1 Singularity in the phase diagram

Many heavy electron systems can be tuned, with pressure, chemical doping, or applied magnetic field, to a point where their antiferromagnetic ordering temperature is driven continuously to zero to produce a 'QCP' (Stewart, 2001, 2006; Coleman, Pépin, Si and Ramazashvili, 2001; Varma, Nussinov and van Saarlos, 2002; von Löhneysen, Rosch, Vojta and Wolfe, 2007; Miranda and Dobrosavljevic, 2005). The remarkable transformation in metallic properties, often referred to as 'non-Fermi liquid behavior', which is induced over a wide range of temperatures above the QCP, together with the marked tendency to develop superconductivity in the vicinity of such 'quantum critical points' has given rise to a resurgence of interest in heavy-fermion materials.

The experimental realization of quantum criticality returns us to central questions left unanswered since the first discovery of heavy-fermion compounds. In particular:

- What is the fate of the Landau quasiparticle when interactions become so large that the ground state is no longer adiabatically connected to a noninteracting system?
- What is the mechanism by which the AFM transforms into the heavy-electron state? Is there a breakdown of the Kondo effect, revealing local moments at the quantum phase transition, or is the transition better regarded as a spin-density wave transition?

Figure 32 illustrates quantum criticality in $YbRh_2Si_2$ (Custers *et al.*, 2003), a material with a 90 mK magnetic transition that can be tuned continuously to zero by a modest magnetic

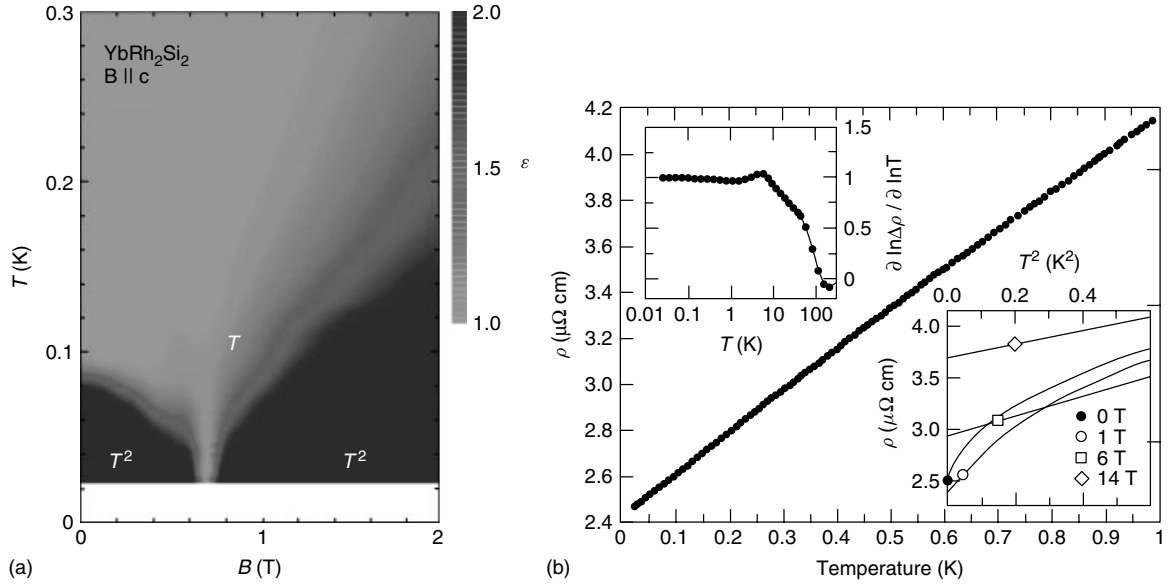

Figure 32. (a) Grayscale plot of the logarithmic derivative of resistivity $d\ln\rho/d\ln T$. (Reproduced from Custers *et al.*, 2003, with permission from Nature Publishing. © 2003.) (b) Resistivity of $YbRh_2Si_2$ in zero magnetic field. Inset shows logarithmic derivative of resistivity. (Reproduced from O. Trovarelli, C. Geibel, S. Mederle, C. Langhammer, F. Grosche, P. Gegenwart, M. Lang, G. Sparn, and F. Steglich, *Phys. Rev. Lett.* **85**, 2000, 626, copyright © 2000 by the American Physical Society, with permission of the APS.)

field. In wedge-shaped regions, either side of the transition, the resistivity displays the T^2 dependence $\rho(T) = \rho_0 + AT^2$ (black) that is the hallmark of Fermi-liquid behavior. Yet, in a tornado shaped region that stretches far above the QCP to about 20 K, the resistivity follows a *linear* dependence over more than three decades. The QCP thus represents a kind of 'singularity' in the material phase diagram.

Experimentally, quantum critical heavy-electron materials fall between two extreme limits that I shall call 'hard' and 'soft' quantum criticality. 'Soft' quantum critical systems are moderately well described in terms quasiparticles interacting with the soft quantum spin fluctuations created by a spin-density wave instability. Theory predicts (Moriya and Kawabata, 1973) that, in a three-dimensional metal, the quantum spin-density wave fluctuations give rise to a weak $\sqrt{T}$ singularity in the low-temperature behavior of the specific heat coefficient

$$\frac{C_V}{T} = \gamma_0 - \gamma_1\sqrt{T} \tag{168}$$

Examples of such behavior include $CeNi_2Ge_2$ (Grosche *et al*., 2000; Küchler *et al*., 2003) chemically doped $Ce_{2-x}La_xRu_2Si_2$ and 'A'-type antiferromagnetic phases of $CeCu_2Si_2$ at a pressure-tuned QCP.

At the other extreme, in 'hard' quantum critical heavy materials, many aspects of the physics appear consistent with a breakdown of the Kondo effect associated with a relocalization of the f electrons into ordered, ordered local moments beyond the QCP. Some of the most heavily studied examples of this behavior occur in the chemically tuned QCP in $CeCu_{6-x}Au_x$ (von Löhneysen *et al*., 1994; von Löhneysen, 1996; Schroeder *et al*., 1998, 2000). and $YbRh_2Si_{2-x}Ge_x$ (Custers *et al*., 2003; Gegenwart *et al*., 2005) and the field-tuned QCP of $YbRh_2Si_2$ (Trovarelli *et al*., 2000) and YbAgGe (Bud'ko, Morosan and Canfield, 2004, 2005; Fak *et al*., 2005; Niklowitz *et al*., 2006). Hallmarks of hard quantum criticality include a logarithmically diverging specific heat coefficient at the QCP,

$$\frac{C_v}{T} \sim \frac{1}{T_0}\ln\left(\frac{T_0}{T}\right) \tag{169}$$

and a quasilinear resistivity

$$\rho(T) \sim T^{1+\eta} \tag{170}$$

where η is in the range 0–0.2. The most impressive results to date have been observed at field-tuned QCPs in $YbRh_2Si_2$ and $CeCoIn_5$, where linear resistivity has been seen to extend over more than two decades of temperature at the field-tuned QCP (Steglich *et al*., 1976; Paglione *et al*., 2003, 2006; Ronning *et al*., 2006). Over the range where linear, where the ratio between the change in the size of the resistivity $\Delta\rho$ to the zero temperature (impurity driven) resistivity ρ_0

$$\Delta\rho/\rho_0 \gg 1 \tag{171}$$

$CeCoIn_5$ is particularly interesting, for, in this case, this resistance ratio exceeds 10^2 for current flow along the c axis (Tanatar, Paglione, Petrovic and Taillefer, 2007). This observation excludes any explanation which attributes the unusual resistivity to an interplay between spin-fluctuation scattering and impurity scattering (Rosch, 1999). Mysteriously, $CeCoIn_5$ also exhibits a $T^{3/2}$ resistivity for resistivity for current flow in the basal plane below about 2 K (Tanatar, Paglione, Petrovic and Taillefer, 2007). Nakasuji, Pines and Fisk (2004) have proposed that this kind of behavior may derive from a *two fluid* character to the underlying conduction fluid.

In quantum critical $YbRh_2Si_{2-x}Ge_x$, the specific heat coefficient develops a $1/T^{1/3}$ divergence at the very lowest temperature. In the approach to a QCP, Fermi liquid behavior is confined to an ever-narrowing range of temperature. Moreover, both the linear coefficient of the specific heat and the the quadratic coefficient A of the resistivity appear to diverge (Estrela *et al*., 2002; Trovarelli *et al*., 2000). Taken together, these results suggests that the Fermi temperature renormalizes to zero and the quasiparticle effective masses diverge

$$T_F^* \to 0 \qquad \frac{m^*}{m} \to \infty \tag{172}$$

at the QCP of these three-dimensional materials. A central property of the Landau quasiparticle is the existence of a finite overlap 'Z', or 'wave function renormalization' between a single quasiparticle state, denoted by $|\mathrm{qp}^-\rangle$ and a bare electron state denoted by $|e^-\rangle = c^\dagger_{\mathbf{k}\sigma}|0\rangle$,

$$Z = |\langle e^-|\mathrm{qp}^-\rangle|^2 \sim \frac{m}{m^*} \tag{173}$$

If the quasiparticle mass diverges, the overlap between the quasiparticle and the electron state from which it is derived is driven to zero, signaling a complete breakdown in the quasiparticle concept at a 'hard' QCP (Varma, Nussinov and van Saarlos, 2002).

Table 3 shows a tabulation of selected quantum critical materials. One interesting variable that exhibits singular behavior at both hard and soft QCPs is the Grüneisen ratio. This quantity, defined as the ratio

$$\Gamma = \frac{\alpha}{C} = -\frac{1}{V}\left.\frac{\partial \ln T}{\partial P}\right|_S \propto \frac{1}{T^\epsilon} \tag{174}$$

Table 3. Selected heavy-fermion compounds with quantum critical points.

	Compound	x_c/H_c	$\frac{C_v}{T}$	$\rho \sim T^a$	$\Gamma(T) = \frac{\alpha}{C_P}$	Other	References
	$CeCu_{6-x}Au_x$	$x_c = 0.1$	$\frac{1}{T_0}\ln\left(\frac{T_0}{T}\right)$	$T + c$	–	$\chi''_{\mathbf{Q}_0}(\omega, T) = \frac{1}{T^{0.7}}F\left[\frac{\omega}{T}\right]$	von Löhneysen *et al*. (1994), von Löhneysen (1996) and Schroeder *et al*. (1998, 2000)
Hard	$YbRh_2Si_2$	$B_{c\|\|} = 0.66\,\mathrm{T}$	–	T	–	Jump in Hall constant	Trovarelli *et al*. (2000) and Paschen *et al*. (2004)
	$YbRh_2Si_{2-x}Ge_x$	$x_c = 0.1$	$\frac{1}{T^{1/3}} \leftrightarrow \frac{1}{T_0}\ln\left(\frac{T_0}{T}\right)$	T	$T^{-0.7}$	–	Custers *et al*. (2003) and Gegenwart *et al*. (2005)
	YbAgGe	$B_{c\|} = 9T$ $B_{c\perp} = 5T$	$\frac{1}{T_0}\ln\left(\frac{T_0}{T}\right)$	T	–	NFL over range of fields	Bud'ko, Morosan and Canfield (2004), Fak *et al*. (2005) and Niklowitz *et al*. (2006)
Soft	$CeCoIn_5$	$B_c = 5\,\mathrm{T}$	$\frac{1}{T_0}\ln\left(\frac{T_0}{T}\right)$	$T/T^{1.5}$	–	$\rho_c \propto T$, $\rho_{ab} \propto T^{1.5}$	Paglione *et al*. (2003, 2006), Ronning *et al*. (2006) and Tanatar, Paglione, Petrovic and Taillefer (2007)
	$CeNi_2Ge_2$	$P_c = 0$	$\gamma_0 - \gamma_1\sqrt{T}$	$T^{1.2-1.5}$	T^{-1}	–	Grosche *et al*. (2000) and Küchler *et al*. (2003)

of the thermal expansion coefficient $\alpha = \frac{1}{V}\frac{\mathrm{d}V}{\mathrm{d}T}$ to the specific heat C, diverges at a QCP. The Grüneisen ratio is a sensitive measure of the rapid acquisition of entropy on warming away from QCP. Theory predicts that $\epsilon = 1$ at a 3D spin density wave critical point, as seen in $CeNi_2Ge_2$. In the 'hard' quantum critical material $YbRh_2Si_{2-x}Ge_x$, $\epsilon = 0.7$ indicates a serious departure from a 3D spin-density wave instability (Küchler *et al*., 2003).

5.2 Quantum versus classical criticality

Figure 33 illustrates some key distinctions between classical and quantum criticality (Sachdev, 2007). Passage through a classical second-order phase transition is achieved by tuning the temperature. Near the transition, the imminent arrival of order is signaled by the growth of droplets of nascent order whose typical size ξ diverges at the critical point. Inside each droplet, fluctuations of the order parameter exhibit a universal power-law dependence on distance

$$\langle \psi(x)\psi(0)\rangle \sim \frac{1}{x^{d-2+\eta}}, \qquad (x \ll \xi) \tag{175}$$

Critical matter 'forgets' about its microscopic origins: Its thermodynamics, scaling laws, and correlation exponents associated with critical matter are so robust and universal that they recur in such diverse contexts as the Curie point of iron or the critical point of water. At a conventional

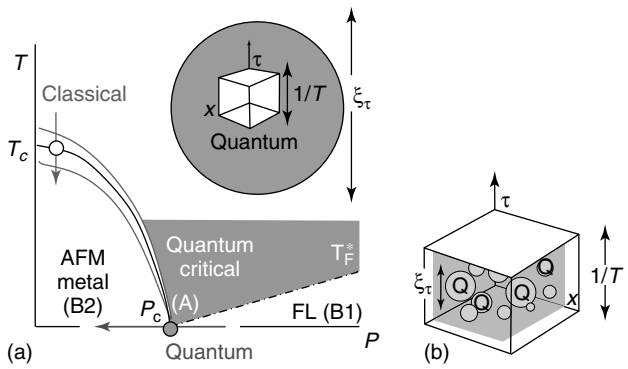

Figure 33. Contrasting classical and quantum criticality in heavy-electron systems. At a QCP, an external parameter P, such as pressure or magnetic field, replaces temperature as the 'tuning parameter'. Temperature assumes the new role of a finite size cutoff $l_\tau \propto 1/T$ on the temporal extent of quantum fluctuations. (a) Quantum critical regime, where $l_\tau < \xi_{\mathrm{tau}}$ probes the interior of the quantum critical matter. (b) Fermi-liquid regime, where $l_\tau > \xi_\tau$, where like soda, bubbles of quantum critical matter fleetingly form within a Fermi liquid that is paramagnetic (B1), or antiferromagnetically ordered (B2).

critical point, order-parameter fluctuations are 'classical', for the characteristic energy of the critical modes $\hbar\omega(q_0)$, evaluated at a wave vector $q_0 \sim \xi^{-1}$, inevitably drops below the thermal energy $\hbar\omega(q_0) \ll k_B T_c$ as $\xi \to \infty$.

In the 1970s, various authors, notably Young (1975) and Hertz (1976), recognized that, if the transition temperature of a continuous phase transition can be depressed to zero, the

critical modes become quantum-mechanical in nature. The partition function for a quantum phase transition is described by a Feynman integral over order-parameter configurations $\{\psi(x,\tau)\}$ in both space *and* imaginary time (Sachdev, 2007; Hertz, 1976)

$$Z_{\text{quantum}} = \sum_{\text{space–time configurations}} \mathrm{e}^{-S[\psi]} \tag{176}$$

where the action

$$S[\psi] = \int_0^{\frac{\hbar}{k_B T}} \mathrm{d}\tau \int_{-\infty}^{\infty} \mathrm{d}^d x L[\psi(x,\tau)] \tag{177}$$

contains an integral of the Lagrangian L over an infinite range in space, but a *finite* time interval

$$l_\tau \equiv \frac{\hbar}{k_{\mathrm{B}} T} \tag{178}$$

Near a QCP, bubbles of quantum critical matter form within a metal, with finite size ξ_x and duration ξ_τ (Figure 33). These two quantities diverge as the quantum critical point is approached, but the rates of divergence are related by a dynamical critical exponent (Hertz, 1976),

$$\xi_\tau \sim (\xi_x)^z \tag{179}$$

One of the consequences of this scaling behavior is that time counts as z spatial dimensions, $[\tau] = [L^z]$ in general.

At a classical critical point, temperature is a tuning parameter that takes one through the transition. The role of temperature is fundamentally different at a quantum critical point: it sets the scale $l_\tau \sim 1/T$ in the time direction, introducing a *finite size correction* to the QCP. When the temperature is raised, l_τ reduces and the quantum fluctuations are probed on shorter and shorter timescales. There are then two regimes to the phase diagram,

$$\text{(a)} \qquad \text{Quantum critical:} \qquad l_\tau \ll \xi_\tau \tag{180}$$

where the physics probes the 'interior' of the quantum critical bubbles, and

$$\text{(b)} \qquad \text{Fermi liquid/AFM} \qquad l_\tau \gg \xi_\tau \tag{181}$$

where the physics probes the quantum fluid 'outside' the quantum critical bubbles. The quantum fluid that forms in this region is a sort of 'quantum soda', containing short-lived bubbles of quantum critical matter surrounded by a paramagnetic (B1) or antiferromagnetically ordered (B2) Landau–Fermi liquid. Unlike a classical phase transition, in which the critical fluctuations are confined to a narrow region either side of the transition, in a quantum critical region (a), fluctuations persist up to temperatures where l_τ becomes comparable the with the microscopic short-time cutoff in the problem (Kopp and Chakravarty, 2005) (which for heavy-electron systems is most likely, the single-ion Kondo temperature $l_\tau \sim \hbar/T_{\mathrm{K}}$).

5.3 Signs of a new universality

The discovery of quantum criticality in heavy-electron systems raises an alluring possibility of *quantum critical matter*, a universal state of matter that, like its classical counterpart, forgets its microscopic, chemical, and electronic origins. There are three pieces of evidence that are particularly fascinating in this respect:

1. Scale invariance, as characterized by E/T scaling in the quantum-critical inelastic spin fluctuations observed in $CeCu_{1-x}Au_x$ (Schroeder *et al.*, 1998, 2000). ($x = x_c = 0.016$),

$$\chi''_{\mathbf{Q}_0}(E,T) = \frac{1}{T^a} F(E/T) \tag{182}$$

   where $a \approx 0.75$ and $F[x] \propto (1 - ix)^{-a}$. Similar behavior has also been seen in powder samples of $UCu_{5-x}Pd_x$ (Aronson *et al.*, 1995).
2. A jump in the Hall constant of $YbRh_2Si_2$ when field tuned through its QCP (Paschen *et al.*, 2004). (see Figure 34a).
3. A sudden change in the area of the extremal Fermi surface orbits observed by de Haas van Alphen at a pressure-tuned QCP in $CeRhin_5$ (Shishido, Settai, Harima and Onuki, 2005). (see Figure 34b).

Features 2 and 3 suggest that the Fermi surface jumps from a 'small' to 'large' Fermi surface as the magnetic order is lost, as if the phase shift associated with the Kondo effect collapses to zero at the critical point, as if the f component of the electron fluid Mott-localizes at the transition. To reconcile a sudden change in the Fermi surface with a second-order phase transition, we are actually forced to infer that the quasiparticle weights vanish at the QCP.

These features are quite incompatible with a spin-density wave QCP. In a spin-density wave scenario, the Fermi surface and Hall constant are expected to evolve continuously through a QCP. Moreover, in an SDW description, the dynamical critical exponent is $z = 2$ so time counts as $z = 2$ dimensions in the scaling theory, and the effective dimensionality $D_{\text{eff}} = d + 2 > 4$ lies above the upper critical dimension, where mean-field theory is applicable and scale-invariant behavior is no longer expected.

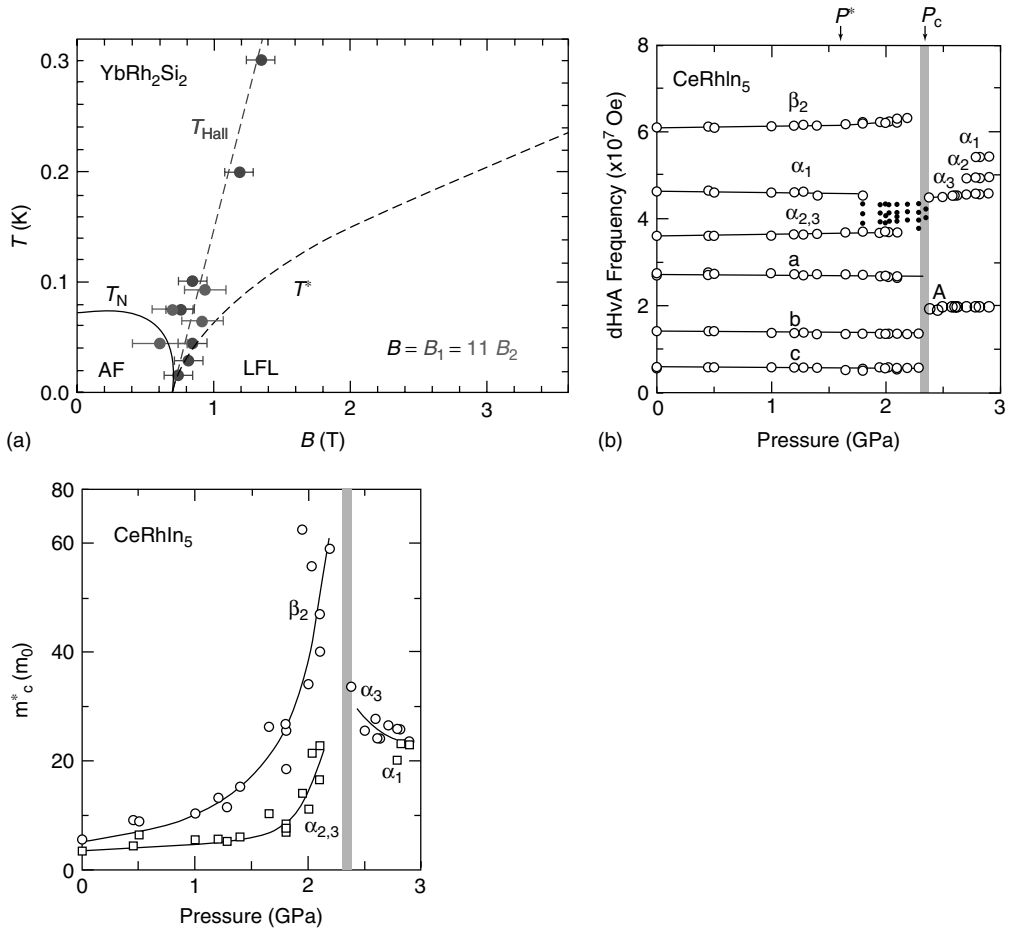

Figure 34. (a) Hall crossover line for sudden evolution of Hall constant in $YbRh_2Si_2$. (Reproduced from Paschen, S., T. Lühmann, S. Wirth, P. Gegenwart, O. Trovarelli, C. Geibel, F. Steglich, P. Coleman, and Q. Si, 2004, *Nature* **432**, 881.) (b) Sudden change in dHvA frequencies and divergence of quasiparticle effective masses at pressure-tuned, finite field QCP in $CeRhIn_5$. (Reproduced from H. Shishido, R. Settai, H. Harima, and Y. Onuki, *Journal of the Physical Society of Japan* **74**, 2005, 1103 weith permission of the Physical Society of Japan.)

These observations have ignited a ferment of theoretical interest in the nature of heavy-fermion criticality. We conclude with a brief discussion of some of the competing ideas currently under consideration.

5.3.1 Local quantum criticality

One of the intriguing observations (Schroeder *et al*., 1998) in $CeCu_{6-x}Au_x$ is that the uniform magnetic susceptibility, $\chi^{-1} \sim T^a + C$, $a = 0.75$ displays the same power-law dependence on temperature observed in the inelastic neutron scattering at the critical wave vector $\mathbf{Q}_0$. A more detailed set of measurements by Schroeder *et al*. (2000) revealed that the scale-invariant component of the dynamical spin susceptibility appears to be momentum independent,

$$\chi^{-1}(\mathbf{q}, E) = T^a[\Phi(E/T)] + \chi_0^{-1}(\mathbf{q}) \tag{183}$$

This behavior suggests that the critical behavior associated with the heavy-fermion QCP contains some kind of *local* critical excitation (Schroeder *et al*., 1998; Coleman, 1999).

One possibility is that this local critical excitation is the spin itself, so that (Coleman, 1999; Sachdev and Ye, 1993; Sengupta, 2000)

$$\langle S(\tau)S(\tau')\rangle = \frac{1}{(\tau - \tau')^{2-\epsilon}} \tag{184}$$

is a power law, but where $\epsilon \neq 0$ signals non-Fermi liquid behavior. This is the basis of the 'local quantum criticality' theory developed by Smith and Si (2000) and Si, Rabello, Ingersent and Smith (2001, 2003). This theory requires that the local spin susceptibility $\chi_{\rm loc} = \sum_{\mathbf{q}} \chi(\mathbf{q}, \omega)_{\omega=0}$ diverges at a heavy-fermion QCP. Using an extension of the methods of DMFT (Georges, Kotliar, Krauth and Rozenberg, 1996; Kotliar *et al*., 2006) Si *et al*. find that it is possible to account

for the local scaling form of the dynamical susceptibility, obtaining exponents that are consistent with the observed properties of $CeCu_{6-x}Au_x$ (Grempel and Si, 2003).

However, there are some significant difficulties with this theory. First, as a local theory, the quantum critical fixed point of this model is expected to possess a finite zero-point entropy per spin, a feature that is, to date, inconsistent with thermodynamic measurements (Custers *et al*., 2003). Second, the requirement of a divergence in the local spin susceptibility imposes the requirement that the surrounding spin fluid behaves as layers of decoupled two-dimensional spin fluids. By expanding $\chi_0^{-1}(\mathbf{q})$ (183) about the critical wave vector $\mathbf{Q}$, one finds that the singular temperature dependence in the local susceptibility is given by

$$\chi_{\rm loc}(T) \sim \int \mathrm{d}^d q \frac{1}{(\mathbf{q}-\mathbf{Q})^2 + T^\alpha} \sim T^{(d-2)\alpha/2} \qquad (185)$$

requiring that $d \leq 2$.

In my judgement, the validity of the original scaling by Schroeder *et al* still stands and that these difficulties stem from a misidentification of the critical local modes driving the scaling seen by neutrons. One possibility, for example, is that the right soft variables are not spin *per se*, but the fluctuations of the phase shift associated with the Kondo effect. This might open up the way to an alternative formulation of local criticality.

5.3.2 *Quasiparticle fractionalization and deconfined criticality*

One of the competing sets of ideas under consideration at present is the idea that, in the process of localizing into an ordered magnetic moment, the composite heavy electron breaks up into constituent spin and charge components. In general,

$$e_\sigma^- \rightleftharpoons s_\sigma + h^- \qquad (186)$$

where s_σ represents a neutral spin-1/2 excitation or 'spinon'. This has led to proposals (Coleman, Pépin, Si and Ramazashvili, 2001; Senthil, Vojta, Sachdev and Vojta, 2003; Pépin, 2005) that gapless spinons develop at the QCP. This idea is faced with a conundrum, for, even if free neutral spin-1/2 excitations can exist at the QCP, they must surely be confined as one tunes away from this point, back into the Fermi liquid. According to the model of 'deconfined criticality' proposed by Senthil *et al*. (2004), the spinon confinement scale ξ_2 introduces a second diverging length scale to the phase transition, where ξ_2 diverges more rapidly to infinity than ξ_1. One possible realization of this proposal is the quantum melting of two-dimensional $S = 1/2$ Heisenberg AFM, where the smaller correlation length ξ_1 is associated with the transition from AFM to spin liquid, and the second correlation length ξ_2 is associated with the confinement of spinons to form a valence bond solid (Figure 35).

It is not yet clear how this scenario will play out for heavy electron systems. Senthil, Sachdev and Vojta (2005) have proposed that, in a heavy-electron system, the intermediate spin liquid state may involve a Fermi surface of neutral (fermionic) spinons coexisting with a small Fermi surface of conduction electrons, which they call an FL* state. In this scenario, the QCP involves an instability of the heavy-electron fluid to the FL* state, which is subsequently unstable to antiferromagnetism. Recent work suggests that the Hall constant can indeed jump at such a transition (Coleman, Marston and Schofield, 2005b).

5.3.3 *Schwinger bosons*

A final approach to quantum criticality, currently under development, attempts to forge a kind of 'spherical model' for the antiferromagnetic QCP through the use of a large N expansion in which the spin is described by Schwinger bosons, rather than fermions (Arovas and Auerbach, 1988; Parcollet and Georges, 1997),

$$S_{ab} = b_a^\dagger b_b - \delta_{ab}\frac{n_b}{N} \qquad (187)$$

where the spin S of the moment is determined by the constraint $n_b = 2S$ on the total number of bosons per site. Schwinger bosons are well suited to describe low-dimensional magnetism (Arovas and Auerbach, 1988). However, unlike fermions, only one boson can enter a Kondo

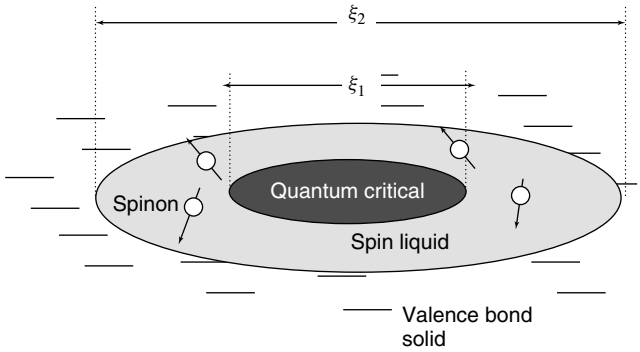

Figure 35. 'Deconfined criticality' (Senthil *et al*., 2004). The quantum critical droplet is defined by two divergent length scales - ξ_1 governing the spin correlation length, ξ_2 on which the spinons confine, in the case of the Heisenberg model, to form a valence bond solid. (Adapted using data from T. Senthil, A. Vishwanath, L. Balents, S. Sachdev and M.P.A. Fisher, *Science* **303** (2004) 1490.)

singlet. To obtain an energy that grows with N, Parcollet and Georges proposed a new class of large N expansion based around the multichannel Kondo model with K channels (Cox and Ruckenstein, 1993; Parcollet and Georges, 1997), where $k = K/N$ is kept fixed. The Kondo interaction takes the form

$$H_{\rm int} = \frac{J_K}{N} \sum_{\nu=1,K,\alpha,\beta} S_{\alpha\beta} c^\dagger_{\nu\beta\mu} c_{\nu\alpha} \qquad (188)$$

where the channel index ν runs from one to K. When written in terms of Schwinger bosons, this interaction can be factorized in terms of a charged, but spinless exchange fermion χ_ν ('holon') as follows:

$$H_{\rm int} \to \sum_{\nu\alpha} \frac{1}{\sqrt{N}} \left[(c^\dagger_{\nu\alpha} b_\alpha) \chi^\dagger_\nu + {\rm H.c} \right] + \sum_\nu \frac{\chi^\dagger_\nu \chi_\nu}{J_K} \qquad (189)$$

Parcollet and Georges originally used this method to study the overscreened Kondo model (Parcollet and Georges, 1997), where $K > 2S$.

Recently, it has proved possible to find the Fermi liquid large N solutions to the fully screened Kondo impurity model, where the number of channels is commensurate with the number of bosons ($K = 2S$) (Rech, Coleman, Parcollet and Zarand, 2006; Lebanon and Coleman, 2007). One of the intriguing features of these solutions is the presence of a gap for spinon excitations, roughly comparable with the Kondo temperature. Once antiferromagnetic interactions are introduced, the spinons pair-condense, forming a state with a *large* Fermi surface, but one that coexists with gapped spinon (and holon) excitations (Coleman, Paul and Rech, 2005a).

The gauge symmetry associated with these particles guarantees that, if the gap for the spinon goes to zero continuously, then the gap for the holon must also go to zero. This raises the possibility that gapless charge degrees of freedom may develop at the very same time as magnetism (Figure 36). In the two impurity model, Rech *et al.* have recently shown that the large N solution contains a 'Jones–Varma' QCP where a static valence bond forms

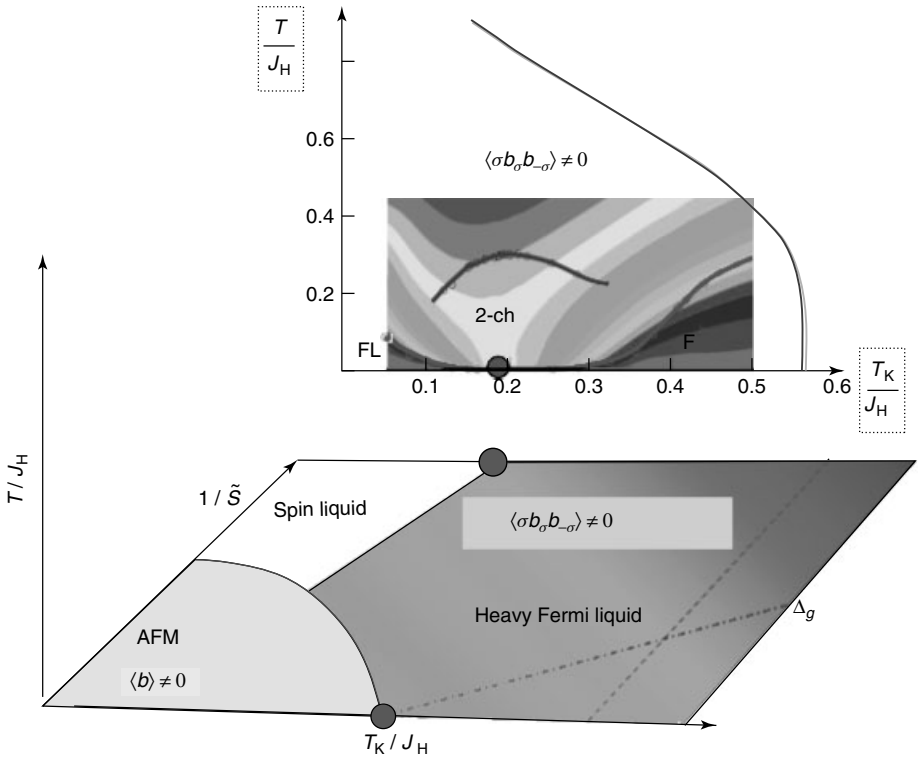

Figure 36. Proposed phase diagram for the large N limit of the two impurity and Kondo lattice models. Background – the two impurity model, showing contours of constant entropy as a function of temperature and the ratio of the Kondo temperature to Heisenberg coupling constant. (Reproduced from Rech, J., P. Coleman, O. Parcollet, and G. Zarand, 2006, *Phys. Rev. Lett* **96**, 016601.) Foreground – proposed phase diagram of the fully screened, multichannel Kondo lattice, where $\tilde{S}$ is the spin of the impurity. At small $\tilde{S}$, there is a phase transition between a spin liquid and heavy-electron phase. At large $\tilde{S}$, a phase transition between the AFM and heavy-electron phase. If this phase transition is continuous in the large N limit, then both the spinon and holon gap are likely to close at the QCP. (Reproduced from Lebanon, E., and P. Coleman, 2007, Fermi liquid identities for the Infinite U Anderson Model, *Phys. Rev. B* (submitted), URL http://arxiv.org/abs/cond-mat/0610027.)

between the Kondo impurities. At this point, the holon and spinon excitations become gapless. On the basis of this result, Lebanon, Rech, Coleman and Parcollet (2006) have recently proposed that the holon spectrum may become gapless at the magnetic QCP (Figure 36) in three dimensions.

6 CONCLUSIONS AND OPEN QUESTIONS

I shall end this chapter with a brief list of open questions in the theory of heavy fermions.

1. To what extent does the mass enhancement in heavy-electron materials owe its size to the vicinity to a nearby quantum phase transitions?
2. What is the microscopic origin of heavy-fermion superconductivity and in theextreme cases UBe_{13} and $PuCoGa_5$ how does the pairing relate to both spin quenching and the Kondo effect?
3. What is the origin of the linear resistivity and the logarithmic divergence of the specific heat at a 'hard' heavy-electron QCP?
4. What happens to magnetic interactions in a Kondo insulator, and why do they appear to vanish?
5. In what new ways can the physics of heavy-electron systems be interfaced with the tremendous current developments in mesoscopics? The Kondo effect is by now a well-established feature of Coulomb blockaded quantum dots (Kouwenhoven and Glazman, 2001), but there may be many other ways in which we can learn about local moment physics from mesoscopic experiments. Is it possible, for example, to observe voltage-driven quantum phase transitions in a mesoscopic heavy-electron wire? This is an area grown with potential.

It should be evident that I believe there is tremendous prospect for concrete progress on many of these issues in the near future. I hope that, in some ways, I have whet your appetite enough to encourage you also to try your hand at their future solution.

NOTES

[1] To calculate the matrix elements associated with valence fluctuations, take

$$|f^1c^1\rangle = \frac{1}{\sqrt{2}}(f^\dagger_\uparrow c^\dagger_\downarrow - c^\dagger_\uparrow f^\dagger_\downarrow)|0\rangle,$$
$$|f^2\rangle = f^\dagger_\uparrow f^\dagger_\downarrow|0\rangle \qquad \text{and} \qquad |c^2\rangle = c^\dagger_\uparrow c^\dagger_\downarrow|0\rangle$$

then $\langle c^2|\sum_\sigma V c^\dagger_\sigma f_\sigma|f^1c^1\rangle = \sqrt{2}V$ and $\langle f^2|\sum_\sigma V f^\dagger_\sigma c_\sigma |f^1c^1\rangle = \sqrt{2}V$

[2] The f-sum rule is a statement about the instantaneous, or short-time diamagnetic response of the metal. At short times $\mathrm{d}j/\mathrm{d}t = (n_c e^2/m)E$, so the high-frequency limit of the conductivity is $\sigma(\omega) = \frac{ne^2}{m}\frac{1}{\delta - i\omega}$. But using the Kramer's Krönig relation

$$\sigma(\omega) = \int \frac{\mathrm{d}x}{i\pi}\frac{\sigma(x)}{x - \omega - i\delta}$$

at large frequencies,

$$\omega(\omega) = \frac{1}{\delta - i\omega}\int \frac{\mathrm{d}x}{\pi}\sigma(x)$$

so that the short-time diamagnetic response implies the f-sum rule.

[3] To prove this identity, first note that any two-dimensional matrix, M, can be expanded as $M = m_0\sigma_2 + \vec{m}\cdot\sigma_2\vec{\sigma}$, $(b = (1, 3))$ where $m_0 = \frac{1}{2}\mathrm{Tr}[M\sigma_2]$ and $\vec{m} = \frac{1}{2}\mathrm{Tr}[M\vec{\sigma}\sigma_2]$, so that in index notation

$$M_{\alpha\gamma} = \frac{1}{2}\mathrm{Tr}[M\sigma_2](\sigma_2)_{\alpha\gamma} + \frac{1}{2}\mathrm{Tr}[M\vec{\sigma}\sigma_2]\cdot(\sigma_2\vec{\sigma})_{\alpha\gamma}$$

Now, if we apply this relationship to the $\alpha\gamma$ components of $\vec{\sigma}_{\alpha\beta}\cdot\vec{\sigma}_{\gamma\delta}$, we obtain

$$\vec{\sigma}_{\alpha\beta}\cdot\vec{\sigma}_{\gamma\delta} = \frac{1}{2}\left(\vec{\sigma}^T\sigma_2\vec{\sigma}\right)_{\delta\beta}(\sigma_2)_{\alpha\gamma} + \frac{1}{2}\sum_{b=1,3}\left(\vec{\sigma}^T\sigma_2\sigma_b\,\vec{\sigma}\right)_{\delta\beta}(\sigma_2\sigma_b)_{\alpha\gamma}$$

If we now use the relation $\vec{\sigma}^T\sigma_2 = -\sigma_2\vec{\sigma}$, together with $\vec{\sigma}\cdot\vec{\sigma} = 3$ and $\vec{\sigma}\sigma_b\vec{\sigma} = -\sigma_b$, we obtain

$$\vec{\sigma}_{\alpha\beta}\cdot\vec{\sigma}_{\gamma\delta} = -\frac{3}{2}(\sigma_2)_{\alpha\gamma}(\sigma_2)_{\delta\beta} + \frac{1}{2}(\vec{\sigma}\sigma_2)_{\alpha\gamma}\cdot(\sigma_2\vec{\sigma})_{\delta\beta}$$

ACKNOWLEDGMENTS

This research was supported by the National Science Foundation grant DMR-0312495. I would like to thank E. Lebanon and T. Senthil for discussions related to this work. I would also like to thank the Aspen Center for Physics, where part of the work for this chapter was carried out.

REFERENCES

Abrikosov, A.A. (1965). Electron scattering on magnetic impurities in metals and anomalous resistivity effects. *Physics*, **2**, 5.

Aeppli, G. and Fisk, Z. (1992). Kondo insulators. *Comments on Condensed Matter Physics*, **16**, 155.

Aeppli, G., Goldman, A., Shirane, G., *et al*. (1987). Development of antiferromagnetic correlations in the heavy-fermion system UPt_3. *Physical Review Letters*, **58**, 808.

Affleck, I., Zou, Z., Hsu, T. and Anderson, P.W. (1988). SU(2) gauge symmetry of the large-U limit of the Hubbard model. *Physical Review B*, **8**, 745.

Alekseev, P.A., Klement'ev, E.S., Lazukov, V., *et al*. (1994). 4f electrons and the formation of the ground state in the Kondo insulator CeNiSn. *JETP*, **79**, 665.

Allen, J.W., Oh, S.J., Maple, M.B. and Torikachvili, M.S. (1983). Large Fermi-level resonance in the electron-addition spectrum of $CeRu_2$ and $CeIr_2$. *Physical Review*, **28**, 5347.

Allen, J.W., Oh, S.J., Cox, L.E., *et al*. (1985). Spectroscopic evidence for the 5f coulomb interaction in UAl_2 and UPt_3. *Physical Review Letters*, **2635**, 54.

Allen, J., Oh, S., Gunnarsson, O., *et al*. (1986). Electronic structure of cerium and light rare-earth intermetallics. *Advances in Physics*, **35**, 275.

Anderson, P.W. (1961). Localized magnetic states in metals. *Physical Review*, **124**, 41.

Anderson, P.W. (1970). Poor Man's derivaton of scaling laws for the Kondo problem. *Journal of Physics C*, **3**, 2346.

Anderson, P.W. (1973). Kondo Effect IV: out of the wilderness. *Comments on Solid State Physics*, **5**, 73.

Anderson, P.W. (1981). Conference summary. In *Valence Fluctuations in Solids*, Falicov, L.M., Hanke, W. and Maple, M.P. (Eds.), North Holland: Amsterdam, p. 451.

Anderson, P.W. (1987). The resonating valence bond state in La_2CuO_4 and superconductivity. *Science*, **235**, 1196.

Anderson, P.W. and Yuval, G. (1969). Exact results in the Kondo problem: equivalence to a classical one-dimensional coulomb gas. *Physical Review Letters*, **45**, 370.

Anderson, P.W. and Yuval, G. (1970). Exact results for the Kondo problem: one-body theory and extension to finite temperature. *Physical Review B*, **1**, 1522.

Anderson, P.W. and Yuval, G. (1971). Some numerical results on the Kondo problem and the inverse square one-dimensional Ising model. *Journal of Physics C*, **4**, 607.

Andrei, N., Furuya, K. and Lowenstein, J. (1983). Solution of the Kondo problem. *Reviews of Modern Physics*, **55**, 331–402.

Andres, K., Graebner, J. and Ott, H.R. (1975). 4f-virtual-bound-state formation in $CeAl_3$ at low temperatures. *Physical Review Letters*, **35**, 1779.

Aoki, H., Sakahibara, T., Shishido, H., *et al*. (2004). Field-angle dependence of the zero-energy density of states in the unconventional heavy-fermion superconductor $CeCoIn_5$. *Journal of Physics: Condensed Matter*, **16**, L13–L19.

Aronson, M., Osborn, R., Robinson, R., *et al*. (1995). Non-Fermi-liquid scaling of the magnetic response in $UCu_{5-x}Pd_x$ ($x = 1, 1.5$). *Physical Review Letters*, **75**, 725.

Arovas, D. and Auerbach, A. (1988). Functional integral theories of low-dimensional quantum Heisenberg models. *Physical Review B*, **38**, 316.

Auerbach, A. and Levin, K. (1986). Kondo bosons and the Kondo lattice: microscopic basis for the heavy Fermi liquid. *Physical Review Letters*, **57**, 877.

Bang, Y., Balatsky, A.V., Wastin, F. and Thompson, J.D. (2004). Possible pairing mechanisms of $PuCoGa_5$ superconductor. *Physical Review*, **70**, 104512.

Barnes, S.E. (1976). New method for the Anderson model. *Journal of Physics*, **F 6**, 1375.

Baskaran, G., Zou, Z. and Anderson, P.W. (1987). The resonating valence bond state and high-T_c superconductivity- a mean field theory. *Solid State Communications*, **63**, 973.

Bauer, E., Michor, G.H.H., Paul, C., *et al*. (2004). Heavy fermion superconductivity and magnetic order in noncentrosymmetric $CePt_3Si$. *Physical Review Letters*, **92**, 027003.

Baym, G. and Pethick, C. (1992). *Landau Fermi-Liquid Theory*, Wiley: New York.

Berlin, T.H. and Kac, M. (1952). The spherical model of a ferromagnet. *Physical Review*, **86**, 821.

Beyerman, W.P., Gruner, G., Dlicheouch, Y. and Maple, M.B. (1988). Frequency-dependent transport properties of UPt_3. *Physical Review B*, **37**, 10353.

Bishop, D.J., Varma, C.M., Batlogg, B., *et al*. (1984). Ultrasonic Attenuation in UPt_3. *Physical Review Letters*, **53**(10), 1009.

Blandin, A. and Friedel, J. (1958). *Journal de Physique et le Radium*, **20**, 160 (1959).

Blount, E.I., Varma, C.M. and Aeppli, G. (1990). Phase diagram of the heavy-fermion superconductor UPt_3. *Physical Review Letters*, **64**, 3074.

Broholm, C., Aeppli, G., Kleiman, R.N., *et al*. (1990). Kondo insulators. *Physical Review Letters*, **65**, 2062.

Bucher, B., Schlessinger, Z., Canfield, P.C. and Fisk, Z. (1994). Charge dynamics in the Kondo insulator Ce_3Bi_4Pt. *Physical Review Letters*, **72**, 522.

Bucher, B., Schlessinger, Z., Mandrus, D., *et al*. (1995). Charge dynamics of Ce-based compounds: connection between the mixed valent and Kondo-insulator states. *Physical Review B*, **53**, R2948.

Bucher, E., Maita, J.P., Hull, G.W., *et al*. (1975). Electronic properties of beryllides of the rare earth and some actinides. *Physical Review B*, **11**, 440.

Bud'ko, S.L., Morosan, E. and Canfield, P.C. (2004). Magnetic field induced non-Fermi-liquid behavior in YbAgGe single crystals. *Physical Review B*, **69**, 014415.

Bud'ko, S.L., Zapf, V., Morosan, E. and Canfield, P.C. (2005). Field-dependent Hall effect in single-crystal heavy-fermion YbAgGe below 1 K. *Physical Review B*, **72**, 172413.

Bulla, R. (2006). Dynamical mean-field theory: from quantum impurity physics to lattice problems. *Philosophical Magazine*, **86**, 1877.

Burdin, S., Georges, A. and Grempel, D.R. (2000). Coherence scale of the Kondo lattice. *Physical Review Letters*, **85**, 1048.

Cardy, J. (1996). *Renormalization in Statistical Physics*, Cambridge University Press: Cambridge.

Clogston, A.M., Mathias, B.T., Peter, M., *et al*. (1962). Local magnetic moment associated with an iron atom dissolved in various transition metal alloys. *Physical Review*, **125**, 541.

Coleman, P. (1983). 1/N expansion for the Kondo lattice. *Physical Review*, **28**, 5255.

Coleman, P. (1984). New approach to the mixed-valence problem. *Physical Review*, **29**, 3035.

Coleman, P. (1987a). Constrained quasiparticles and conduction in heavy-fermion systems. *Physical Review B*, **35**, 5072.

Coleman, P. (1987b). Mixed valence as an almost broken symmetry. *Physical Review Letters*, **59**, 1026.

Coleman, P. (1999). Theories of non-Fermi liquid behavior in heavy fermions. *Physica B*, **259–261**, 353.

Coleman, P. and Andrei, N. (1989). Kondo-stabilized spin liquids and heavy fermion superconductivity. *Journal of Physics: Condensed Matter*, **C 1**, 4057.

Coleman, P., Tsvelik, A.M., Andrei, N. and Kee, H.Y. (1999). Cooperative Kondo effect in the two-channel Kondo lattice. *Physical Review*, **B60**, 3608.

Coleman, P., Pépin, C., Si, Q. and Ramazashvili, R. (2001). How do Fermi liquids get heavy and die?. *Journal of Physics: Condensed Matter*, **13**, 273.

Coleman, P., Paul, I. and Rech, J. (2005a). Sum rules and Ward identities in the Kondo lattice. *Physical Review B*, **72**, 094430.

Coleman, P., Marston, J.B. and Schofield, A.J. (2005b). Transport anomalies in a simplified model for a heavy-electron quantum critical point. *Physical Review*, **72**, 245111.

Coqblin, B. and Schrieffer, J.R. (1969). Exchange interaction in alloys with cerium impurities. *Physical Review*, **185**, 847.

Cox, D. and Grewe, N. (1988). Transport properties of the Anderson lattice. *Zeitschrift fur Physik B*, **71**, 273.

Cox, D. and Maple, M. (1995). Electronic pairing in exotic superconductors. *Physics Today*, **482**, 32.

Cox, D. and Zawadowski, A. (1999). *Exotic Kondo Effects in Metals*, CRC Press: Boca Raton.

Cox, D.L. and Ruckenstein, A.E. (1993). Spin-flavor separation and non-Fermi-liquid behavior in the multichannel Kondo problem: a large-N approach. *Physical Review Letters*, **71**((Sept.)), 1613–1616.

Curro, N.J., Caldwell, T., Bauer, E.D., *et al*. (2005). Unconventional superconductivity in $PuCoGa_5$. *Nature*, **434**, 622.

Custers, J., Gegenwart, P., Wilhelm, H., *et al*. (2003). The break-up of heavy electrons at a quantom critical point. *Nature*, **424**, 524.

de Haas, W.J., de Boer, J. and van der Berg, D. (1933). *Physica*, **1**, 1115.

Degiorgi, L. (1999). The electrodynamic response of heavy-electron compounds. *Reviews of Modern Physics*, **71**, 687.

Degiorgi, L., Anders, F., Gruner, G. and Society, E.P. (2001). Charge excitations in heavy electron metals. *Journal B*, **19**, 167.

DiTusa, J.F., Friemelt, K., Bucher, E., *et al*. (1997). Metal-insulator transitions in the Kondo insulator FeSi and classic semiconductors are similar. *Physical Review Letters*, **831**, 78.

Doniach, S. (1977). Kondo lattice and weak antiferromagnetism. *Physica B*, **91**, 231.

Dordevic, S.V., Basov, D.N., Dilley, N.R., *et al*. (2001). Hybridization gap in 16 heavy fermion compounds. *Physical Review Letters*, **86**, 684.

Engelbrecht, J. and Bedell, K. (1995). Robustness of a local Fermi liquid against ferromagnetism and phase separation. *Physical Review Letters*, **74**, 4265.

Estrela, P., de Visser, A., Naka, T., *et al*. (2002). Resistivity of non-Fermi liquid UPtIn under pressure. *Physica B*, **312–313**, 482.

Fak, B., McMorrow, D.F., Niklowitz, P.G., *et al*. (2005). An inelastic neutron scattering study of single-crystal heavy-fermion YbAgGe. *Journal of Physics: Condensed Matter*, **17**, 301.

Flouquet, J. (2005). *On the Heavy Fermion Road*, http://www.citebase.org/abstract?id=oai:arXiv.org:cond-mat/05 01602.

Fowler, M. and Zawadowskii, A. (1971). Scaling and the renormalization group in the Kondo effect. *Solid State Communications*, **9**, 471.

Fulde, P., Keller, J. and Zwicknagl, G. (1988). Theory of heavy fermion systems. *Solid State Physics*, **41**, 1.

Gegenwart, P., Custers, J., Tokiwa, Y., *et al*. (2005). Ferromagnetic quantum critical fluctuations in $YbRh_2(Si_{0.95}Ge_{0.05})_2$. *Physical Review Letters*, **94**, 076402.

Geibel, C., Schank, C., Thies, S., *et al*. (1991a). Heavy-fermion superconductivity at $T_c = 2K$ in the antiferromagnet UPd_2Al_3. *Zeitschrift fur Physik B*, **84**, 1.

Geibel, C., Thies, S., Kacrowski, D., *et al*. (1991b). A new heavy-fermion superconductor: UNi_2Al_3. *Zeitschrift fur Physik B*, **83**, 305.

Georges, A. and Kotliar, G. (1992). Hubbard model in infinite dimensions. *Physical Review B*, **45**, 6479.

Georges, A., Kotliar, G., Krauth, W. and Rozenberg, M. (1996). Dynamical mean-field theory of strongly correlated fermion systems and the limit of infinite dimensions. *Reviews of Modern Physics*, **68**, 13–125.

Grempel, D.R. and Si, Q. (2003). Locally critical point in an anisotropic Kondo lattice. *Physical Review Letters*, **91**, 026401.

Grewe, N. and Steglich, F. (1991). Heavy Fermions. In *Handbook on the Physics and Chemistry of Rare Earths*, Gschneider, K.A. and Eyring, L. (Eds.), Elsevier: Amsterdam, p. 343, Vol. 14.

Grosche, F.M., Agarwal, P., Julian, S.R., *et al*. (2000). Anomalous low temperature states in $CeNi_2Ge_2$ and $CePd_2Si_2$. *Journal of Physics: Condensed Matter*, **12**, L533.

Gruner, G. and Zawadowski, A. (1974). Magnetic impurities in non-magnetic metals. *Reports on Progress in Physics*, **37**, 1497.

Gunnarsson, O. and Schönhammer, K. (1983). Electron spectroscopies for Ce compounds in the impurity model. *Physical Review B*, **28**, 4315.

Haldane, F.D.M. (1978). Scaling theory of the asymmetric anderson model. *Physical Review Letters*, **40**, 416.

Hertz, J.A. (1976). Quantum critical phenomena. *Physical Review B*, **14**, 1165.

Hess, D.W., Tokuyasu, T.A and Sauls, J.A. (1990). Vortex states in an unconventional superconductor and the mixed phases of UPt_3. *Physical Review B*, **41**, 8891.

Hewson, A.C. (1993). *The Kondo Problem to Heavy Fermions*, Cambridge University Press: Cambridge.

Hirsch, J.E. (1985). Attractive interaction and pairing in fermion systems with strong on-site repulsion. *Physical Review Letters*, **54**, 1317.

Hundley, M.F., Canfield, P.C., Thompson, J.D., *et al*. (1990). Hybridization gap in $Ce_3Bi_4Pt_3$. *Physical Review B*, **42**, 6842.

Iga, F., Kasaya, M. and Kasuya, T. (1988). Specific heat measurements of YbB_{12} and $Yb_xLu_{1-x}B_{12}$. *Journal of Magnetism and Magnetic Materials*, **76–77**, 156.

Ikeda, H. and Miyake, K. (1996). A theory of anisotropic semiconductor of heavy fermions. *Journal of the Physical Society of Japan*, **65**, 1769.

Izawa, K., Suzuki, T., Fujita, T., *et al*. (1999). Metallic ground state of CeNiSn. *Physical Review*, **59**, 2599.

Isawa, K., Goryo, Y.N.J., Matsuda, Y., *et al*. (2003). Multiple Superconducting Phases in New Heavy Fermion Superconductor $PrOs_4Sb)_{12}$. *Physical Review Letters*, **90**, 117001.

Jaccarino, V., Wertheim, G.K., Wernick, J.H., *et al*. (1967). Paramagnetic excited state of FeSi. *Physical Review*, **160**, 476.

Jarrell, M. (1995). Symmetric periodic Anderson model in infinite dimensions. *Physical Review B*, **51**, 7429.

Jarrell, M., Pang, H. and Cox, D.L. (1997). Phase diagram of the two-channel Kondo lattice. *Physical Review Letters*, **78**, 1996.

Jones, B.A. (2007). Kondo effect. In *Handbook of Magnetism and Advanced Magnetic Materials*, Kronmüller, H. and Parkin, S. (Eds.), John Wiley & Sons: Chichester, Vol. 1.

Joynt, R. (1988). Phase diagram of d-wave superconductors in a magnetic field. *Speculations in Science and Technology*, **1**, 210.

Julian, S.R., Teunissen, P.A.A. and Wiegers, S.A.J. (1992). Fermi surface of UPt_3 from 3 to 30 T: field-induced quasiparticle band polarization and the metamagnetic transition. *Physical Review B*, **46**, 9821.

Kadowaki, K. and Woods, S. (1986). Universal relationship of the resistivity and specific heat in heavy-fermion compounds. *Solid State Communications*, **58**, 507.

Kagan, Y., Kikoin, K. and Prokof'ev, N. (1993). Nature of the pseudogap in the energy spectrum of CeNiSn. *JETP Letters*, **57**, 600.

Kasuya, T. (1956). Indirect exchange coupling of nuclear magnetic moments by conduction electrons. *Progress of Theoretical Physics*, **16**, 45.

Kim, K.H., Harrison, N., Jaime, M., *et al*. (2003). Magnetic-field-induced quantum critical point and competing order parameters in URu_2Si_2. *Physical Review Letters*, **91**, 256401.

Kimura, N., Komatsubara, T., Aoki, D., *et al*. (1998). Metamagnetic transition in UPt_3 studied by high-field magnetization and de Haas van Alphen experiments. *Journal of the Physical Society of Japan*, **67**, 2185.

Kondo, J. (1962). g-shift and anomalous Hall effect in gadolinium metals. *Progress of Theoretical Physics*, **28**, 772.

Kondo, J. (1964). Resistance minimum in dilute magnetic alloys. *Progress of Theoretical Physics*, **32**, 37.

Kopp, A. and Chakravarty, S. (2005). Criticality in correlated quantum matter. *Nature Physics*, **1**, 53.

Kotliar, G. (1988). Resonating valence bonds and d-wave superconductivity. *Physical Review B*, **37**, 3664.

Kotliar, G., Savrasov, S.Y., Haule, K., *et al*. (2006). Electronic structure calculations with dynamical mean-field theory. *Reviews of Modern Physics*, **78**, 865.

Kouwenhoven, L. and Glazman, L. (2001). Revival of the Kondo effect. *Physics World*, **14**, 33.

Küchler, R., Oeschler, N., Gegenwart, P., *et al*. (2003). Divergence of the Grüneisen ratio at quantum critical points in heavy fermion metals. *Physical Review Letters*, **91**, 066405.

Kuramoto, Y. and Watanabe, T. (1987). Theory of momentum-dependent magnetic response in heavy-fermion systems. *Physica B*, **148**, 80.

Lacroix, C. and Cyrot, M. (1979). Phase diagram of the kondo lattice. *Physical Review B*, **20**, 1969.

Landau, L. (1957). The theory of a Fermi liquid. *Soviet Physics JETP*, **3**, 920–925.

Langer, J.S. and Ambegaokar, V. (1961). Friedel sum rule for a system of interacting electrons. *Physical Review*, **121**, 1090.

Langreth, D. (1966). Friedel sum rule for Anderson's model of localized impurity states. *Physical Review*, **150**, 516.

Lebanon, E. and Coleman, P. (2007). Fermi liquid identities for the Infinite U Anderson Model, *Physical Review B*, in press, http://arxiv.org/abs/cond-mat/0610027.

Lebanon, E., Rech, J., Coleman, P. and Parcollet, O. (2006). Conserving many body approach to the infinite-U Anderson model. *Physical Review Letters*, **97**, 106604.

Lee, P.A., Rice, T.M., Serene, J.W., *et al*. (1986). Theories of heavy-electron systems. comments condens. *Comments on Condensed Matter Physics*, **12**, 99.

Liu, L.Z., Allen, J.W., Seaman, C.L., *et al*. (1992). Kondo resonance in $Y_{1-x}U_xPd_3$. *Physical Review Letters*, **68**, 1034.

Luttinger, J.M. (1960). Fermi surface and some simple equilibrium properties of a system of interacting fermions. *Physical Review*, **119**, 1153.

Luttinger, J.M. and Ward, J.C. (1960). Ground-state energy of a many-Fermion system. *Physical Review*, **118**, 1417.

Machida, K. and Ozaki, M. (1989). Unconventional superconducting class in a heavy Fermion system UPt_3. *Journal of the Physical Society of Japan*, **58**, 2244.

Maple, B., Fertig, W., Mota, A., *et al*. (1972). The re-entrant superconducting-normal phase boundary of the Kondo system $(La,Ce)Al_2$. *Solid State Communications*, **11**, 829.

Martin, R.M. (1982). Fermi-surface sum rule and its consequences for periodic Kondo and mixed-valence systems. *Physical Review Letters*, **48**, 362.

Mathur, N., Grosche, F.M., Julian, S.R., *et al*. (1998). Magnetically mediated superconductivity in heavy fermion compounds. *Nature*, **394**, 39.

McCollam, A., Julian, S.R., Rourke, P.M.C., *et al*. (2005). Anomalous de Haas van 19 Alphen oscillations in $CeCoIn_5$. *Physical Review Letters*, **94**, 186401.

Meisner, G.P., Torikachvili, M.S., Yang, K.N., *et al*. (1985). UFe_4P_{12} and $CeFe_4P_{12}$: nonmetallic isotypes of superconducting $LaFe_4P_{12}$. *Journal of Applied Physics*, **57**, 3073.

Mekata, M., Ito, S., Sato, N., *et al*. (1986). Spin fluctuations in dense Kondo alloys. *Journal of Magnetism and Magnetic Materials*, **54**, 433.

Menth, A., Buehler, E. and Geballe, T.H. (1969). Magnetic and semiconducting properties of SmB_6. *Physical Review Letters*, **22**, 295.

Metzner, W. and Vollhardt, D. (1989). Correlated lattice fermions in $d = \infty$ dimensions. *Physical Review Letters*, **62**, 324.

Millis, A.J. and Lee, P.A. (1987a). Large-orbital-degeneracy expansion for the lattice Anderson model. *Physical Review B*, **35**(7), 3394–3414.

Millis, A.J., Lavagna, M. and Lee, P.A. (1987b). Plasma oscillations in heavy-fermion materials. *Physical Review*, **36**, 864–867.

Miranda, E. and Dobrosavljevic, V. (2005). Disorder-driven non-Fermi liquid behaviour of correlated electrons. *Reports on Progress in Physics*, **68**, 2337.

Miyake, K., Rink, S.S. and Varma, C.M. (1986). pin-fluctuation-mediated even-parity pairing in heavy fermion superconductors. *Physical Review B*, **34**, 6554.

Monod, M.T.B., Bourbonnais, C. and Emery, V. (1986). Possible superconductivity in nearly antiferromagnetic itinerant fermion systems. *Physical Review B*, **34**, 7716.

Monthoux, P. and Lonzarich, G. (1999). p-wave and d-wave superconductivity in quasi-two-dimensional metals. *Physical Review B*, **59**, 14598.

Moreno, J. and Coleman, P. (2000). Gap-anisotropic model for the narrow-gap Kondo insulators. *Physical Review Letters*, **84**, 342.

Moriya, T. and Kawabata, J. (1973). Effect of spin fluctuations on itinerant electron ferromagnetism. *Journal of the Physical Society of Japan*, **34**, 639.

Nakamura, K., Kitaoka, Y., Asayama, K., *et al*. (1994). NMR investigation of energy gap formation in the valence fluctuating compound CeNiSn. *Journal of the Physical Society of Japan*, **63**, 433.

Nakasuji, S., Pines, D. and Fisk, Z. (2004). Two fluid description of the kondo lattice, *Physical Review Letters*, **92**, 16401–16404.

Niklowitz, P.G., Knebel, G., Flouquet, J., *et al*. (2006). Field-induced non-fermiliquid resistivity of stoichiometric YbAgGe single crystals. *Physical Review B*, **73**, 12501.

Norman, M.R. (2007). High-temperature superconductivity – magnetic mechanisms. In *Handbook of Magnetism and Advanced Magnetic Materials*, Kronmüller, H. and Parkin, S. (Eds.), John Wiley & Sons: Chichester, Vol. 5.

Norman, M.R., Oguchi, T. and Freeman, A.J. (1988). Magnetism in the heavy-electron superconductors UPt_3 and URu_2Si_2. *Physical Review*, **38**, 11193.

Nozières, P. (1976). A "Fermi Liquid" description of the Kondo problem at low tempertures. *Journal de Physique C*, **37**, 1.

Nozières, P. (1985). Magnetic impurities and Kondo effects. *Annales de Physique (Paris)*, **10**, 19–35.

Nozières, P. and Blandin, A. (1980). Kondo effect in real metals. *Journal de Physique*, **41**, 193.

Nozières, P. and Luttinger, J.M. (1962). Derivation of the landau theory of Fermi liquids. *Physical Review*, **127**, 1423.

Oguchi, T. and Freeman, A.J. (1985). Local density band approach to f-electron systems-heavy fermion superconductor UPt_3. *Journal of Magnetism and Magnetic Materials*, **52**, 174.

Okiji, A. and Kawakami, N. (1983). Thermodynamic properties of the Anderson model. *Physical Review Letters*, **50**, 1157.

Onuki, Y. and Komatsubara, T. (1987). Heavy fermion state $CeCu_6$. *Journal of Magnetism and Magnetic Materials*, **63–64**, 281.

Oshikawa, M. (2000). Topological approach to Luttinger's theorem and the Fermi surface of a Kondo lattice. *Physical Review Letters*, **84**, 3370.

Ott, H.R. (1987). Heavy Electron Materials. *Progress in Low Temp Physics*, Brewer, D.F. (ed.), North Holland: Amsterdam, p. 215 Vol. 11.

Ott, H.R., Rudigier, H., Fisk, Z. and Smith, J.L. (1983). UBe_{13}: an unconventional actinide superconductor. *Physical Review Letters*, **50**, 1595.

Ott, H.R., Rudigier, H., Rice, T.M., *et al*. (1984). p-wave superconductivity in UBe_{13}. *Physical Review Letters*, **52**, 1915.

Ott, H.R., Rudigier, H., Fisk, Z. and Smith, J.L. (1985). Superconducting Ground State of a Strongly Interacting Electron System: UBe_{13}. In *Valence Fluctuations in Solids*, Buyers, W.J.L. (Ed.), Plenum, p. 309; *Proceedings of the NATO Advanced Study Institute on Moment Formation in Solids*, Vancouver Island, August 1983.

Paglione, J., Tanatar, M.A., Hawthorn, D.G., *et al*. Field-induced quantum critical point in $CeCoIn_5$. (2003). *Physical Review Letters*, **91**, 246405.

Paglione, J., Tanatar, M.A., Hawthorn, D.G., *et al*. (2006). Nonvanishing energy scales at the quantum critical point of $CeCoIn_5$. *Physical Review Letters*, **97**, 106606.

Palstra, T.T.M., Menovsky, A.A., van den Berg, J., *et al*. (1985). Superconducting and magnetic transitions in the heavy-fermion system URu_2Si_2. *Physical Review Letters*, **55**, 2727.

Parcollet, O. and Georges, A. (1997). Transition from overscreening to underscreening in the multichannel Kondo model: exact solution at large N. *Physical Review Letters*, **79**, 4665.

Paschen, S., Lühmann, T., Wirth, S., *et al*. (2004). Hall-effect evolution across a heavy-fermion quantum critical point. *Nature*, **432**, 881.

Pépin, C. (2005). Fractionalization and Fermi-surface volume in heavy-fermion compounds: the case of $YbRh_2Si_2$. *Physical Review Letters*, **94**, 066402.

Petrovic, C., Pagliuso, P.G., Hundley, M.F., *et al*. (2001). Heavy-fermion superconductivity in $CeCoIn_5$ at 2.3 K. *Journal of Physics: Condensed Matter*, **13**, L337.

Pitaevskii, L.P. (1960). On the superfluidity of liquid He^3. *Zhurnal Eksperimentalnoi i Teoreticheskoi Fiziki*, **37**, 1794.

Puttika, W. and Joynt, R. (1988). Stability of anisotropic superconducting phases in UPt_3. *Physical Review B*, **37**, 2377.

Ramakrishnan, T.V. (1981). In *Valence Fluctuations in Solids*, Falicov, L.M., Hanke, W. and Maple, M.P. (Eds.), North Holland: Amsterdam, p. 13.

Read, N. and Newns, D.M. (1983a). A new functional integral formalism for the degenerate Anderson model. *Journal of Physics C*, **29**, L1055.

Read, N. and Newns, D.M. (1983b). On the solution of the Coqblin-Schreiffer Hamiltonian by the large-N expansion technique. *Journal of Physics C*, **16**, 3274.

Read, N. and Sachdev, S. (1991). Large-N expansion for frustrated quantum antiferromagnets. *Physical Review Letters*, **66**, 1773.

Rech, J., Coleman, P., Parcollet, O. and Zarand, G. (2006). Schwinger Boson approach to the fully screened Kondo model. *Physical Review Letters*, **96**, 016601.

Reinders, P.H.P., Springford, M., Coleridge, P.T., *et al*. (1986). de Haas-van Alphen effect in the heavy-electron compound $CeCu_6$. *Physical Review Letters*, **57**, 1631.

Riseborough, P. (2000). Heavy fermion semiconductors. *Advances in Physics*, **49**, 257.

Ronning, F., Capan, C., Bauer, E.D., *et al*. (2006). Pressure study of quantum criticality in $CeCoIn_5$. *Physical Review*, **73**, 064519.

Rosch, A. (1999). Interplay of disorder and spin fluctuations in the resistivity near a quantum critical point. *Physical Review Letters*, **82**, 4280.

Rozenberg, M.J., Kotliar, G. and Kajueter, H. (1996). Transfer of spectral weight in spectroscopies of correlated electron systems. *Physical Review B*, **54**, 8452.

Ruderman, M.A. and Kittel, C. (1954). Indirect exchange coupling of nuclear magnetic moments by conduction electrons. *Physical Review*, **96**, 99–102.

Sachdev, S. (2007). Quantum phase transitions. In *Handbook of Magnetism and Advanced Magnetic Materials*, Kronmüller, H. and Parkin, S. (Eds.), John Wiley & Sons: Chichester, Vol. 1.

Sachdev, S. and Ye, J. (1993). Gapless spin-fluid ground state in a random quantum Heisenberg magnet. *Physical Review Letters*, **70**, 3339.

Sarachik, M., Corenzwit, E. and Longinotti, L.D. (1964). Resistivity of Mo-Nb and Mo-Re Alloys Containing 1% Fe. *Physical Review*, **135**, A1041.

Sarrao, J.L., Morales, L.A., Thompson, J.D., *et al*. (2002). Plutonium-based superconductivity with a transition temperature above 18 K. *Nature*, **420**, 297.

Sato, N., Aso, N., Miyake, K., *et al*. (2001). Strong coupling between local moments and superconducting 'heavy' electrons in UPd_2Al_3. *Nature*, **410**, 340.

Scalapino, D.J., Loh, E. and Hirsch, J.E. (1986). d-wave pairing near a spin-density-wave instability. *Physical Review B*, **34**, 8190.

Schlessinger, Z., Fisk, Z., Zhang, H.T. and Maple, M.B. (1997). s FeSi a Kondo insulator? *Physica B*, **237–238**, 460–462.

Schrieffer, J.R. and Wolff, P. (1966). Relation between the Anderson and Kondo Hamiltonians. *Physical Review*, **149**, 491.

Schroeder, A., Aeppli, G., Bucher, E., *et al*. (1998). Scaling of magnetic fluctuations near a quantum phase transition. *Physical Review Letters*, **80**, 5623.

Schroeder, A., Coldea, G.A.R., Adams, M., *et al*. (2000). Onset of antiferromagnetism in heavy-fermion metals. *Nature*, **407**, 351.

Schweitzer, H. and Czycholl, G. (1991). Resistivity and thermopower of heavy-fermion systems. *Physical Review Letters*, **67**, 3724.

Sengupta, A.M. (2000). Spin in a fluctuating field: the Bose (+ Fermi) Kondo models. *Physical Review*, **61**, 4041.

Senthil, T., Vojta, M., Sachdev, S. and Vojta, M. (2003). Fractionalized Fermi liquids. *Physical Review Letters*, **90**, 216403.

Senthil, T., Vishwanath, A., Balents, L., *et al*. (2004). Deconfined quantum critical points. *Science*, **303**, 1490.

Senthil, T., Sachdev, S. and Vojta, M. (2005). Deconfined quantum critical points. *Physica B*, **9**, 359–361.

Shishido, H., Settai, R., Harima, H. and Onuki, Y. (2005). A drastic change of the Fermi surface at a critical pressure in $CeRhIn_5$: dHvA study under pressure. *Journal of the Physical Society of Japan*, **74**, 1103.

Si, Q., Rabello, S., Ingersent, K. and Smith, J.L. (2001). Ocally critical quantum phase transitions in strongly correlated metals. *Nature*, **413**, 804.

Si, Q., Rabello, S., Ingersent, K. and Smith, J.L. (2003). Local fluctuations in quantum critical metals. *Physical Review*, **68**, 115103.

Sidorov, V.A., Nicklas, M., Pagliuso, P.G., *et al*. (2002). Superconductivity and quantum criticality in $CeCoIn_5$. *Physical Review Letters*, **89**, 157004.

Sigrist, M. and Ueda, K. (1991a). Unconventional superconductivity. *Reviews of Modern Physics*, **63**, 239.

Sigrist, M. and Ueda, K. (1991b). Phenomenological theory of unconventional superconductivity. *Reviews of Modern Physics*, **63**, 239.

Smith, J.L. and Riseborough, P.S. (1985). Actinides, the narrowest bands. *Journal of Magnetism and Magnetic Materials*, **47–48**, 545.

Smith, J.L. and Si, Q. (2000). Spatial correlations in dynamical mean-field theory. *Physical Review*, **61**, 5184.

Steglich, F., Aarts, J., Bredl, C.D., *et al*. (1976). Superconductivity in the presence of strong pauli paramagnetism: $CeCu_2Si_2$. *Physical Review Letters*, **43**, 1892.

Stewart, G. (1984). Heavy-fermion systems. *Reviews of Modern Physics*, **56**, 755.

Stewart, G. (2001). Heavy-fermion systems. *Reviews of Modern Physics*, **73**, 797.

Stewart, G. (2006). Addendum: non-Fermi-liquid behavior in d-and f-electron metals. *Reviews of Modern Physics*, **78**, 743.

Stewart, G.R., Fisk, Z. and Wire, M.S. (1984a). New Ce heavy-fermion system: $CeCu_6$. *Physical Review*, **30**, 482.

Stewart, G.R., Fisk, Z., Willis, J.O. and Smith, J.L. (1984b). Possibility of coexistence of bulk superconductivity and spin fluctuations in UPt_3. *Physical Review Letters*, **52**, 697.

Suhl, H. (1965). Formation of Local Magnetic Moments in Metals. *Physical Review*, **38A**, 515.

Taillefer, L. and Lonzarich, G.G. (1988). Heavy-fermion quasiparticles in UPt_3. *Physical Review Letters*, **60**, 1570.

Taillefer, L., Newbury, R., Lonzarich, G.G., *et al*. (1987). Direct observation of heavy quasiparticles in UPt_3 via the dHvA effect. *Journal of Magnetism and Magnetic Materials*, **63–64**, 372.

Takabatake, T., Teshima, F., Fujii, H., *et al*. (1990). Formation of an anisotropic energy gap in the valence-fluctuating system of CeNiSn. *Physical Review B*, **41**, 9607.

Takabatake, T., Nagasawa, M., Fujii, H., *et al*. (1992). Anisotropic suppression of the energy gap in CeNiSn by high magnetic fields. *Physical Review*, **45**, 5740.

Takabatake, T., Tanaka, H., Bando, Y., *et al*. (1994). Neling evidence for the quasiparticle Gap in Kondo semiconductors CeNiSn and CeRhSb. *Physical Review B*, **50**, 623.

Tanatar, M.A., Paglione, J., Petrovic, C. and Taillefer, L. (2007). Anisotropic violation of the Wiedemann-Franz law at a quantum critical point. *Science* (in press).

Tou, H., Kitaoka, Y., Asayama, K., *et al*. (1995). d-wave superconductivity in antiferromagnetic heavy-fermion compound UPd_2Al_3-evidence from ^{27}Al NMR/NQR studies. *Journal of the Physical Society of Japan*, **64**, 725.

Trovarelli, O., Geibel, C. Mederle, S., *et al*. (2000). $YbRh_2Si_2$: pronounced non-Fermi-liquid effects above a low-lying magnetic phase transition. *Physical Review Letters*, **85**, 626.

Tsujji, H., Kontani, H. and Yoshimora, K. (2005). Universality in heavy fermion systems with general degeneracy. *Physical Review Letters*, **94**, 057201.

Tsunetsugu, H., Sigrist, M. and Ueda, K. (1997). The ground-state phase diagram of the one-dimensional Kondo lattice model. *Reviews of Modern Physics*, **69**, 809.

Tsvelik, A. and Wiegman, P. (1983). The exact results for magnetic alloys. *Advances in Physics*, **32**, 453.

Varma, C.M. (1976). Mixed-valence compounds. *Reviews of Modern Physics*, **48**, 219.

Varma, C., Nussinov, Z. and van Saarlos, W. (2002). Singular Fermi liquids. *Physics Reports*, **361**, 267.

Vekhter, I., Hirschfield, P., Carbotte, J.P. and Nicol, E.J. (1998). Anisotropic thermodynamics of d-wave superconductors in the vortex state. *Physical Review B*, **59**, R9023.

Vidhyadhiraja, N.S., Smith, V.E., Logan, D.E. and Krishnamurthy, H.R. (2003). Dynamics and transport properties of Kondo insulators. *Journal of Physics: Condensed Matter*, **15**, 4045.

Volovik, G.E. (1993). Superconductivity with lines of GAP nodes: density of states in the vortex. *Soviet Physics JETP Letters*, **58**, 469.

von Löhneysen, H. (1996). Non-Fermi-liquid behaviour in the heavy-fermion system $CeCu_{6-x}Au_x$. *Journal of Physics: Condensed Matter*, **8**, 9689.

von Löhneysen, H., Pietrus, T., Portisch, G., *et al*. (1994). Non-Fermi-liquid behavior in a heavy-fermion alloy at a magnetic instability. *Physical Review Letters*, **72**, 3262.

von Löhneysen, H., Rosch, A., Vojta, M. and Wolfe, P. (2007). Fermi-liquid instabilities at magnetic quantum phase transitions. *Reviews of Modern Physics* (submitted) http://arxiv.org/abs/cond-mat/0606317.

Vorontsov, A. and Vekhter, I. (2006). Nodal structure of quasi-two-dimensional superconductors probed by a magnetic field. *Physical Review Letters*, **96**, 237001.

Wang, C.S., Norman, M.R., Albers, R., *et al*. (1987). Fermi surface of UPt_3 within the local-density approximation. *Physical Review*, **35**, 7260.

White, R.H. and Geballe, T.H. (1979). Long Range Order in Solids. Chap. VII. In *Solid State Physics*, Ehrenreich, H., Seitz, F. and Turnbull, D. (Eds.), Academic Press: New York, p. 283, Vol. 15.

Wiegmann, P.B. (1980a). Towards an exact solution of the Anderson model. *Physics Letters*, **80A**, 163.

Wilson, K.G. (1976). The renormalization group: Critical phenomena and the Kondo problem. *Reviews of Modern Physics*, **47**, 773.

Witten, E. (1978). Chiral symmetry, the 1/N expansion and the SU(N) Thirring model. *Nuclear Physics B*, **145**, 110.

Won, H., Parker, D., Maki, K., *et al*. (2004). Gap symmetry of superconductivity in UPd_2Al_3. *Physical Review B*, **70**, 140509.

Yamada, K. (1975). Perturbation expansion for the Anderson Hamiltonian. II. *Progress of Theoretical Physics*, **53**, 970.

Yoshida, K. and Yamada, K. (1975). Perturbation expansion for the Anderson Hamiltonian. III. *Progress of Theoretical Physics*, **53**, 1286.

Yosida, K. (1957). Magnetic properties of Cu-Mn alloys. *Physical Review*, **106**, 896.

Young, A.P. (1975). Quantum effects in the renormalization group approach to phase transitions. *Journal of Physics C: Solid State Physics*, **8**, L309.

Yuan, H.Q., Grosche, F.M., Deppe, M., *et al*. (2006). Non-Fermi liquid states in the pressurized $CeCu_2(Si_{1-x}Gex)_2$ system: two critical points. *Physical Review Letters*, **96**, 047008.

Zwicknagl, G., Yaresko, A.N. and Fulde, P. (2002). Microscopic description of origin of heavy quasiparticles in UPt_3. *Physical Review*, **65**, 081103.

FURTHER READING

Kawakami, N. and Okiji, A. (1981). Exact expression of the ground-state energy for the symmetric Anderson model. *Physical Review Letters*, **86A**, 483.